Bedryfsingenieurswese
Industrial Engineering

University of Stellenbosch

Department of Industrial Engineering

An air suspension cushion to reduce human exposure to vibration

Andre Francois van der Merwe

student number 10880232

Dissertation presented for the degree of Doctorate of Philosophy (Engineering) at Stellenbosch University.

Promotor: Prof JL van Niekerk

08 March 2007

Declaration

I, the undersigned, hereby declare that the work contained in this dissertation is my own original work and has not previously in its entirety or in part been submitted at any university for a degree.
Ek, die ondergetekende verklaar hiermee dat die werk gedoen in hierdie tesis my eie oorspronklike werk is wat nog nie voorheen gedeeltelik of volledig by enige universiteit vir ’n graad aangebied is nie.

Signature: Date:

Synopsis

Off-road working vehicles are subjected to high levels of vibration input on the rough terrain and irregular roads they work. The human operators are therefore exposed to high levels of whole body vibration (WBV) and at risk of developing health problems. A number of international standards address the matter of whole body vibration, and the European Union issued a directive which limits the exposure of workers in the EU to WBV. Unfortunately, to date there is no law in South Africa requiring compliance with any of these EU standards nor guidelines.

There are vehicles which are not fitted with suspension and/or suspension seats. The three wheeled logger used in forestry is a highly manoeuvrable and effective bulk handler, but without any form of suspension and no space under the operator's seat to install a suspension seat. However, a suspension cushion can be retrofitted to existing vehicles largely alleviating the problem.

To isolate low frequency vibration large suspension travel is required which makes an air suspension cushion attractive, as it can fully collapse. Additionally, a Helmholtz resonator if added to the cushion in the form of a pipe and tank, provides anti-resonance at a specific frequency. The resonator can be tuned by adjusting the pipe's length and diameter as well as the volume of the tank. Larger diameter pipes have less friction and give better reduction of the transmissibility curve at the anti-resonance frequency.

The SEAT value is a single number used to compare suspension seats for a specific input vibration. It is calculated from the weighted input acceleration power spectral density curve and the suspension seat transmissibility curve. The former is obtained from the vehicle and is vehicle, path and speed dependent. The latter is the only variable that can be improved by using a better suspension seat/cushion. The input power spectral density often contains significant energy at frequencies where the human operator is most sensitive. The cushion resonator could be tuned to position the anti-resonance in the transmissibility curve at these frequencies. The resultant output vibration would thus be lower than the input vibration at that frequency.

In this dissertation an analytical model describes the state variables in the cushion, pipe and tank. A Simulink model predicts the transmissibility curve with a solid mass as well as with a two degree of freedom seated human model. Initially the prototype was tested with a solid mass to compare the transmissibility curve produced by the simulation with the experimental results. It was required to evaluate the contribution of the resonator without the complexity of the human impedance. Subsequent tests were carried out with human subjects. Test results showed high inter subject similarity at the anti-resonance frequencies.

Design guidelines are formulated that can be used by the suspension cushion designer to specify the pipe diameter and length and the volume of the tank to determine the optimal transmissibility. Input psd from ISO7096 class EM3 vehicles is used as an example during the design process.

A prototype air suspension cushion was designed to reduce output vibration on the three wheeled logger. Laboratory tests with human subjects showed a significant improvement at the problematic frequencies through the tuning of the resonator. Using a Helmholtz resonator with the air suspension cushion the overall SEAT value improved by 25% compared with a 100mm foam cushion. However, the current tank and pipe need to be reduced in size for practical implementation to the vehicle.

Future work would include finding an alternative mass to replace the air in the pipe. This should reduce the size of the tank and the pipe required. Additionally the simultaneous effect of multiple resonators at different frequencies should be investigated. This is required for vehicles having an input psd with significant energy at more than one frequency band.

Opsomming

Veldwerk voertuie word onderwerp aan hoë vlakke van vibrasie as gevolg van die rowwe terrein waaroor dit beweeg. Die operateur is blootgestel aan hoë vlakke van heelliggaam vibrasie (HLV) en gevolglik die risiko van mediese ongeskiktheid. Sekere internasionale standaarde hanteer HLV en die Europese Unie het riglyne uitgereik wat werkers in die EU se blootstelling tot HLV beperk. Ongelukkig is daar tot op datum geen wet in Suid Afrika wat voldoening aan hierdie standaarde en riglyne vereis nie.

Daar bestaan sekere voertuie wat met geen suspensie stelsel of suspensie sitplek toegerus is nie. Die driewiel stomper wat in bosbou gebruik word is ’n baie effektiewe vrag hanteerder, maar het geen suspensie nie. Daar is ook geen spasie onder die operateur se sitplek om ’n suspensie sitplek te installeer nie. Die behoefte ontstaan dus vir ’n suspensie kussing wat in ’n bestaande voertuig geïnstalleer kan word.

Om lae frekwensie vibrasie te isoleer is ’n lang suspensie verplasing nodig. Dit maak die lugsuspensie kussing aantreklik omdat dit ten volle kan platvou. Die byvoeging van ’n Helmholtz resonator in die vorm van ’n pyp en tenk verskaf ook ’n anti-resonans by ’n spesifieke frekwensie. Die resonator frekwensie word verstel deur die pyplengte en pypdiameter asook die tenk volume te verander. Groter deursnee pype het minder wrywing en ’n laer transmissie kurwe by die anti-resonans frekwensie.

Die SEAT waarde is ’n enkel syfer wat gebruik word om sitplekke vir ’n spesifieke inset vibrasie te vergelyk. Dit word bereken van twee frekwensie veranderlikes naamlik die geweegde inset versnelling se drywing digtheid spektrum en die sitplek se transmissiekurwe. Die eerste veranderlike word bepaal van die voertuig en is voertuig, pad en spoed afhanklik. Die tweede veranderlike is die enigste wat verbeter kan word deur ’n beter suspensie sitplek / kussing te gebruik. Die inset drywingdigtheidspektrum het soms hoë energie by frekwensies waar die mens op sy sensitiefste is. Die kussing resonator kan verstel word tot die anti-resonator by die frekwensie lê. Die resulterende uitset vibrasie is dus laer as die inset vibrasie by daardie frekwensie.

In hierdie navorsing beskryf ’n analitiese model die toestand veranderlikes in die kussing, pyp en tenk. ’n Simulink model voorspel die transmissie kurwe met ’n soliede massa en ’n tweede vryheidsgraad mensmodel. Aanvanklik is die prototipe met ’n soliede massa getoets om die transmissie kurwe van die simulasie met die eksperimentele resultate te vergelyk. Dit was nodig om die bydrae van die resonator te beoordeel sonder die kompleksiteit van die mensmodel. Verdere toetse is met proefpersone gedoen. Resultate toon dat min verskil bestaan tussen persone by die anti-resonans frekwensies.

Ontwerp riglyne word geformuleer vir die gebruik deur ’n suspensie kussing ontwerper om die pyp deursnee, lengte en die volume van die tenk te bepaal vir die optimum transmissie. Die inset drywing digtheid spektrum van ISO7096 klas EM3 voertuie word gebruik as voorbeeld tydens die ontwerp proses.

’n Prototipe lugsuspensie kussing is ontwerp om uitset vibrasie op die driewiel stomper te verminder. Laboratoriumtoetse met proefpersone het ’n beduidende verbetering getoon by die probleem frekwensies. Die gebruik van ’n Helmholtz resonator met die lug suspensie kussing het die algehele SEAT waarde met 25% verbeter in vergelyking met ’n 100mm

dik sponskussing. Die grootte van die tenk en die pyp moet egter verklein word voor dit prakties op die voertuig aangewend kan word.

Verdere werk verlang die gebruik van ’n alternatiewe massa in die pyp om die lug te vervang. Dit sal die grootte van die pyp en tenk verklein. Die gesamentlike effek van veelvoudige resonators moet ook ondersoek word vir voertuie waar hoë energie by meer as een frekwensie op die drywingdigtheidspektrum voorkom.

Acknowledgements

Gratitude extends to JL van Niekerk for his detailed mentorship in finalising this research; DC Page, D Pienaar, N Theron, T Terblanche who all contributed through many years; EJ Hendrikse who originated my interest in human vibration; my wife M van der Merwe for her endless patience and support, and my two sons for all the times I told them I cannot come out to play ball; most importantly to my God for lending me the knowledge to create.

Table of Contents

LIST OF FIGURES

LIST OF TABLES

Glossary

acceleration	a vector quantity that specifies the rate of change of the velocity (units in meter per second per second, m/s^2)
acoustic	related to the science of sound
amplitude	the maximum value of sinusoidal quantity
endocrinology	the branch of medicine dealing with the endocrine glands and their secretions
ergonomics	scientific study of the comfort, performance and health of people in their work environments
infra sound	sound at frequency lower than the ear can perceive - subsonic
linear system	a system in which the response is proportional to the magnitude of the excitation
ISO	International organization for standardization
modulus	the modulus of a complex number is its absolute value
narrow band	vibration having frequency components only within a narrow band e.g. 1/3 octave or less
psd	power spectral density
rmq	root mean quad
rms	root mean square
SEAT	Seat effective amplitude transmissibility value. A non-dimensional measure of the efficiency of a seat isolating the body from vibration or shock. ISO 7096 (2000) refers to a SEAT factor which has the same meaning.
floor	movement of supporting base
sdof	single degree of freedom; a system will be defined as such if it requires only one co-ordinate to define its configuration completely at any instant
transmissibility	the non-dimensional ratio of the response amplitude of a system in steady state forced vibration to the excitation amplitude expressed as a function of the vibration frequency.
vdv	vibration dose value (units in $m/s^{1.75}$)
velocity	a vector quantity that specifies the rate of change of displacement (meter per second, m/s)
vibration	the variation with time of the magnitude of quantity which it descriptive of the motion or position of a mechanical system, when the magnitude is alternately larger or smaller than some average value
viscera	internal organs of the human body

1. Introduction

Whole body vibration experienced by humans has been researched for more than a century and published literature dates back to before the Second World War (Muller 1939). Human vibration is a health necessity categorised into two major fields of study: hand arm vibration and whole body vibration. Hand arm vibration is concerned with vibration induced into the hands by handheld tools and equipment. White finger disease is a common symptom of excessive exposure to hand arm vibration. Whole body vibration is induced by the vibration of the surface that supports the body. Seated operators rely on the seat suspension to protect them against floor vibration. A standing person can use his legs to isolate his body against floor vibration.

1.1. International

Early international standards organisation ISO 2631(1997) standard considered the rms of the acceleration signal measured on the seat-human interface as an indication of vibration exposure. Subsequently, following direction from BS 6841 (1987) and the later ISO 2631 (1997) standards on whole body human vibration require more focus on peak acceleration values. As late as 2004 the latest addition to theses standards addresses multiple shocks. ISO 2631 part5 (2004) addresses shock in both the horizontal and vertical directions. As expected some recent publications question the validity of this standard, which gives reason to argue that this field of research is still developing.

Currently the number of researchers around the world focusing on the subject of whole body human vibration is estimated at fewer than 100, whilst the number of operators subjected to this health risk daily in forestry, mining, agricultural and industrial sectors outnumbers that by many multiples. Health deteriorations caused by vibration are grouped with hearing loss, asbestoses and tuberculosis, where the symptoms don't appear immediately, but often months and years after the exposure. Normally the operator at that stage has changed jobs, retired, or boarded for medical reasons. It is thus difficult to prove and link that such later illness had been caused by the earlier exposure to whole body vibration.

1.2. European Union

International legislation is increasingly addressing the issue. The EU Human Vibration Directive (2002) establishes action values whereby certain protective procedures must be set in place and limit values which may never be breached. The vibration directive has action values set at 2.5 m/s^2 for hand-arm vibration and 0.5 m/s^2 for whole-body vibration with a hand-arm exposure limit value of 5 m/s^2 and a whole-body exposure limit value of 1.15 m/s^2 equivalent continuous acceleration values. These values are suggested for eight hours exposure period. The values are such that workers are afforded good protection. In addition, many companies will be forced to change their work tools or methods.

Measurements are made according to the latest ISO standards. For hand-arm vibration, it is important to note that ISO-5439-2:2002 "Mechanical vibration - Measurement of human exposure to hand-transmitted vibration - Part 2: Practical guidance for measurement at the workplace" requires that regular checks of functionality are made both before and after a sequence of measurements. For whole body vibration ISO 2631 is used with a choice of

using vdv or rms levels: (a) the daily exposure limit value standardised to an eight-hour reference period shall be 1,15 m/s^2 or, at the choice of the Member State concerned, a vibration dose value (vdv) of 21 $m/s^{1.75}$; (b) the daily exposure action value standardised to an eight hour reference period shall be 0,5 m/s^2 or, at the choice of the Member State concerned, a vibration dose value of 9,1 $m/s^{1.75}$. Many have chosen the rms levels as the vdv levels are more restrictive.

Member States are to comply with this directive since 6th July 2005. However, Member States have a maximum transitional period of five years (2010) where work equipment given to workers before 2007 does not permit the exposure limit values to be adhered to (taking into account the latest technical advances and/or the organisational measures taken). In addition, for agriculture and forestry, this deadline can be extended by up to four years (2014).

1.3. South Africa

To date the South African Buro of Standards has accepted ISO 2631 (1997) part 1 as SABS/ISO 2631. However, no other whole body vibration standards have been promulgated to protect operators in South Africa. Experts suggest South Africa follows European Union law action and limit levels for an eight hour workday. Then again, considering the implication for the employers, it may only be affordable to the bigger, more publicly responsible companies and those under enough pressure from the unions. Consequently a cost effective solution is sought to at least partially protect the operator.

The cost of vibration isolation is like the cost of sound proofing. A little money goes a long way, but to isolate for absolutely every possible floor vibration input would escalate the costs beyond viability. It is therefore important to focus a vibration isolation solution on a specific floor input. ISO 7096 (2000) divides earth moving machinery into nine different spectral classes. The vibration isolation seat designer can therefore claim that the design meets any one or more of the spectral classes according to ISO 7096 (2000). This does not guarantee that when installed in a vehicle of that class, the ISO 2631 and the law are met. Two other factors will still require consideration, the input acceleration which depends on the vehicles speed and terrain and the exposure time.

Management would, in addition to providing vibration isolating suspension, have to educate the operators and their team leaders on the allowed exposure limits. This might be considered counter productive as management would normally push for higher productivity rates. Management's duty remains to evaluate every operation in accordance with ISO 2631, and to set limits to operating tempo, vehicle speed and exposure time. Job rotation is a cost effective tool to manage exposure time.

It could be worth considering an example; in forestry trees are lumbered down, stacked in-field with a logger, transported to road side with a logger, and loaded onto the trucks with the logger. Ideal job rotation solution would be to form groups of five, all trained to operate the logger and the cutting of trees. Each would operate the logger for a fifth of the work day, and spend the rest cutting trees

As a general principle every employer is responsible for managing the whole body vibration that his operators are exposed to. Standards organisations merely suggest exposure limits and methods to assess exposure levels but do not enforce adherence thereto. Government lawmakers have the duty of ensuring that employers are obliged by

law to adhere to these standards. Needless to say, it is pointless to make a law and never police it. However, to get any government to police such laws could prove onerous, especially in developing countries where forestry and agriculture make up a large part of the GDP.

The South African Occupational Health and Safety Act (1993) does not refer directly to human vibration. However, it contains specific reference to the employer's responsibility towards occupational hazards. Additionally it is the employers duty to advise and make aware the employee of any hazards his duties may entail. Whole body vibration isolation under adverse conditions is therefore the undisputed responsibility of the employer.

Another driving mechanism is unions expecting the employer to provide equipment that is compliant with the law. Arguing for the employer is cost and availability of equipment that meet the standards. In South African a successful local manufacturer of forestry and mining equipment still markets a three-wheeled logger vehicle with no consideration of protecting the operator against whole body vibration. To aggravate the problem, these vehicles are still acquired and operated by the government and forestry companies.

In 1992 the author was part of a team of ergonomists consulted by three manufacturers of three-wheeled logger vehicles to evaluate vibration exposure. The outcome of the study indicated that none of the three-wheeled loggers were suitable to be operated by a human for any economical length of time. The vertical vibration induced by the vehicle to the operator exceeded the limits of BS 6841 and ISO 2631 at the time.

Years later the "Airseat" concept originated during a noise survey at a South African brewery company where the author was approached to improve the seat suspension on the forklift trucks that allegedly caused health problems in its drivers. The drivers made their own effort to reduce the shock and vibration with pieces of mattress foam and pillows on top of the seat bases fitted in the forklifts. For the design various suspension seat systems were considered, however the amount of height available for the seat base to fit into was merely 150mm. None of the commercially available suspension seats would meet this criterion. Investigation showed that the workers would almost be satisfied with anything that makes them feel better. This led to the manufacturing and testing of an air bubble plastic cushion called AIRSEAT. After installation tests showed that the AIRSEAT did reduce the shock, but less than what the piece of mattress foam did. The AIRSEAT bubble plastic concept was scrapped

Although the AIRSEAT did not actually isolate the vibration, it surely put management in favour with the drivers as it seemed that they were actually recognising the problem and was doing something about it. This led the author to investigate the AIRSEAT as a vibration isolator. The challenge in the three-wheeled logger also remained unsolved. This gave focus to this research. The topic was defined: "a seat suspension cushion solution".

1.4. The three wheeled logger vehicle

Due to the lack of suspension the divers of these vehicles are subjected to excessively high levels of vibration. The only suspension is the tyres, and no seat suspension is provided. The rear castor wheel is also out of sight of the driver and is often driven over tree stumps that generate high levels of shock. Figure 1 shows the three-wheeled logger during an in-field operation. Normally these machines are used to move logs from where they were felled to the roadside for pickup by transportation trucks. These operations are often

amongst tree stumps, and when driven over, induce high acceleration levels into the operator. The second picture was captured from a video where the operator clearly compensates for the low frequency oscillation by moving his upper body forward and backward. The picture shows the upper body at the forward limit of the oscillation.

Figure 1 :- Three-wheeled loggers used in forestry

This research considers a possible solution which can be retrofitted cost effectively to existing vehicles. A recognised research procedure is followed starting with the formal definition of the problem.

1.5. Problem statement

Five challenges define the problem statement of this research. 1) the solution should fit into the vehicle; 2) it should not restrict the operational ergonomics; 3) provide lateral support of the seated operator's body; 4) solution must be affordable; 5) it should reduce the vibration

The vibration isolation solution should fit in:

Retrofitting a solution into any vehicle should change as little as possible of the original vehicle. Ideally the solution should just bolt onto the existing. However, in certain cases a small part of the existing seat may be removed to increase the efficacy of the retrofit.

Low frequency floor vibration is characterised by large cyclic displacement. Suspension systems capable of isolating such vibration require large travel. The vibration isolation solution would therefore require distance between the seat base and the buttock interface. Consider the limited space in the three-wheeled logger in Figure 9. Also note other volumetric space around the operator. If the existing seat base is removed, a suspension cushion of 100mm thick can be fitted. No space is available for a conventional suspension seat.

The solution should not restrict the operational ergonomics:

Mechanical suspension seats could employ a soft metal spring to achieve a single degree of freedom natural frequency (f_n) of below 2Hz. If a subject with a seated mass of 65kg would sit on such a seat the spring stiffness coefficient k can be calculated from:

$$f_n = \frac{1}{2\pi}\sqrt{\frac{k}{m}} \qquad (1)$$

At k equal 20.55kN/m and the operator pushing down on a pedal with one foot with a force of 200N, the seat would rise 20mm. If he would push down harder in event of an emergency stop, the seat could rise as far as 60mm. A stiff suspension cushion with less vertical travel would therefore be preferred.

Hand, arm, leg and head movements should not be restricted by the system. Vision should not be impaired, and no additional heat and sweat build-up would be acceptable if caused by a seat cushion. The operator interface would have to 'feel' normal with no additional attachments to the operator's body.

Importantly the pressure distribution at the buttock interface that supports the operator's body should be considered. Ischial tuberosities, shown in Figure 2, mainly support 75% of the seated human body mass. The other 25% is by the legs, and greater buttock area. A pressurized air filled cushion would evenly distribute the force supporting the body over the interface area. This would not 'feel' normal and could result in blood flow restriction due to higher pressure under the thighs. The cushion would require a hard interface that provides 75% of the support to the operator's body under the ischial tuberosities and the balance to the other areas.

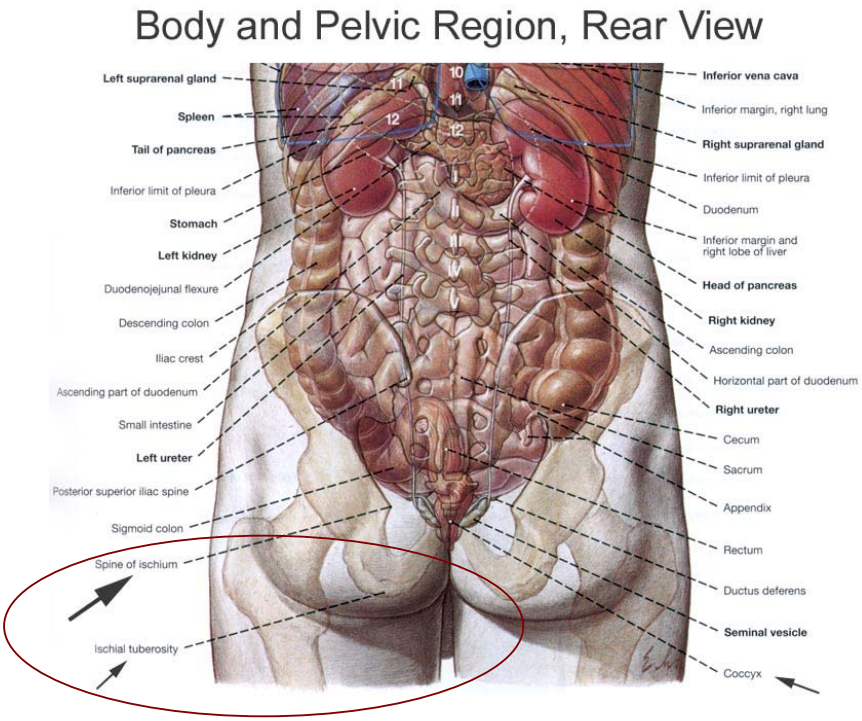

Figure 2 :- The human body to illustrate the position of the ischial tuberosities

Lateral support of the seated operator's body

The main purpose of a suspension cushion is to isolate vibration in the vertical (z-axis) direction. The other five degrees of freedom of body motion; lateral (y-axis), fore-aft vibration (x-axis), roll (around the x-axis), pitch (around the y-axis) and yaw (around the z-axis) have to be considered in the cushion design. With feet on the floor using the backrest, the operator can resist fore-aft, pitch and yaw movements. More difficult is to resist roll and lateral movement as the upper body has little side support. The operator has to hang onto hand controls and press against arm supports fixed to the chair base, which oscillates out of phase with his upper body.

The solution must be affordable

Affordability would motivate a manufacturer to design a vehicle which meets safety standards. However if the buyer does not care whether safety standards are met, and is more attracted by low capital cost, the motivation for designing safety into vehicles is lost. The increase of costs in passenger and commercial vehicles is often frowned upon by those ignoring all the additional safety features inherent to modern vehicles.

How much would the forestry department of the South African government be willing to spend on upgrading a single three-wheeled logger to comply with the vibration standards suggested by the SABS/ISO 2631? A solution that often finds its way to such a government decision maker is to contract the job out, and thus the responsibility of protecting his employees. The smaller contractor could even hire the equipment 'as is' from the department and take the responsibility for the maintenance.

An affordable solution may motivate the management to take the responsible step and retrofit the vehicles. Suspension seats could cost in excess of R3000, but cannot be retrofitted into the logger due to height restriction. A suspension cushion could be marketed at R2000, but will have to guarantee adherence to SABS/ISO 2631. If the cost of research to design a suspension cushion for one vehicle only is considered, many multiples will have to sell to break even.

If a generic solution exists, which with small modifications can be applied to more than one vehicle, it may become viable. Ideally the off the shelf cost of a generic cushion solution should not exceed R2000 and include certification to at least one spectral class according to ISO 7096:1999.

The solution must isolate the vibration

Vibration isolation versus cost closely follows Pareto's 20-80 principle. Twenty percent of the cost will isolate 80% of the vibration, but it will cost the other 80% to isolate the rest. It is accepted that all vibration can not be isolated; however, it is possible to reduce vibration in the critical frequencies where the human is most sensitive. In Figure 3 the ISO 2631 (1997) W_k weighting filter to show at which frequencies the human body is the most sensitive to vertical whole body vibration.

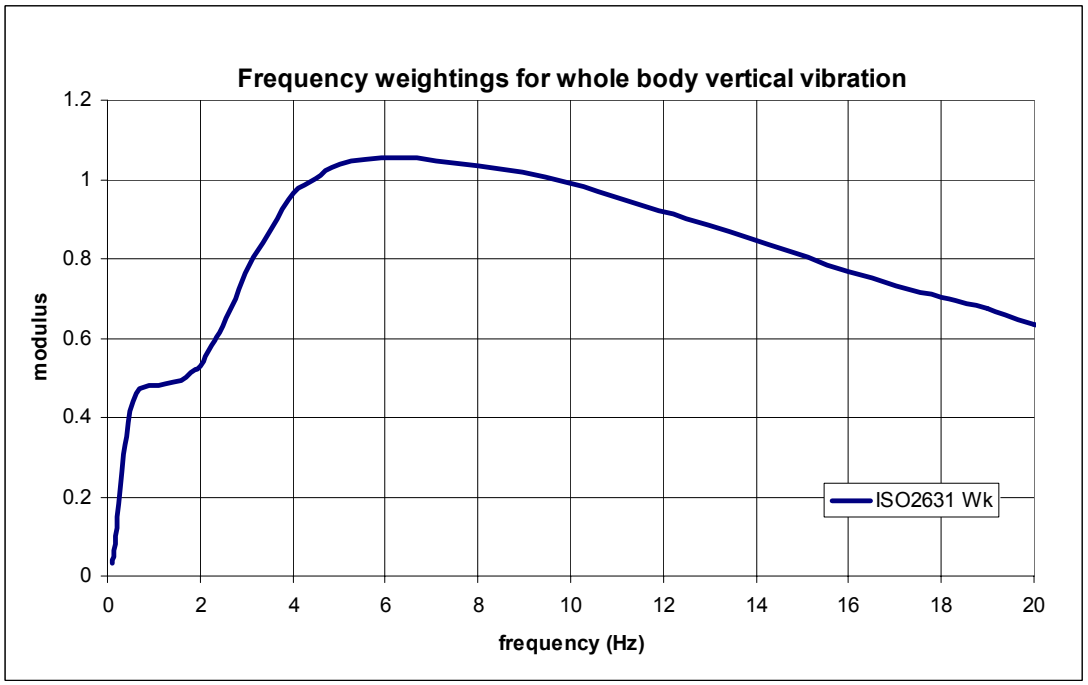

Figure 3 :- ISO 2631 (1997) – W_k filter for vertical whole body vibration (z-axis)

Between 0 and 1.6Hz, the body experiences less than 50% of the induced floor vibration. However, between 4.4 and 9.5Hz the body's vibration experience is more than 100% of the induced value. The latter range is where the vibration isolation is sought. Ideally, the vibration-isolating cushion should act as a band stop filter between 4Hz and 10Hz.

1.6. Helmholtz resonator

A band stop filter technique applied in this study is that of the Helmholtz resonator. Similar to the resonator used in exhaust systems to reduce acoustic resonance at certain frequencies, the acoustic pressure between 4 and 10Hz is reduced in the cushion. The Helmholtz resonator is tuned to act as a band stop filter at frequency f_h by changing its dimensions according to the following formula:

$$f_h = \frac{c}{2\pi}\sqrt{\frac{A}{LV}} \qquad (2)$$

Where: c = speed of sound; A=Area of the pipe; L=length of the pipe;

V=volume of the drum or tank

The Helmholtz resonator works like a vibration absorber without damping. Air in the pipe between the cushion and a secondary chamber (tank) acts as the secondary mass. At resonance, the air oscillates out of phase with the floor force and reduces the oscillation at the buttock interface.

The disadvantage is that a second resonance peak at a higher frequency is generated. If the anti-resonance system is designed correctly, the second resonance peak exists at a frequency where the human body is again less sensitive. The summed gain therefore improves the cushion's vibration isolation capabilities. Ideally, the suspension cushion

would act as a non-linear system, which is firm during small floor displacements of the seat base and soft during high peak acceleration. Additionally a mechanism that would stiffen the spring when no floor acceleration of the seat base occurs would reduce the transmissibility curve amplitude at the systems natural frequency.

1.7. This dissertation

In chapter 3 several concepts were evaluated using an objective selection process. The major challenge was to maintain stability of the cushion at a stiffness low enough to isolate vibration at low frequencies. Chapter 4 analyses the physics of the phenomena and suggests a simulation model which approximates the transmissibility curve. Power spectral density data measured in-field on a three-wheeled logger vehicle was used to choose pipe and tank configuration that would minimise the SEAT value of a cushion. Chapter 5 provides details on the experimentation carried out on the chosen cushion. This is concluded in chapter 6. Due to the variable nature of floor vibration under vehicle seats no attempt was made to design a generic air suspension cushion, but rather to propose a procedure which the designer should follow. Chapter 7 guides the designer through a step-by-step design process. The ideal route would be for the designer to measure floor spectra of an operating vehicle. If however for some reason this cannot be done, specification such as ISO7096:2000 for earth moving vehicles could be used as guidelines of the floor character against which the cushion should protect the human operator. Chapter 8 concludes this document with some recommendations.

2. Literature study

Whole body human vibration in off road vehicles was first studied in Germany before the Second World War in publications by Muller (1939), Coermann (1940) and Von Bekesy (1939). Mainly medical symptoms originated these first studies. At the time military personnel endurance and efficiency were the primary fields of study. Various characteristics were found to influence the magnitude of the effect of whole body vibration. Later studies in the military field included helicopter rotor isolation systems and vibration in aerospace. Others studied vibration in tracked and wheeled vehicles. It was found that the problem was not only with combat vehicles, but also with passenger vehicles that deliver infantry to the front line in a fighting fit condition.

Today forestry, mining, and agriculture are the main commercial fields where off road vehicles are driven on a daily basis for long hours (Village & Morrison, 1989; Van Niekerk et al, 2000; Paddan and Griffin, 2002). Sophisticated air suspension for seats and cabs are designed into many modern vehicles. Unfortunately many older and lower budget vehicles in use are not fitted with vibration isolation seats. These vehicles require retrofit suspension seats and cushions to abide by the new vibration standards and laws.

The effects of vibration will fall broadly into either of two categories. The first are those responses which are attributable directly to the differential vibratory movement or deformation of the organs or tissues of the body. The second category of reaction to vibration contains generalised responses to the stress acting non-specifically. Guignard (1965) was first to formally address the following topics:

- Cardiopulmonary responses - Strong vibration can cause hyperventilation at frequencies between 1 and 10Hz. Arterial carbon dioxide partial pressures can fall to below 25mmHg after only two minutes' exposure to 1g z-axis vibration at 9.5Hz.
- Cardiovascular and electrocardiogram - During whole body vibration of man at infrasonic frequencies, increases in the heart rate are commonly observed, however not correlated with changes in arterial blood pressure.
- Metabolic and endocrinological - Various changes in the cellular and biochemical composition of the blood and urine have been observed in response to low frequency vibration, which in general appear to reflect the body's reaction to stress acting non-specifically.
- The central nervous system - Sensory mechanisms, the cutaneous vibration sense, deeper somatic vibration receptors, vestibular apparatus all feed information to the central nervous systems which in turn is aroused in various ways. Low-frequency steady state oscillation can be soporific in man. In man, habituation occurs, as it does with noise if the stimulus is unchanging, even when the precocity is complex. One can quite quickly cease to notice the vibration and noise aboard an aircraft. Non-stationary vibration on the other hand is likely to oppose habituation and to increase arousal.
- The electroencephalogram (EEG) during vibration - The electrical activity of the brain can be observed during vibration using surface electrodes. He speculated that the human EEG can be "driven" by low – frequency vibration.

- Severe acute vibration exposure - Whole body vibration exposures of 5 to 10g in range 10 to 25Hz can provoke thoracic pain resembling angina pectoris. This is due to mechanical deformation receptors in the chest wall. Gastro-intestinal bleeding has also been observed after severe exposures. Regular provocation of haematuria was observed in when a subject that had renal calculus was exposed to high levels vibration at 30Hz.

More recently Griffin (1990) summarized from several references that various responses are due to whole body vibration such as cardiovascular, respiratory, endocrine and metabolic, motor processes, sensory processes, central nervous system, and skeletal.

The successful treatments of ailments with vibration exercise programs were investigated by Rittweger et al (1999). They claim vibration exercise (VE) is a type of exercise that has recently been developed for the prevention and treatment of osteoporosis. It elicits neuromuscular training reflectorily, without much effort and in short periods.

Griffin (1990) suggests both simple and complex activities can be disturbed by vibration i.e. the inputs (vision) and outputs (hand control). Three stressors are common: interference with comfort; interference with activities; interference with health. The frequencies most often associated with effects of whole-body vibration on health, activities and comfort are approximately 0.5 to 100Hz. At frequencies below 0.5Hz the principal effect of oscillation is a type of motion sickness. A series of "comfort" contours are published. This is similar to those that BS 6841 is based on.

Van der Merwe (1989) studied the combined effect of noise and vibration on task performance. An increase in weighted vibration affected tracking task performance. Higher noise levels had a negative influence on reaction times at low vibration levels, but had a subtractive effect at higher vibration levels.

Nishiyama et al (2000) showed the vibration magnitude ratios for seven body parts relative to a vertically induced vibration signal. From his graphs it is interesting that the first mode (4Hz) of the human body is significantly the same measured on the head, chest, upper arm and hip. However at the hip, a second mode (above 6Hz) is apparent. This second mode is the most significant for the measurements on the thigh and shin. The second peak often seen on the magnitude graphs is therefore due to the vibrating mass of the leg. In this case the feet were vibrated with the base of the seat and the steering wheel. They also studied different angles of the arm (and leg), from 90^0 to 180^0, without influence on the frequency of first mode of the body trunk, however with a significant influence on the natural frequency of the vibration of the legs.

Guignard (1965) defined the first group of physiological effects of vibration on the body that are attributable directly to the differential vibratory movement or the deformation of the organs or tissues of the body. Such responses are in the main frequency dependent and can be related to the body resonance phenomena described earlier. Steady state low frequency vibration such as rocking motion can create pleasant and relaxing feeling. Non-stationary vibration with respect to frequency and/or magnitude will normally increase the arousal level. Motion sickness occurs even at levels of low vibration magnitude, and is mainly due to frequency content of the motion. Nashash et al (1996) reported the effect vibration has on the elevation and depression of the heart's ST segment which indicates heart muscle fatigue. The maximum effect was found to be at 8Hz, which is thought to be around the resonance frequency of the heart. The frequency content of vibration of low

magnitude (near the threshold of perception) has little effect on the psychological state. However at higher magnitude, the frequency plays an increasingly significant roll.

Guignard (1965) defined a second group of physiological effects of vibration on the human body related to the stress that acts non-specifically. Contrary to the first (discussed earlier), it is less frequency dependent, but more intensity dependent and to the exposure marked with it. At low frequencies (3-4Hz) and high intensities (>0.5g) of vibration several occurrences of hyperventilation have been recorded. The occurrence is normally well below that of any mechanical resonance of the respiratory system. It is reasoned that it is due to Pavlovian response to a strong environmental influence. Others suggested it is a response due to the stimulation of the labyrinth. Increases in the heart rate are often observed due to vibration stimulation. Research has no specific correlation between vibration magnitude and exact heart rate increase. Arterial blood pressure increase is also not correlated with vibration magnitude. Many receptors in the body will pick up the vibratory sensation and transfer the condition to the brain. Guignard (1965) mentions cutaneous receptors, mechanoreceptors and vestibular apparatus. The most sensitive mechanoreceptors are muscles, tendons, viscera and their suspensionary attachments.

Griffin (1990) stated that the magnitudes of general interest are within the $0.01 m/s^2$ and $10 m/s^2$ (peak) range. He noted:

- Below $0.01 m/s^2$ will rarely be felt
- Below 1Hz and above 20Hz higher magnitudes are required for perception

Whole body vibration of $10 m/s^2$ rms may be reasonably assumed to be hazardous. Some hazard may be associated with vibration of about $1 m/s^2$ depending on duration, direction and frequency. Road vehicles may encounter 0.2 to$1.0 m/s^2$ rms.

The rms (root-mean-square) measurements are primarily restricted to the assessment of motion, which are continuous, statistically stationary and do not contain shocks. Acceleration must be frequency weighed before determining the rmq (root-mean-quad) or vdv (vibration dose value). The rmq value is intended for the comparison of motions, which contain high peak values, but can be quantified over fixed period of time. Vdv is a robust method of assessing the severity of all motions (deterministic or random, stationary or non-stationary, transient or shock), which are above the threshold of perception and fall within the frequency range of the analysis method.

When driving over a rough road, most subjects would agree that any reduction in the number of potholes would improve the ride. It is likely that any adverse effect on comfort, activities or health will be reduced if a high magnitude of vibration occurs less often. The simplest time dependency in current use, involves a "fourth power" relationship between acceleration, “a”, and exposure time, “t”, (i.e. a^4t = constant).

After Griffin and Whitham (1977) failed to find any substantial evidence of a time constant, they proposed the rmq. The idea of time constant was suggested by Miwa (1968). He concluded that discomfort increased with increasing duration up to a limit and suggested that beyond 2 seconds for vibration in 2-60Hz, and beyond 0.8 seconds for vibration in 60 - 200Hz, there may be no further increases in sensation.

Very early Mallock (1902) reported on how vibration due to the London underground affects the residential properties under which it passes. Often irritation is caused by vibration levels not much above the lower threshold level. A private motor car is expected

to have much lower vibration levels than public transport and the owner will probably be alarmed when the levels reach that of the public transport.

Kitazaki and Griffin (1998) reported 8 modes of spinal vibration with resonance frequencies from 1.1Hz to 9.3Hz. Sitting in a 'normal' posture the principal resonance at 4.9Hz did not seem to contain any deformation of the lumbar spine. The fifth mode resonated at 5.6Hz and contained a bending of the lumbar and lower thoriac spine and was located close to the principle mode. It seems likely that the greatest stress and potential damage to the back will arise from bending deformation of the spine such as contained in the fifth mode. Principle resonances for other postures were 5.2Hz in the erect and 4Hz in the slouched.

2.1. Research on vehicles

Paddan and Griffin (2002) evaluated 100 vehicles for vibration exposure levels. They found that on average a dumper, helicopter and excavator vehicles reach the ISO recommended levels before a full work shift can be worked. In descending order of severity the following were amongst the vehicles tested: dumper, helicopter, excavator, armoured vehicle, milk float, lift truck, tractor and mower. The most severe accelerations were measured in the dumper at 1.28m/s^2 (vdv_{1min} of 4.99m/s$^{1.75}$), helicopter at 1.08m/s^2 (vdv_{1min} of 4.21m/s$^{1.75}$), and in the excavator at 0.91m/s^2 (vdv_{1min} of 3.55m/s$^{1.75}$).

Research in the mining environment - Village & Morrison (1989) concluded that in load haul mining vehicles excessive vibration levels were recorded during driving full and empty. Space limitations in the cab prevented the use of hydraulic suspension seats. A solution would be to either reduce the level of vibration acceleration across all frequency bands, or shift the dominant frequency band to one at which the human body is less sensitive.

The South African mining industry is still on of the largest contributors to the country's gross domestic product. However few health and safety studies have been done on human vibration in this industry. One comprehensive study by Van Niekerk et al (2000) was carried out on 70 different machines at 15 different mines and workshops. Data was obtained for at least 24 different types of equipment and machines. It was primarily earth moving equipment such as haul trucks, bulldozers, front-end loaders and shovels, which measured the highest levels of vibration for the whole body. The major conclusion from this study was that the measured vibration levels are sufficiently high to create an enhanced level of risk of vibration-induced disorders in a significant proportion of operators.

Independent tests were carried out in the forestry environment as part of this research. Results showed that vdv values of 15 were exceeded for a 4 hour work shift. The report in the appendices of this document shows that the vdv on the seat is normally higher than the vdv below the seat. This is a common problem found in most vehicles tested in rough off-road conditions. The operator would be at lower risk if seated on the hard floor than on his seat.

Figure 4 :– Three-wheeled logger tractor in a forestry operation

Schomer and Neathammer (1987) studied the role of helicopter noise induced vibration in human response. Narrowband vibration occurred due to rotor frequency. It was mentioned that a narrowband vibration isolator is required to reduce the exposure level. Jones (1975) investigated the qualities of an anti-vibration seat suspension system in a helicopter. The system worked on a single frequency anti-resonance principle, and was considered a feasible concept for achieving a substantial reduction in vertical vibration load. The weight of the system increased that of the helicopter by 1.5%.

2.2. Measurement of whole body vibration

Three axes of vibration are defined to act upon the human body namely vertical z-axis, backward forward x-axis and sideways y-axis. Three additional degrees of freedom are defined as roll around the x-axis, pitch around the y-axis and yaw around the Z-axis. The z-axis vibration is considered the most critical. A further refinement is to focus only on the seated human body with backrest, which is typical of the driver position in the logger tractor. As an introduction guideline Safetyline Institute (2006) maintains quick reference guidelines on the methods to measure whole body vibration.

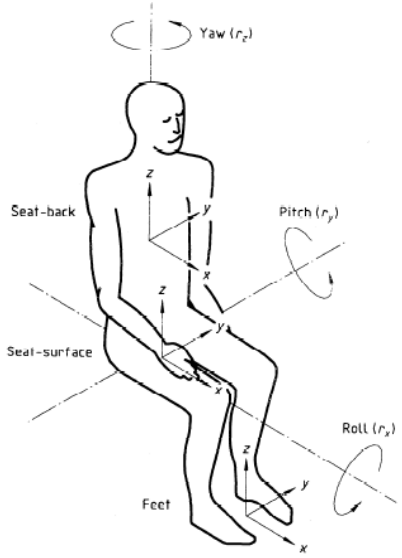

Figure 5 :- Axes of vibration for the seated human body ISO 2631:1 (1997)

The ISO 2631 part 1 (1997) is the latest standard to follow for measuring whole body vibration. A W_k filter is suggested for vertical vibration and a W_D filter for the two horizontal directions. Motion sickness is considered using a W_f filter in the vertical axis only. In this research we are only concerned with the vertical (z-axis) and will therefore use the W_k filter in Figure 6.

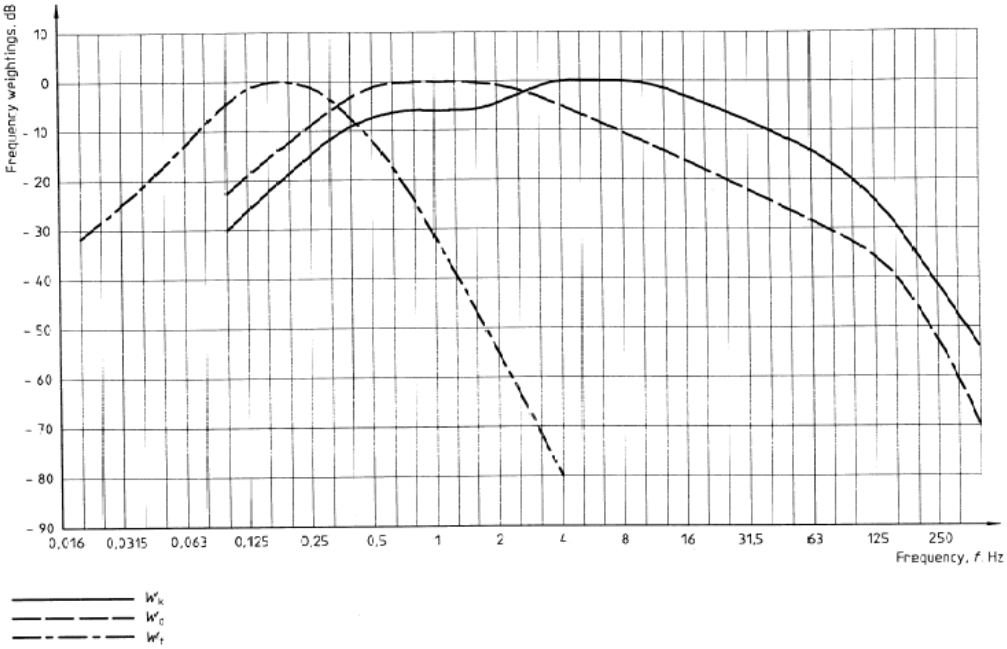

Figure 6 :- ISO 2631–1(1997) :- Frequency weighting curves

The newer ISO 2631-5:2004 Mechanical vibration and shock -- Evaluation of human exposure to whole-body vibration -- Part 5: Method for evaluation of vibration containing multiple shocks addresses specific mechanical shock in the horizontal and vertical direction. A linear single degree of freedom (SDOF) is used to determine horizontal acceleration dose. For vertical vibration a non-linear model is used. Measured acceleration is analysed in the time domain and a single figure is obtained by raising to the power of six before summing and taking the sixth root. The resultant dose is a quantification in pressure (MPa) and compared with action and limit levels.

ISO 7096 (2000) set the standard of input vibration towards that seat designers should work. As seen from the SEAT calculation, the power spectral density (psd) of the floor input signal $G_{ff}(f)$ is paramount in determining the vibration isolation qualities of a seat. This standard sets down the $G_{ff}(f)$ for several groups of vehicles. Conformance of a generic suspension seat to meet ISO2361 on a class 6 vehicle can typically be claimed by a manufacturer. The designer can use the EM curves in the laboratory to determine the ideal transmissibility curve for a new cushion. More details on ISO 7096 are in section 5.1.2.

2.3. Human modelling

Body resonance can be defined as the condition in which a forcing vibration is applied to the living body at such a frequency that some anatomical structure, part or

organ is excited into measurable or subjectively noticeable oscillation of greater amplitude than that of the related structures according to Guignard (1965).

The dynamic human body can be modelled as a system, containing several principle masses, the passive motion of which is controlled by elastic elements with varying degrees of stiffness and damping. Many models of the human body have been proposed in the literature, from simple one degree of freedom spring mass models to complex multidimensional models. Here we will focus on seated models that will suite the purpose of this study, i.e. a model with which basic suspension seat dynamics can be evaluated in the z-axis. By definition for the human body, the z-axis is vertical, x-axis fore-aft and the y-axis left right.

Before the Second World War, German research found, that when the body is excited in the spinal (z) axis, there is a dominant response at the frequencies 4 to 6Hz. Von Bekesy (1939) at the time suggested that below 3Hz the body moves as a single mass without internal resonances. Coermann (1962) showed that above 15Hz no major resonances occur. At 100Hz only 5% of vertical force induced into the seated body reaches the head. In the years following the methods of mechanical impedance and transmissibility were more commonly used to study the human dynamic model.

Guignard (1965) described the first two modes of the human body resonance in the z-axis is 5Hz and 12Hz. The 5Hz being due to the upper torso and shoulder girdle; much the same as the Germans found earlier. Damping ratio is at 0.3 to 0.4. Coermann (1962) described the thoraco-abdominal viscera having a resonant frequency of 4Hz. It also plays a major roll in damping low-frequency vibration, and therefore the main system that limits the human body tolerance of vibration. The second mode is mainly controlled by the elastic properties of the spinal column and its supporting musculature. The relaxed legs of the seated operator have little effect on response to the 5Hz and 12Hz modes.

An erect body posture influences the resonant mode differently to that of a slumped mode. The bodies of passengers transported in an infantry troop carrier will be slumped rather than be erect after a long journey. This is due to the bodies' natural ability to protect itself by minimising vibration of the vital parts like the lungs, hart and brain. Mansfield and Griffin (2002) proved that this kyphotic posture improves the damping in the biodynamic system.

Fairley and Griffin (1989) reported that the apparent mass resonance frequency for 65 subjects is on average 5Hz using a static footplate. Under real conditions a vehicle's footplate moves with the cushion input with lower magnitude at resonance than the cushion output (cushion/buttock interface). Above cushion resonance, the footplate and cushion output is also out of phase. Literature does not state whether this footplate condition actually helps with reduction in vibration energy transferred to the upper body. The previously mentioned kyphotic posture could work as a see-saw effect between the footplate and cushion oscillations to reduce the effect of input vibration. Again literature and international standards only address vibration output of the seat cushion and not the effect of the vibration input through the legs.

Qassem et al (1993) developed a complex human model with 12 degrees of freedom to investigate the natural response of the 100kg human body. He applied specific

mass to each part of the human body, however if considered that the body consists of infinite parts, each oscillating at its own frequency due to its mass, stiffness and damping, this approach is not an ideal model. More correctly would be to do reverse engineering on the apparent mass as seen on the cushion/buttock interface for a given degree of freedom human model. The degrees of freedom would be determined by the accuracy of the experimental data required as well as inter- and intra subject variability. Seating posture as well as whether the footrest moves with the seat/buttock interface is important to note. A footplate that moves with the seat buttock interface is not common in vehicles though.

Rakheja et al (1994) modelled one and two degree of freedom approaches of the human body on a suspension seat with cushion (two degree of freedom model). They compared an air spring with a mechanical spring and recorded all the stiffness and damping characteristics of the systems. They found that the three and four DOF models had the same acceleration transmissibility characteristics below 5.5Hz. Above 6Hz secondary resonances of the upper and lower body dynamics showed considerable differences between the models. The non-linear suspension seat models responded well to the 12.5mm, 25mm and 37.5mm peak to peak sinusoidal inputs.

Boileau et al (1997) compared 12 biomechanical models with respect to difference between driving point impedance and seat to head transmissibility resonant frequencies. The models by Patil, Payne and Mertens had the lowest difference in resonant frequency. Synthesised data, from several earlier publications, magnitudes were also compared, where models by Fairley and Griffin, Mertens, Suggs, were found to reflect the experimentally measured results the best. Interestingly, the ISO CD 5982 did not do well in either comparison. The model by Mertens (1978) was noted to be second best in both the frequency and magnitude, therefore possibly the best choice of model.

Wei & Griffin (1998a) suggested that a two degree of freedom model provides adequate parameters to represent the human body mathematical model to assess suspension seats. In their article they published a table of spring constants, masses, and damping coefficients to represent a range of body weights from 40 to 90 kilogram. Wei & Griffin (2000) have subsequently employed this model to evaluate the effect of subject weight on predictions of seat foam cushion transmissibility.

Boileau & Rakheja (1998) described the method of human model development in detail to evaluate seat characteristics. They used a three degree of freedom model based on 73.6% of the bodyweight supported by the seat. They compared seat to head transmissibility with mechanical driving point impedance to qualify their model and concluded that the latter method was the more accurate for use in model predictions.

Cho and Yoon (2001) tested a 9 degree of freedom model with 3 masses, each with its moment of inertia, against 10 subjects. They compared their model with 1DOF, 2DOF and 3 DOF models in the z-axis and x-axis by evaluating the transmissibility from buttock-cushion contact to the head. Interestingly, the 3 masses used for the 9 DOF model were exactly the same as for the 3DOF model. It is therefore apparent that the rotational inertia of the various parts of the human body does influence the transmissibility to the head. They ignored the foot support as they claimed it

transfers vibration into the body only partially. A backrest support was used at an inclination of 21 degrees rearward from vertical.

Boileau et al (2002) in their model pointed out that the higher the mass of the seated subject, the lower the resonant frequency of the apparent mass. He used a 4 mass model and distinguished the mass ranges <60, 60.5-70, 70.5-80, >80. Rakheja et al (2002) describe the indirect linear relationship between the frequency increase and mass decrease. They also fitted a linear relationship between the increasing body mass and the increasing peak magnitude at resonance.

Rosen & Arcan (2003) based a three dimensional model on specific experimental results obtained in the literature. They investigated the influences of backrest, footrest height, and vibration magnitude and muscle tension on the apparent mass curve at the seat buttock interface. They continued to investigate the influence of different cushion materials on the vertical contact stress distribution for different frequencies. They found that the first mode of the human body was at 4.25Hz with a normalised apparent mass modulus factor of 1.5 with respect to the static mass. The 1.5 factor was evenly distributed over the seat / buttock contact area.

Belytschko and Privitzer (1979) found that the 5Hz resonance is due to three factors: seat body mode; flexural response of spine; axial response of viscera. Griffin (1990 p.383) stated the 5Hz resonance is not due to axial resonance of the spine. Axial resonance of the spine is at 20Hz. 5Hz is possibly from spinal bending. He made five assumptions when using the single degree of freedom spring mass system to model the seated human body:

- There is only one important resonance frequency in the body
- The response of the body is virtually independent of frequency below half the resonant frequency
- The response of the body decreases below its low-frequency response at frequencies in excess of 1.4 times the resonant frequency
- At high frequencies the response tends to decrease at 12dB per octave
- The relevant body response occurs in single axis i.e. vertical compression of spine with no bending - which is a contradiction with the findings of Belytschko et al (1976)

Using the formula for damping ratio below, Vogt et al (1968) showed a good fit to a single degree of freedom model with a natural frequency (f_n) of 5.2Hz and damping ratio of 0.58.

$$\zeta = \frac{c}{c_c} = \frac{c}{2mf_n}$$

$$c_c = 2\sqrt{mk} = mf_n$$

where c is the linear viscous damping coefficient

c_c is the critical linear viscous damping coefficient

m = mass of upper torso

k = spring stiffness of the spine

Note that variable c in the above formula is different from c elsewhere in this document.

Fairley and Griffin (1989a) showed natural frequency of 5.0Hz and damping ratio of 0.475. Griffin (1990 p.384) states that when seated on a rigid flat surface with no backrest, vertical vibration of the seat causes vibration in all six axes of the head. The greatest head motions occur in the x-axis between 5 and 10Hz in the z-axis up to 20Hz and in the pitch axis around 5Hz. This ties up with Belytschko et al (1976). Griffin (1990) states that when the impedance is non-linear: increases in vibration magnitude produce a decrease in resonance frequency.

2.4. Seat suspension

Mansfield & Griffin (2002) showed in a study that for all postures of the human body, the natural frequency of the apparent mass decreases with an increase in vibration magnitude. The magnitude at resonance was statistically similar for all input magnitudes. Fairley (1990) stated that the response of a suspension seat is largely dominated by the mass, not by the stiffness or the damping of the subject on the seat. The normalised apparent mass of the body, which does not include the mass of the subject, therefore has little effect on the predicted transmissibility of a suspension seat. Transmissibility is measured as the ratio between the amplitudes of vibration measured at some point on the body and another point such as the seat. Resonances of the human body are seen as absolute maxima in the graphs of impedance or transmissibility plotted as a function of frequency.

Qassem (1996) tested a complex human model on three cushions with known mass, stiffness and damping characteristics. He concluded that a heavier human sitting on a cushion with lower stiffness will have a lower vertical resonance frequency. He based his research on cushion design by Patil et al (1980). His research addressed a human model with 8 degrees of freedom which separated the various body elements. Typically the resonance frequency for the head varied between 2.4 and 4.8Hz when seated on 15kg cushion with stiffness of 2550 kgf/m and damping 37.8 kgfs/m.

Wan and Schimmels (1997) designed a theoretically optimal cushion that would render the best results according to international suspension seat evaluation standards. They evaluated their 4 DOF human model on a modified ISO 7096 standard as well as the Corbridge and Griffin (1986) standard using white noise as an input. Combining the characteristics of the seat and cushion, they recommend lower bound stiffness of 1666 N/m and damping of 327.34 Ns/m and upper bound stiffness of 6666 Nm^{-1} and damping of 1555 Ns/m. Mass of seat and cushion is 12kg.

Amirouche et al (1994) computed the optimal stiffness and damping coefficients at cushion/body contact to be 10000Nm^{-1} and 100Ns/m. Demic (1991) showed that non-linear programming can be used to optimise cushion dynamics. Wu et al (1999) found that on softer cushions the pressure area of the human-seat interface changes during vertical vibration. They found that harder cushions have a smaller distribution area and softer cushions a larger area, with respective inverse proportional pressure. They suggested that a linear pressure model at the interface is not accurate due to a change of contact area during acceleration and deceleration.

Patten & Pang (1998) suggested that a low-order, lumped parameter model is used to predict the characteristics of an open cell foam cushion. Their study combined this model with the ISO human model which evaluated well in an experimental study with a human subject. An increase in the subject weight and change on the input vibration signal gave results similar to that predicted by the model. Through reverse engineering and curve fitting they obtained the published stiffness and damping coefficients for sports and luxury cars.

2.5. Air suspension seats

The literature has many examples of air suspension seat designs. Several manufacturers have patents to their design which can be purchased commercially. Isringhausen, Zhangjiagang Youbang, Northen Tool, Caterpillar, Cobo, Knoedler, Sears Seating, Bostrom Seating, Wise, Seats Inc, Industrial Seats and National Seating are to name a few.

Fairley (1990) described the measurement of the characteristics of an air suspension seat loaded with a mass or a human body. Gouw et al (1990) evaluated various suspension types used for off-road vehicles. In their model the influence on the transmissibility of each parameter was separately evaluated. Hosten (2004) suggested that air suspension seat has higher efficiency than mechanical links in damping vibration. However, Kornhauser (1994) insisted that the air spring can best be described by an anelastic model consisting of isothermal and adiabatic springs in parallel. Some manufacturers of air suspension systems have investigated adding an auxiliary reservoir to the air suspension chamber. One system is commercially available from Firestone.

The commercial tendency is towards air suspension. Consider the many air suspension systems commercially available to substitute coil and leaf springs. Consumer's perception is that it gives a softer ride. Land Rover's Range Rover and Volkswagen's Touareg are examples of vehicles with full air suspension systems. They utilise the air suspension not only to give superb ride comfort, but also to offer suspension height adjustability between on and off road conditions. Citroen was probably the first commercially available vehicle to offer this type of suspension. They combined a hydraulic and pneumatic system that linked the suspension actuators at the wheels to the air suspension cushion situated in the engine compartment. The Citroën was never considered a good option as a getaway car for bank robbers, as it took time to "pump up" before it could be driven. However, the ride it offered was considered excellent by many enthusiasts. The system was complex and consequently had reliability problems. The fact that the system lost pressure was probably one of the major drawbacks.

2.6. Auxiliary chambers in air suspension

The literature Quaglia and Sorli (2001) describes the use of a twin chamber vibration isolator that uses an orifice between the chambers. Quaglia and Sorli (2001) studied the non-linear characteristics of an auxiliary chamber and orifice added to a passive air suspension system. They found that the auxiliary chamber reduces the need for using a shock absorber in parallel to the air spring. A non-linear orifice system was compared with a linear system and they suggest that an orifice that can provide near

linear performance is preferred. The purpose of the orifice is to provide damping and should be chosen with the spring and reservoir to ensure correct stiffness and damping relationship. Interesting in this article is that a choked orifice conductance can influence the natural frequency of the system. A system with a closed orifice has a smaller air spring volume than an open orifice therefore a higher natural frequency of the system. The air spring with auxiliary chamber and flow restrictive orifice model is relevant as it would hypothetically be indicative of the aircushion characteristics at frequencies lower than that of the Helmholtz resonance frequency. Two natural frequencies exist, depending on whether the orifice, connecting the air spring and the auxiliary chamber, is choked or not.

It has been commercialised by Firestone Air springs, but only to extend the volume of the air chamber, thus providing a softer air spring. They add that a free flow of air is required between the air spring chamber and the auxiliary chamber. An additional auxiliary volume would affect the natural frequency directly. The air path between the air spring and the second volume has been described in the literature, however not tuned to counteract a specific frequency bandwidth. The orifice between the chambers has been varied to control the damping of the system by Quaglia and Sorli (2001). Nell and Steyn (1994) used a two state unsophisticated semi-active damper. Kashani (2004) used a liquid in an "inertia path" between the chambers to act at a specific frequency. The results were varied although when applied to their specific applications, deemed successful. The concept was based on a Helmholtz resonator. Toyofuku et al (1999) analysed the dynamic characteristic of the air spring with an auxiliary chamber, with focus on the dynamic spring stiffness of an air spring. They concluded that the extra chamber helps little at high frequencies, and that the phenomenon is due to the inertia of the air in the pipe and not due to the friction in the pipe. The only relevant reference in their article is to a Japanese article by Kagawa et al (1992) with title 'A study of unsteady flow in pneumatic pipe – chamber system'.

BS 6841 (1987) and ISO 2631 (1997) standards specify procedures to evaluate the health risk of an operator exposed to in any whole body vibration environment. A single value is used to describe the efficiency of any vibration isolation seat for a given environment namely SEAT. Van Niekerk (2000) found a 94% correlation between SEAT and subjective opinion. Equation (3) shows that the SEAT is obtained from the measured input vibration spectrum G_{ff}, the isolation characteristic spectrum (transmissibility), and the applicable frequency weighting (W_b for BS 6841 and W_k for ISO 2631).

$$SEAT = 100\sqrt{\frac{\int_{0.5}^{80} G_{ff} H_c^2 W_k^2 df}{\int_{0.5}^{80} G_{ff} W_k^2 df}} \qquad (3)$$

where W_k is frequency domain vector of ISO 2631 W_k filter,

H_c is frequency domain transmissibility curve of the air suspension cushion measured in the laboratory

G_{ff} is the frequency domain floor acceleration signal power spectral density

It is important that the suspension seat is developed for the environment where it will be used. Quaglia and Sorli (2001) confirmed this in their air suspension research. A suspension seat that works well in one vibration environment, will not necessarily work well in another. A lower SEAT value is the aim. The only variable that the seat/cushion designer can control is the isolation characteristic spectrum Hc. Ideally the numerator integral in equation (3), should be at a minimum. Therefore the transmissibility H_c should be low especially at the frequencies where weighted $G_{ffw} = G_{ff}.W_k$ is high. The fact that $G_{ffw}(f)$ is squared before the frequencies are summed (integrated) means that any natural resonance of the vehicle resulting in a high $G_{ffw}(f)$ will dramatically increase the resultant SEAT value. The same applies to the transmissibility of the suspension cushion that supports the human body.

If the weighted transmissibility of the suspension seat has a peak in the same frequency range as the floor acceleration dominates, then that frequency range will determine the SEAT value. The air suspension seat designer is therefore looking for a suspension system where for any frequency the product of $W_k.H_c.G_{ff}$ is a minimum. W_k is only non-zero in the frequency range 0.5 to 80Hz (ISO 2631) which means the effect of other frequencies can be ignored for vertical whole body vibration except for motion sickness.

The air suspension cushion design procedure would start with a measurement to determine the G_{ff} power spectrum during a typical in-field operation. The duration of this measurement would be typical of a task that the operator normally performs during his day. It will be important to determine which daily task has the highest vdv for a given time during the day, and to measure the G_{ff} for this task. The reason is that the task with the highest vdv should be reduced the most, and only then the task with the second highest vdv value, and so on. Consequently the improved air suspension cushion should aim to reduce the vdv value to allow the operator to work longer hours without endangering his health.

Weight the G_{ff} spectrum measured in-field with the ISO 2631 W_k frequency weighting filter to obtain G_{ffw}. The peaks on this spectrum are the challenge that the designer face. Ideally the transmissibility of the suspension cushion should reduce the peaks of G_{ffw}. Theoretically the designer should aim to achieve the transmissibility H_{ideal} where:

$$1 > H_{ideal}(f) < G_{ffw}.^{-1}(f) \quad \text{for } 0.5 < f < 80\text{Hz}$$

If the cushion offers no suspension, then the SEAT value would equal 1 as the numerator and denominator in Equation 1 are equal. Smaller H_{ideal} transmissibility will offer better vibration isolation. Of course ultimately we would wish for $H_{ideal} = 0$. This is not achievable in practice. The air suspension designer therefore aims for the H_c that will reduce the acceleration peaks in G_{ffw} as far as possible.

2.7. Helmholtz resonator theory

From acoustics and low frequency acoustic absorbers often called bass traps it followed to use a Helmholtz cavity resonator to absorb the sound pressure wave that exists in an air suspension cushion. The cushion will remain under static pressure due to the weight of the subject it supports, but any infra-acoustic pressure wave, which is generated by acceleration, will force air into the auxiliary chamber. The air

pressure in the auxiliary chamber will rise, and in return force air back to the air suspension cushion when the cushions pressure drops again. Helmholtz found that the mass of air in the pipe and the spring action of the compressible air in the auxiliary chamber will resonate similar to a simple spring mass vibration system. At certain frequencies, the displacement of the air mass in the pipe due to the systems resonance can be 180 degrees out of phase with the pressure wave in the cushion. Many low frequency acoustic absorbers employ this phenomenon to absorb low frequency acoustic pressure waves.

Herman von Helmholtz (1863) described the ringing sound of a spherical glass container with a small open throat. The effect is caused by the air in the throat acting as a mass and the air in the container as a spring. This mass spring system vibrates at its natural frequency whenever set in motion by external pressure variations. Various publications have since been made on this topic.

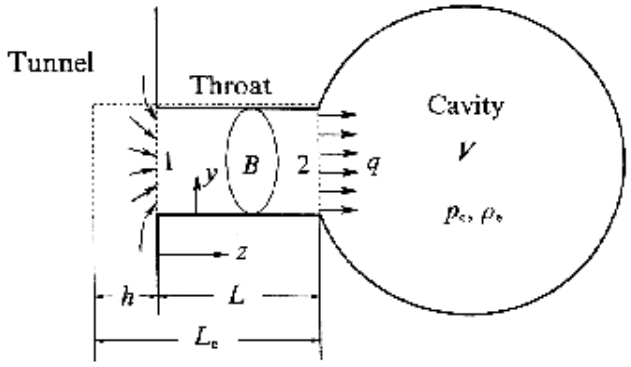

Figure 7 :- Helmholtz resonator theory

The Helmholtz resonator in Figure 7 is a flask. It consists of a closed volume V of air, with a narrow neck of area B and length L. The air in the neck oscillates in and out depending on the pressure inside the volume. If the pressure is high in the volume, the air moves out, and vice versa. The air in the volume acts as a spring, the air in the neck acts as a mass creating a simple spring mass system. It can be put in motion by blowing over the neck which, if tuned, will often produce a sound. The Helmholtz frequency is calculated by the equation:

$$f_h = \frac{c}{2\pi}\sqrt{\frac{A_p}{L_p V_d}} \tag{4}$$

Where c = speed of sound;

A_p = Area of the pipe (area B in the figure);

L_p = length of the pipe (effective throat length L_e in the figure);

V_d = volume of the tank (cavity V in the figure)

An example of a Helmholtz resonator is a 2 litre plastic soda drink bottle:

$V_d = 0.002\ m^3$ - volume of the bottle; $A_p = 0.00031\ m^2$ – area of the neck

$L_p = 0.04$ m – length of the neck; $c = 343$ (m/s) – speed of sound

Therefore

$$f_h = 1/(2pi)(A_p\, c^2 / (V_d\, L_p))^{0.5} = \frac{343}{2\pi}\sqrt{\frac{0.00031}{0.002 * 0.04}} = 107.5Hz \text{ - frequency}$$

Helmholtz resonators are commonly used in acoustics to effectively absorb sound. Wooden slats spaced slightly apart on the back and side walls of auditoria utilise this phenomenon. The disadvantage it that a tuned resonator will only absorb sound waves of a narrow frequency band. It is possible to broaden the frequency band. However, the absorption magnitude (Q-factor) is reduced.

Selamet et al (1995) warned that the individual volume dimensions of a Helmholtz resonator can significantly affect the resonance frequency and the transmission loss characteristics.

2.8. Pipe theory

Helmholtz found the resonator phenomenon to exist in a volume with a relatively short neck. Longer necks have not been addressed. Many musical instruments use air movement in pipes to generate sound. It is therefore expected that a long neck to the resonator would generate its own resonance. Basic pipe resonance theory (Bueche, 1979) calculates resonance on long pipes with open and closed ends. Mohring (1999) suggested that pipe resonance would be insignificant where the pipe is shorter than one tenth of the wavelength.

Daugherty and Franzini (1984) presented the adiabatic flow of a compressible fluid in a pipe in Figure 8. Important to note the pressure, temperature and velocity profiles of adiabatic air flow in the pipe. Subsonic flow, with Mach number (N_m) less than unity, flow has a limited distance along the pipe, until the pressure increase rate over distance reaches infinity. The velocity curve indicates this point as when the speed of sound is reached. The velocity increase rate over pipe distance beyond this point approaches infinity. It is important is the speed of sound in the pipe and ensure that during a simulation exercise it is not exceeded by the speed of air in the pipe.

It is anticipated that at low frequencies and low excitation amplitudes, the flow velocity in the pipe will be low enough to be in the linear region on the left side of the graph. At high frequencies and higher amplitudes of vibration excitation of the cushion, the pressure difference can increase and the velocity can reach N_m=1. At this condition, it is anticipated that the pipe flow will be throttled so much, that the cushion will exchange little air mass with the tank.

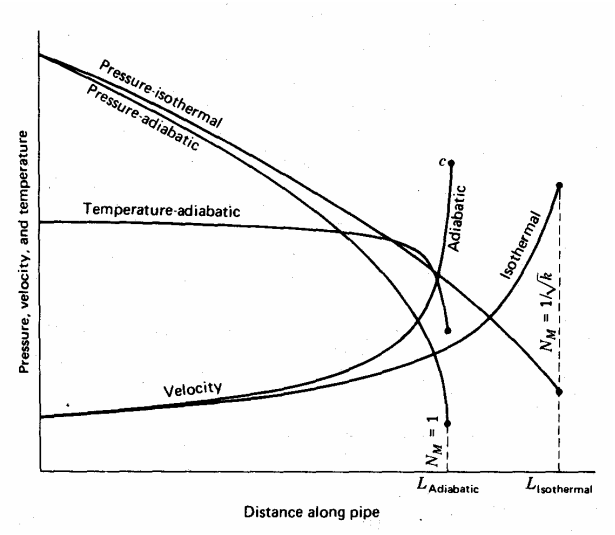

Figure 8 :- Airflow properties in a pipe

The spring rate of the system will then be that of an air spring with the cushion volume only. The tank will not contribute to the spring rate, and the natural frequency of the mass on the cushion will be that of a mass on the cushion only without the tank. Although the graph has no dimensions, it is interesting to note the temperature curve near to horizontal, except when it approached the critical point of N_m=1. It can be useful to say that up to a pipe distance of half a pipe length where N_m=1, the temperature of the air in the pipe remains constant. The calculation to determine the pipe distance at which Nm=1 will have to be done as part of the simulation every time any of the parameters of the air in the pipe changes.

2.9. Seat ergonomics

An ergonomic approach to vibration environments should include a consideration for the influence of the controls and the visual environment on the posture of the operator. The workstation should be designed in order for the operator can do the job while sitting in a seat in a satisfactory posture (Griffin 1990). Lee and Ferraiuolo (1993) found a correlation between pressure and muscle activity and sweat impulse and subjective comfort opinion.

Commercial advertising suggest that consumer perception of a good ergonomic seat includes; pressure mapping , placement of control handles, ease of service, for/aft adjustment, height adjustment, backrest angle adjustment, seat cushion tilting, adjustable suspension stroke, weight adjustment – infinitely, headrest height adjustment, moisture barrier cover, lateral support.

Ebe and Griffin (2001) reported on the subjective static comfort of various seat cushions. They employed a pressure mat to measure pressure in the whole seating area. A 40mm x 40mm square area beneath the ischial bones was correlated with seat comfort; samples with less pressure in this area were judged to be more comfortable than samples with greater total pressure. They concluded that the pressure beneath the ischial bones may reflect both comfort factors: the bottoming effect and the foam hardness feeling. Liu et al (2004) researched the cause of

pressure ulcers and suggested lower pressure under the ischial tuberosities. Griffin (1990) commented that generally cushions with softer foam were considered more comfortable that cushions with harder foam. However, cushions that were too soft and bottomed out were considered worst. An air suspension cushion will distribute pressure evenly and eliminate pinch points under the ischial bones. However, under extreme conditions progressive bottoming may still be acceptable to the operator (Wu et al 1999). They studied the pressure distribution under vertical vibration conditions. Air pressure will have to be adjusted to prevent cushion bottoming under normal operating conditions.

Griffin (1990) suggested that pressure comfort contours should be determined with non-complaint seating. The contours obtained on rigid seats are then applied to vibration measurements, obtained on the surface of complaint seats at a position directly beneath the ischial tuberosities of a subject. The vibration of the ischial tuberosities arises from the dynamics interaction of the response of the body and the response of the seat. If the seat is not rigid, the vibration of the body will influence the vibration of the seat and, in the extreme, it is possible to be near-zero vibration at the seat, but significant vibration in the body.

On the relation between seat pressure and perceived comfort, Gyi and Porter (1999) found very little coherence. They however found that taller thinner subjects have higher pressure in the ischial tuberosities area those shorter fatter subjects. The latter group again had higher pressure under the thighs. This is important in an air suspension cushion as the pressure distribution is near equal over the interface.

Seat adjustability depends on the anthropometric range of the indented operator population. It can be perceived by consumers that a seat with more adjustability is better. In air suspension seats the most important adjustment would be automatic height control. Lateral and anti roll seat support assist the body in balancing itself during adverse conditions. Arm rests would also contribute during worse lateral acceleration.

3. Conceptual design

The conceptual design process used consists of four stages;

- product design specification
- concept generation
- concept evaluation
- concept refinement.

Stated design specifications are for ergonomics, vibration isolation, manufacturing, marketing and operating. Eleven initial concept ideas were generated for the cushion. The tank and pipe design was postponed until the refinement stage. The cushion concept designs were evaluated according to Ulmann's (2003) method. Two concepts were refined and subjected to laboratory experimentation. One concept was chosen to analytically model and for final design.

3.1. Product design specification:

A conceptual design guideline specification was required to give direction to the design development of the air-cushion. Some design criteria were noted:

3.1.1. Ergonomic specification for the cushion:

- Support the weight of light to heavy operator;
- Allow the cushion buttock not more that 5 degrees tilt from the static plane – i.e. stable to tilt;
- Allow maximum vertical travel under low frequency shock conditions ;
- The seat should not travel vertically more than 20mm when pressing any foot on a pedal;
- Cushion buttock interface to be shaped to centre seated position;
- No pinch points (high pressure points) on the buttocks at the interface;
- The body's weight centre axis to be the same as the cushion;
- The spring coefficient of the cushion linear for analytical modelling purposes;
- Utilise a pipe and tank to increase isolation properties at given frequencies;
- No mechanical scissors mechanism or similar to stabilise the cushion;
- Operating and safety instructions printed on the cushion;
- Pressure area increase with increased load should be limited
- A hard interface is suggested to spread pressure force and prevent cut of blood flow.
- Allow air flow through to reduce sweat build-up at the seat interface

- Lateral forces support requirement - Design according to the maximum lateral acceleration measured on the Three-wheeled in-field tests
- Roll support requirement - Design to the moment forces expected when the operators body compensates for roll during maximum lateral acceleration
- Anthropometric size and design considerations - Use anthropometric tables for size calculations. Design the three dimensional shape of the cushion semi rigid frame.

Figure 9 :– Limited space in three-wheeled logger operator cabin

The picture shows that no space is available below the seat for a normal suspension seat. The measured distance between the cabin floor and the operator buttocks is less than 200mm.

3.1.2. Vibration isolation specification

The cushion should reduce the SEAT value for the vehicle by at least 20% alternatively increase the maximum operating time allowed according to EU Directive (2002) as determined in accordance with ISO 2631:1 (1997).

3.1.3. Manufacturing specification:

- manufacturing in South Africa from locally produced materials
- simple moulding / assembly process
- no moving parts other than due to pressure changes within the cushion due to external forces

3.1.4. Marketing specification:

- marketable as a stand alone product
- off the shelf sellable
- replacement guarantee policy for first year
- Material will receive paint or colouring for branding

- pricing under R2000 in 2006

3.1.5. Operating specification:

- operate without separate instruction manual
- air reservoir sealed against leaks
- inflatable to specified operating pressure
- standard car / bicycle pump inflator connection
- mountable/demountable with limited tools
- 50,000 rub resistant material
- Crip 5 fire resistance
- Cover must be replaceable when damaged
- Tear resistant to normal use as indented
- Attachable to existing seat bases with or without cushions

3.2. Concept generation

Eleven concepts were generated. These were cushions of bubble plastic, open cell foam rubber, closed cell foam rubber, inflatable plastic ball, stabilised inflatable plastic ball, flat cylinder shape, two horizontal cylinders, three flat cylinders, square torus, round torus concept with non-constant pressure area, round torus concept with constant pressure area. A short description of each of the concepts follows. Initial experimentation on some concepts are discussed. However, detailed experimentation to assist design refinement is in a later chapter. In each case after the heading, the concept codename is between brackets for referencing from the later section on concept evaluation.

3.2.1. Bubble Plastic Concept (Airbubble):

This first concept originated from a specific need of a company with several forklift drivers. The drivers were using mattress foam as a cushion on top of the seat fitted in the forklift. The concept air bubble cushion was approximately 80mm thick and consisted of black synthetic rubber outer layer and multiple layers of large bubble plastic (at the time used for thermal roof insulation), mounted on the existing seat cushion with wide Velcro strips. This cushion was actually manufactured and fitted into the forklifts, which was accepted favourably by the drivers. However, from vibration tests carried out it was found that this favour was merely due to the fact that the drivers then felt that their problem was being recognised by management, and no vibration isolation was actually provided by the cushions.

Figure 10 :- Inside of the original AIRSEAT

Advantages of bubble plastic concept were that it is stable against the driver's lateral body roll; can be made in virtually any thickness by just adding more layers of bubble plastic; plastic was found to be tear resistant and no punctures could be made even when jumping heals first onto the cushion; bubble plastic is almost as cheap as foam; the cushion can be shaped to fit the buttocks by puncturing some of the bubbles in some of the layers.

Disadvantages of bubble plastic concept identified were that air is contained in multiple cells making the fitment of an anti-vibration resonator impossible; the plastic was noisy when the driver changes position; the total area of the air bubbles in a stable air suspension cushion is too high for the spring coefficient to be low enough for adequate vibration isolation at low frequencies

3.2.2. Open cell foam rubber concept (OpenFoam):

Although originally frowned upon, a sleeping mattress type open cell foam was also considered as a concept for the air suspension cushion. During compression and expansion, air moves in and out of this cushion through the millions of air holes in the structure of the material. Due to the open cell configuration, the spring stiffness was however not provided by the compression and expansion of trapped air, but rather by the foam itself. A characteristic of open cell foams is deterioration of structure when subjected to continuous compression and expansion.

Advantages were simplicity, off the shelf, just cut it to size; stable against human lateral body roll; foam can be manufactured to any hardness the seat manufacturer may require; cheap and easy to install and replace. Disadvantages were air is not contained to act as the air spring; deteriorate after many strenuous cycles of compression / expansion; the support is spread over the full area of the buttocks, which results in a harder spring coefficient, than what may be required to meet the

sought isolation coefficients; the Helmholtz anti-resonance concept will not work with the open cell foam rubber

This concept is used as reference when the final air suspension cushion is evaluated experimentally. It is due to its similarity to the foam used in commercial seat bases.

3.2.3. Closed cell foam rubber concept (ClosedFoam):

Closed cell rubber contains air that can be compressed to function as an air spring. The multiple cells can act together as an airspring. Although closed cell foam rubbers have a small amount of plastic reformation under continuous load, it was found to recover to almost 100% of its original size after a short time. Advantages were simplicity, off the shelf, just cut it to size; stable against human lateral body roll; foam can be manufactured to any hardness the seat manufacturer may require; almost as cheap as open cell foams, as well as easy to install and replace. Disadvantages were that the support is spread over the full area of the buttocks, which results in a harder spring coefficient than what may be required to meet the sought isolation coefficients; air is contained in multiple cells making the fitment of an anti-vibration resonator impossible

3.2.4. Inflatable plastic ball concept (PlasticBall):

A simple air inflatable beach ball of spherical shape flattened at two support ends. It is inflated to support the weight of the driver at a working thickness of 100mm. the sides of the ball will be unrestricted and can stretch sideways under increased pressure. The ball is fitted with a tank connector and pipe to a tank which will act as the absorption resonator. Advantages are simplicity; easy to connect to pipe and tank; reliability; pressure on buttocks is spread. Disadvantages identified were firstly instability – will roll sideways and forward under force; and secondly the spring coefficient is not linear; as the weight / acceleration changes - the pressure area changes.

This concept is unstable; tilt could be excessive and operator will concentrate more on balancing on the cushion than on his task.

3.2.5. Inflatable plastic ball concept – side stabilised (StablePlasticBall):

As above, but the ball lies in a pan with 100mm high sides to restrict lateral movement. Advantages were simplicity; easy to connect to pipe and tank; reliability; pressure on buttocks is spread Disadvantages noted are that its unstable, although sideways and forward movement can be restricted by the pan, the support to the buttocks will not be adequate for human lateral roll stability. The ball construction is a sphere and it will tend to roll the subject off to regain its shape. A large pressure area results in high air spring stiffness.

Although the lateral stability was improved, it is still too unstable to be used as a cushion. Tilt could be excessive and operator will concentrate more on balancing on the cushion than on his task.

3.2.6. Flat cylinder shape concept (FlatCylinder):

The idea is similar to the above, but the shape is that of a flat cylinder and not of a sphere. This could reduce the action of rolling the subject off the cushion.

Advantages are simplicity; easy to connect to pipe and tank; reliability. Disadvantages are when applying a lateral force, the subject, to counteract will roll his hips and one buttock will apply more force on the cushion than the other. The side of the cushion under higher force will simply sink and the air pressure will push the other side up, still unstable to roll forces. The cylinder shape is stable when fully inflated, however as soon as the subject sits on it, it compresses and the result can be as unstable as the beach ball The sides will crumble and change shape when changing the pressure area i.e. the linearity of the spring.

In conclusion this is too unstable to be used as a cushion. A cushion with better anti-roll support is needed.

3.2.7. Two horizontal cylinders concept (TwoHorisontalCylinder):

This concept consists of two long cylinders laid horizontally at a designed distance apart. The two cylinders provide pressure independently and the distance between them increases the resistive moment and roll stability. A small pipe connects the two air chambers to even out static pressure. This pipe is small enough to restrict periodic flow between the two volumes during lateral and roll acceleration at frequencies in excess of 0.5Hz.

Advantages are sideway stability as the cylinders can be long and far apart. Disadvantages are that fore-aft stability is not improved; the cylinders will change shape under variation of weight/acceleration, therefore change the pressure area and the linearity of the spring. The pressure area is large and might not achieve low system natural frequencies. Two springs with interconnecting pipe are more complex and therefore less reliable due to leaks and more costly in long term.

3.2.8. Three flat cylinders concept with side stabilisers (ThreeFlatCylinders):

Three flat cylinders positioned in a triangle. The triangle is positioned to achieve maximum sideways and fore-aft stability. Small interlinking pipes are used to even out static pressure differences between cylinders. Each cylinder sits in a pan with high sides to prevent sideways roll.

Advantages are more stable against body roll, as the cylinders, can be placed far apart. It is stable against lateral sideways force due to the pan sides. Disadvantages could be that the pan sides could restrict vertical movement; the cylinder's sides will crumble and changes shape when changing the pressure area and the linearity of the spring. The three springs with interconnecting pipe is more complex and therefore less reliable and more costly to maintain. An additional hard seat plate will be required to keep the cylinders together

3.2.9. Square torus concept (SquareTorus):

A square torus manufactured of non-stretch material to maximise linearity of the spring. The torus consists of 4 sides of a certain length each within a cover creating a sausage shape. The ends are stitched together to form a square. However, the four

air chambers remain separate. The torus is then placed within a shaped block to ensure its shape stays uniform. Another block, with edges shaped, acts as the piston. At variable height positions of the spring, the pressure area stays the same. The spring rate is dependant on the compression of the air volume only.

Advantages are that it is stable against roll as the square torus shaped spring can be enlarged. Disadvantages are that four auxiliary chambers and pipes are required as resonators; the stitches at the ends of the sausages may have a different stiffness than the rest of the tube; the stitches may prove unreliable and cause leaks.

3.2.10. Round Torus concept with non-constant pressure area (TorusInFoam):

A foam cushion is hollowed out to contain a small inner tube Figure 11. The semi rigid foam sides acts against the lateral roll as well as the sideways force problem. A cut out can be made in the area of the ischial tuberosities. Moulding material should be of low stiffness synthetic rubber, or similar material. Although the spring coefficient is expected to be non-linear, the round torus can be more stable if used as is. When roll occurs to one side, the round torus is compressed more on that side. The pressure area on that side will increase, causing an increase in the resulting force whilst the pressure inside the torus remains constant. On the other side where the roll causes lift; the pressure area reduces, causing a reduction in the resultant supporting force. The difference between the forces provides the anti-roll support moment.

Advantages of this concept are:

- stable against lateral roll as the round torus shaped spring diameter can be enlarged and the block shaped to enlarge the area when compressed
- it consists of one volume which is easily connectable to the pipe and tank
- a simple vehicle tyre inner tube can be used
- rubber is known as a reliable material when stretched and released periodically
- commercial air springs use rubber even though it does not have a linear spring coefficient.
- the torus if fitted to a shaped block can be designed to resist lateral forces

Disadvantages:

- rubber stretches and therefore allow variance in the volume of the airspring when subjected to dynamic weight (gravitational plus acceleration force). The shaped block can however be engineered to increase the area of pressure when the volume increased due to the stretch of rubber.

Conclusion:

On first impressions this concept is a simple and deemed reliable, however it needs refinement and the effects of the expected non-linearity of this airspring requires investigation.

Figure 11 :- The tube torus in foam

3.2.11. Round Torus concept with constant pressure area (RoundTorus):

The round torus consists of a shaped torus block that guides the shape of a membrane (inner tube) forming an air spring that gives constant pressure area irrespective of the height of the "piston" in Figure 12. The advantage of this concept is that the spring rate can be controlled by adjustment of the pressure area, and the volume of the cushion. The linearity of the constant pressure area could be easier to describe analytically and model for simulation. This concept would be expensive to manufacture as a prototype. However, with modern plastic injection moulding processes high quantities could prove economical.

Disadvantages are that a stretchable material is required, as the specific points on the material moves from position A to position B (Figure 12) as the piston moves up and down. The circumference of the torus at A is larger than the circumference at B. The stretch of the rubber will cause the rubber to move against the metal block at the point of contact. In the long run, the rubber will wear through and perish here. When the pressure area stays constant as the cushion height is decreased, the same body roll instability found with the flat cylinder concept recurs.

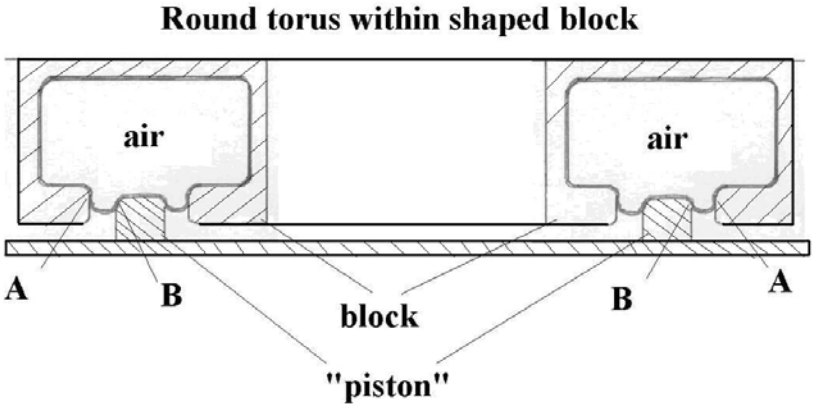

Figure 12 :- Section through Round Torus Concept in block with constant pressure area

3.3. Concept design evaluation

From the above analysis it is concluded that there are several major design criteria that have to be met. It is therefore essential to formalize the concept evaluation. Ullman (2003) described a conceptual design evaluation based on a basic decision matrix. This method was followed in the following steps:

- Step 1 - Draw up a list of criteria that are important factors that will in the experts opinion influence the performance of the cushion. Start by noting the obvious factors, followed by the less obvious factors.
- Step 2 - Scratch out the factors that all the concepts obviously fully comply with.
- Step 3 - Sort the factors from least to most important, and subsequently number them from 1 to n.
- Step 4 - Shuffle the factors now whilst keeping the number and factor linked.
- Step 5 - Prepare a questionnaire for experts to complete with -1, 0, 1 numbers respectively for non-compliant, not applicable and comply with each concept for each factor.
- Step 6 - Sum the products of the compliance numbers and respective weight for each concept.
- Step 7 - The concept with the highest score is deemed the one to pursue.

The factors used in this study were:

- a cushion with three separate pressure chambers will solve the anti-roll problem.
- a mechanical link will hold the backrest (tanks) to allow vertical movement only.
- a simple off the shelf material can be used
- a single moulding with air chambers can be used for the seat cushion
- a tuned pipe exists between each air chamber in the cushion and each tank
- allow maximum vertical travel under low frequency shock conditions
- allow the cushion buttock no more that 5 degrees tilt from the static plane – i.e. stable to tilt
- the membrane used will stretch under increased pressure in the airspring, and the membrane will have a rolling resistance.
- constant pressure area as the cushion height is decreased; the same body roll instability that was found with the “cake” concept recurs.
- cushion buttock interface to be shaped to centre seated position
- high linearity
- ideally the tanks will move with the suspended seat plate.
- lateral forces can cause the piston to move and bring the inner face in contact with the outer face, which could cause damage to the membrane.
- manufacturing simple to keep cost low
- moulding material to be of closed cell low stiffness synthetic rubber
- no mechanical scissors mechanism or similar to stabilise the cushion
- no pinch points (high pressure points) on the buttocks at the interface
- one pipe and tank rather than multiple pipes and tanks.

- one volume which is easily connectable to the pipe and tank
- provide support against fore aft body roll of the subject
- provide support against fore aft horizontal force
- provide support against sideways body roll of the subject
- provide support against sideways force
- rubber is used which is a reliable material when stretched and released periodically
- seat does not have vertical travel of more than 20mm due to pressing foot on the pedals
- stable as the shaped spring can be made large in diameter
- stable support against body roll
- support the weight of light to heavy operator
- the air-cushion will ideally replace the existing seat base in the vehicle and not be placed on top of it
- the body's weight centre axis the same as the cushion
- the tanks are interlinked with a small hole to balance the static pressure
- the tanks can be structurally connected to the seat plate of the cushion
- the tanks can ideally form the backrest of a seat.
- the linearity of the pressure area can best be handled by a rolling membrane piston spring.
- the pressure area increase under high acceleration force should ideally be zero to maintain spring coefficient linearity at working height
- the pressure filler valve is mounted in the tanks
- the rolling membrane air spring has its own spring coefficient due to the membrane rolling from the larger circumference outer face to the lower circumference inner face.
- the sideways force can be prevented by mechanical connection between the cushion base plate and cushion seat plate.
- the spring coefficient of the cushion linear for analytical modelling purposes
- the stretch of the rubber will not cause the rubber to move against the metal block at the point of contact and perish here.
- the three pressure chambers will have to function pressure independently during exposure to vibration.
- three long tanks (cylindrical or rectangular) can be mounted vertically alongside in the position of the seat backrest.
- utilise a pipe and tank to increase isolation properties at given frequencies

See Appendix D for the factors, weights and results used in this study. Concept designs "G" and "K" received the highest score in this evaluation. The Round torus – constant pressure area (RoundTorus) and the Round torus in Foam (TorusInFoam) were chosen for refinement.

3.4. Refinement of two concepts and the pipe tank connection

The design evaluation suggested refinement of the 'round torus in foam' concept and the 'round torus with constant pressure area' concept. Due to uncertainty the latter was refined first due to its assumed linearity. The former concept was subsequently refined and evaluated under laboratory conditions. Both were connected with the same tank and pipe and tested extensively under controlled

laboratory conditions. This section describes the refined designs and the next chapter the experimental work. During experimentation the round torus in foam concept proved the most suitable. The round tube torus with constant pressure area was used to understand the contribution of the pipe and tank to the transmissibility curve.

In this section the design of the pipe and tank is discussed as well as other concepts that could improve the specification of the system.

3.4.1. Round Torus concept – constant pressure area

The challenges faced during the design of the laboratory prototype air-cushion were that the airspring "piston" had to be as linear as possible. Often air suspension cushions with soft sides would bulge out when the pressure increase and the height decrease, this would increase the pressure area rendering the spring non-linear. The torus concept discussed earlier was used in the design.

The air was to be contained by a rolling membrane and a 12inch inner tube was used here. Three cross section designs were considered to be used in the torus:

- Firstly in Figure 13 the symmetrical expanded volume cross section offers the lowest stiffness spring by using more volume (A x B) for a smaller pressure area G.

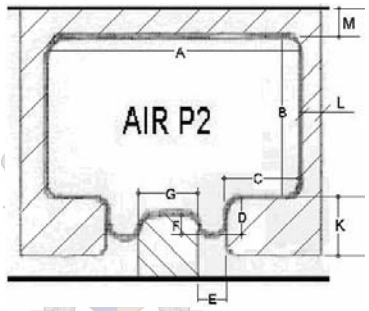

Figure 13 :- Constant area shape1

- Secondly in Figure 14 dimension C on the one sided expanded volume cross section, can be extended to the centre vertical axis of the torus, to give maximum volume for an even softer air spring.

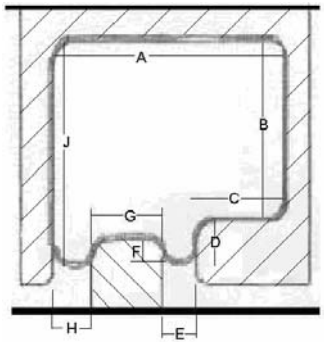

Figure 14 :- Constant area shape2

- Thirdly in Figure 15 the rectangular cross section minimises the volume to area ratio to provide stiffer springs, whilst maintaining the travel (dimension B - dimension F).

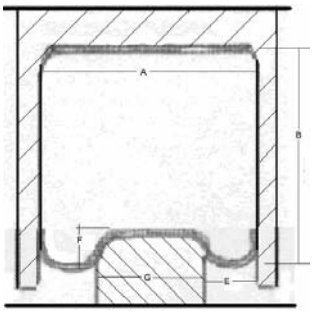

Figure 15 :- Constant area shape3

- The use of an inner tube placed certain restrictions on the length of the membrane, as maximum vertical travel was required. An iteration model was used to obtain the most effective cross sectional design that offers the required pressure area necessary for the air spring stiffness. The initial air spring stiffness was chosen from the literature study to be 1666 kN/m< k < 6666 kN/m. the air spring required at least 100mm travel to accommodate high amplitudes at low frequency.

Mild steel was chosen as the material for the prototype in Figure 16. It has adequate strength and already contributed to the required mass of the suspended part of the cushion. Additional mass was suspended to the moving part of the cushion to make up the total mass required for the experiment. The volume of the air suspension cushion had to be determined accurately. With the air suspension cushion fixed at normal working height, it was weighted empty, and weighted filled with water.

It should be noted that the intention was not to use a steel cushion in a vehicle. The steel cushion prototype was used to eliminate unknown non-linear air spring volume changes during pressure fluctuation and shape changes. The pressure area was reduced by using a torus shape piston instead of a flat cylindrical shape. The torus had better anti-roll stability.

Another challenge was that should the moving part of the cushion be tilted at a large angle it could get stuck to and damages the membrane? The diagram in Figure 17 was used to ensure that the upper and lower parts of the cushion could bottom out and continue functioning normally after maximum tilt.

This concept developed into a design that was laboratory tested in order to investigate the effect of various resonator parameters. The design had to eliminate as many variables as possible in order to refine the results of the laboratory tests. To determine the transmissibility of the air-cushion, a static mass load was used. This eliminated the complexities and risks of human subject testing.

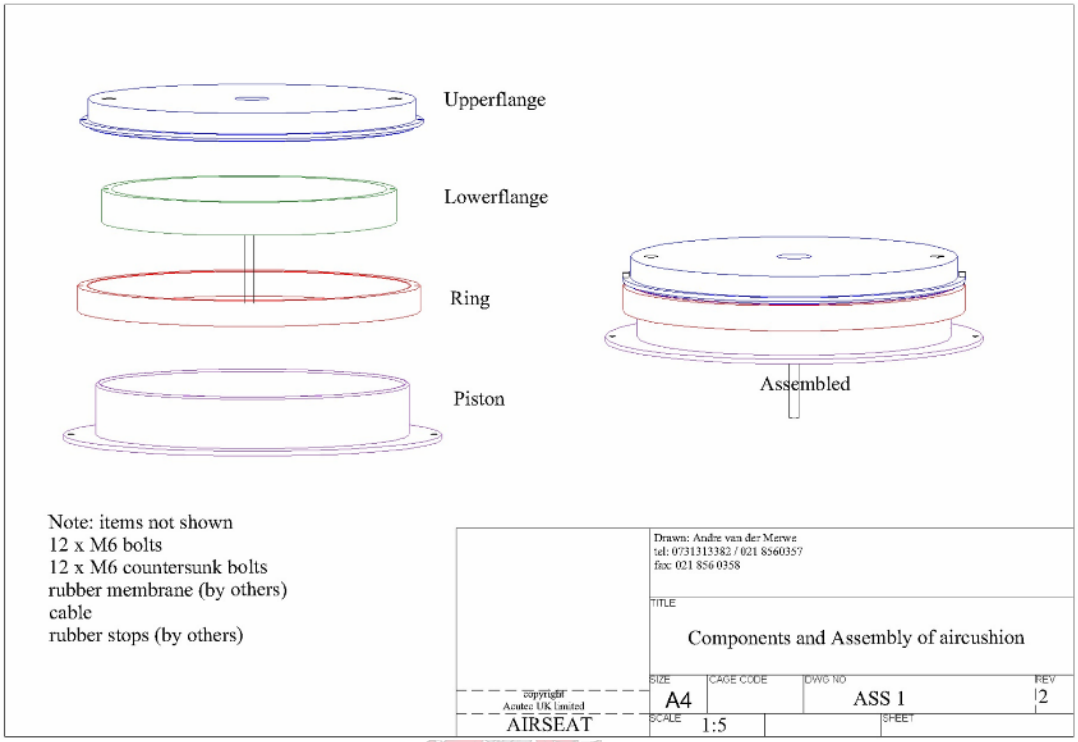

Figure 16 :- Steel cushion with constant pressure area – assembly drawings

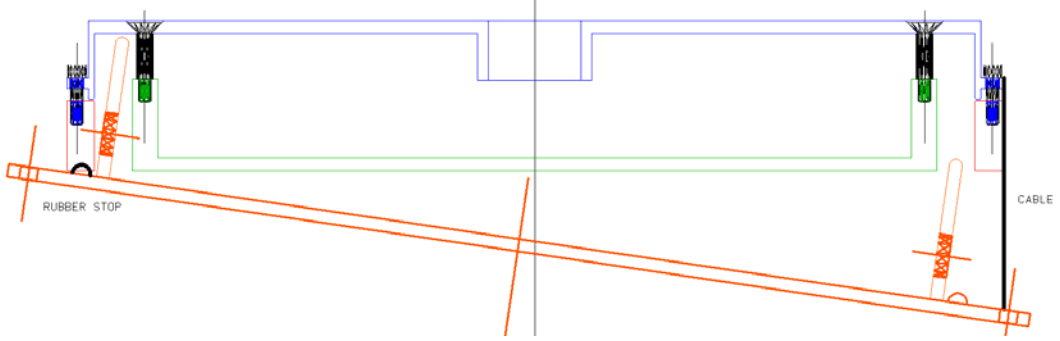

Figure 17 :- Angular test to maintain membrane integrity during bottoming out

3.4.2. Round torus in foam – non-constant pressure area

The semi-rigid foam frame is designed to house the torus rubber which contains the compressed tube. The purposely designed shape of the cushion frame helps with support against body roll, and sideways forces. It also shapes the torus during peak vertical accelerations to allow maximum vertical compression of the cushion before bottoming out. Other refinements are:

- Material - The semi-rigid seat cushion frame is manufactured from open cell synthetic rubber of a medium-high density.
- Interface to torus - The torus rubber is partly glued to the foam surround
- Manufacturing - The cushion moulding is a single piece moulded in a normal foam expansion process.

When the operator is subjected to sideways forces his body tends to roll away from the force. Compensating he will rotate his hips to counter this roll whilst expecting support from the cushion. The cushion will compress in the side where the force is high and expand on the other. Compression of the torus will enlarge the pressure area and increase the force. The opposite occurs on the other side of the expansion. The force difference between the two sides is only regulated by the change in difference of pressure area, as the pressure in the torus remains constant on both sides. When it just supports the static body weight, the vertical cross sectional shape of the torus is therefore required to be a circle rather than a flat ellipse. This is possible by increasing the pressure in the torus enough to support the static body weight with only a small area at the top of the torus. Under increased force the pressure area will quickly enlarge to support the force. Figure 42 illustrates how the shape changes are quantified by digitising the different shapes of the torus when subjected to different loadings.

An upward movement of the seat base will increase the pressure in the cushion resulting in an increase in the force supporting the body at the buttock interface. Due to the inertia of the body, the force will be resisted, and the pressure area will increase, which in turn will increase the force. This increase of pressure area is affected by the vertical cross sectional shape of the torus, which is controlled by the shape of the cushion frame. Section 3.4.5 deals with influence of variation in supported mass. It is considered similar to increased constant acceleration.

A seat board in Figure 18 on the tube spreads the force supporting the body at the interface with the buttocks. An extension of the board under the legs prevents cut of blood flow, which could occur when seated directly on the tube.

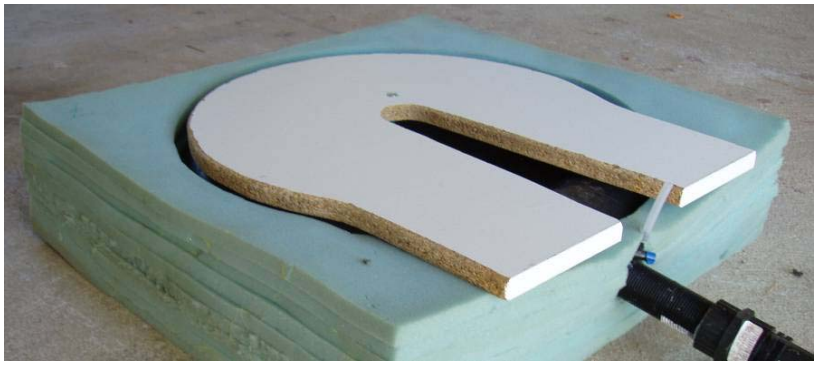

Figure 18 :- Hard seat board spreads force below the thighs

3.4.3. Tank and pipe design

The air suspension cushion is extended to a larger volume by adding the tank. The pipe connects the two volumes. The pipe and tank combination forms the

resonator. From the literature in sections 2.7 and 2.8 we learned that the Helmholtz resonator absorbs acoustic energy, and that a pipe length needs to be limited to avoid standing waves. Pipe and tank design is therefore critical to ensure that the air suspension cushion is an improvement over other seat cushions.

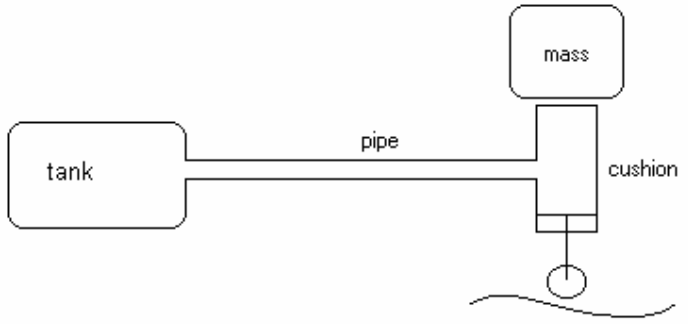

Figure 19 :- pipe and tank resonator extension to the air suspension cushion

In an air suspension cushion (Figure 19) pressure changes occur due to differences in displacement between the upper and lower surfaces of the cushion. Such differences in displacement are normally due to unequal acceleration of these surfaces. A closed air suspension cushion supporting a single mass is also a single degree of freedom spring mass system. The compressible air acts as the spring supporting the mass. However, due to the static weight of the mass, the static pressure inside the cushion is higher than in a Helmholtz resonator at atmospheric pressure as discussed earlier. The question can be asked whether this phenomenon is static pressure dependent. Helmholtz equation (4) shows that frequency is independent of pressure. It can therefore be expected that the Helmholtz formula will apply at higher system pressures inside an air suspension cushion.

Floor movement would cause displacement differences between the upper and lower surfaces to result in acoustic pressure fluctuations within the cushion. The static pressure remains constant. If the displacement differences are periodic, the acoustic pressure fluctuation inside the cushion is periodic. The most expected occurrence of this periodic acoustic pressure fluctuation will be, when the air spring mass system oscillates at its natural frequency. If this periodic acoustic pressure fluctuation in the air suspension cushion is reduced, the natural frequency oscillation of the spring mass system could be reduced.

A Helmholtz resonator will "absorb" acoustic pressure fluctuations present in an air suspension cushion at the tuned frequency of the resonator. Of course the Helmholtz resonator could be tuned to absorb periodic acoustic pressure at exactly the natural frequency of the spring mass system of the aircushion. The natural frequency of the mass on cushion with the Helmholtz resonator attached will reduce to that of the spring on a bigger air suspension cushion that now includes the resonator's volume. At a higher frequency an amplitude peak will occur due to the now two degrees of freedom system. This peak is normally small and could be reduced by ensuring that adequate damping is present in the system.

Ideally the resonator should reduce the resonance peak in the transmissibility curve. Figure 20 shows the difference between a cushion with and without a resonator. A solid mass of 86 kg on a cushion of 550mm diameter at a working height of

120mm was tested. A resonator consisted of a 2220mm long 25mm diameter pipe and a 25liter tank. The graph was generated from initial trials.

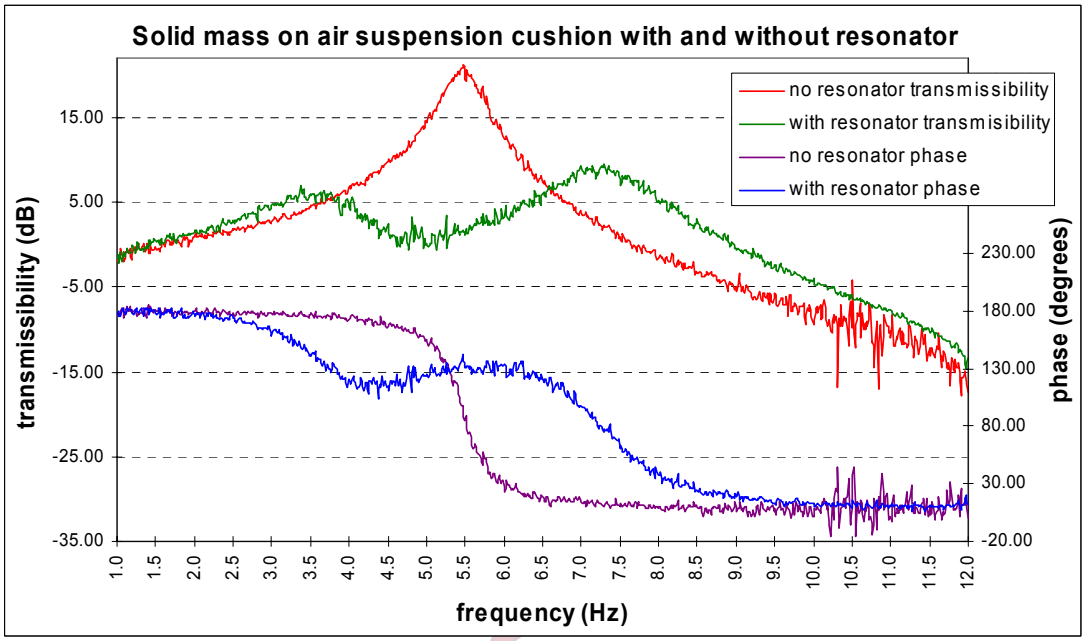

Figure 20 :- The effect of a Helmholtz resonator fitted to the air suspension cushion

Unfortunately Helmholtz' cavity absorber can only be tuned to one specific frequency, and will only absorb an acoustic pressure wave at that frequency (and neighbouring frequencies if damping is present). Many questions arose from this:

- What size should the cavity absorber's resonating volume be?
- Can one use more than one absorber at the same time?
- What happens when the system is a closed system under pressure – Helmholtz resonators were found to work at ambient pressure?
- How does the volume of the cushion influence the working of the resonator, which normally functions as a volume with a neck which is open to an infinite volume?
- How will one achieve stability in the cushion, where sitting on an air suspension cushion is as unstable as sitting on a beach ball on water?
- Will the system work at subsonic (<20Hz) frequencies?
- Will air pressure influence the isolation frequency of the resonator?
- What happens during and immediately after a shock input?
- Interface to cushion - The rigid pipe attaches to the cushion torus with a specially manufactured interface, similar to that of the inflator valve. Leaks in this area are likely due to the amount of movement and pressure changes that it is subjected to.

- Integration of simulation results into design - The simulation results are critical in deciding which cushion area, pipe diameter, pipe length and tank volume should be used for a specific cushion design. The transmissibility of the cushion depends on these factors, which can be optimized to provide maximum vibration isolation for vehicles with high floor acceleration of the operators' seat.

Certain design criteria were noted during the conceptual phase and the subsequent experimental planning. For the final product ideally the tank could be moulded in the shape of a backrest and mounted vertically to function as the backrest. The pressure filler valve could be mounted in the tank rather than in the cushion. Ideally, the tank (backrest) will move with the suspended top of the cushion. A linear bearing could hold the backrest (tank) to allow vertical movement only.

For experimentation, the tank volume had to be variable, which allowed testing at various tank volumes. Water is not compressible and was ideal to reduce the air volume of the tank. Air volume was indicated on a transparent vertical tube on the side of the tank. The tank was completely filled with water, weighted and then gradually emptied whilst calibrating the volume based on the weight. Water supply and outlet were at the bottom and air pressure supply at the top of the tank. See laboratory picture of the tank in Figure 21 and manufacturing drawing in Figure 63.

Figure 21 :- Tank with clear tube to monitor air volume

3.4.4. Cushion volume for low natural frequency

Ideally the air suspension cushion designer will consider a system that can be "pumped up" using normal tyre air pressure at a filling station or similar. The internal static pressure should therefore not exceed 300kPa. This means that for a

seated man with apparent mass of 60kg the minimum pressure area would be P=mg/A:

$$area = \frac{seatedmass \times gravitational\_acceleration}{\Pr essure} = \frac{60 \times 9.81}{300000} = 0.01962m^2$$

This is also the area that will be considered in the calculation of the air suspension cushion dynamic characteristics. If the piston is round, then its diameter will be 158mm.

An ideal piston type air suspension cushion with rigid sides and only the upper and lower surfaces moving relative to each other can have the following spring coefficient:

$$k = \frac{A_c^2 \times \gamma \times P_0}{V_c} \tag{5}$$

Where γ is the specific heat ratio of air normally 1.4

A_c is the area of the piston / cushion

P_0 is the static pressure in the system

V_c is the volume of the system

It is known that for a single degree of freedom spring mass system the natural frequency is described as follows:

$$f_n = \frac{1}{2\pi}\sqrt{\frac{k}{m}} \tag{6}$$

Ideally a human sitting (60kg seated mass) on a suspension cushion should have a natural frequency of lower than 2Hz. Solve equation (6) with natural frequency f =2 and seated mass m = 60kg. The result is k = 9474.8 N/m. Substituting k = 9474.8 N/m, A=0.01962 m^2, γ =1.4 and P_0=300000 Pa into Equation 2; we calculated the cushion volume to be V=0.017m^3 - roughly a minimum of 17 litres. The sizes and capacities determined above are within designable reach and therefore we can assume that such a cushion design is viable and can be implemented.

3.4.5. The influence of mass on the performance of the cushion

It may be important to note at this stage that the natural frequency of an air spring (or air suspension cushion) is independent of the mass on the airspring as long as V_0 is constant. Stiffness of an adiabatic air spring is given by:

$$k = \frac{\gamma A^2 P_0}{V_0} \tag{7}$$

The pressure inside the airspring is due to the gravitational force of the supported mass:

$$P_0 = \frac{Mg}{A} \tag{8}$$

Substituting

$$k = \frac{\gamma A M g}{V_0} \tag{9}$$

Calculate natural frequency

$$f_n = \frac{1}{2\pi}\sqrt{\frac{k}{M}} = \frac{1}{2\pi}\sqrt{\frac{\gamma A g}{V_0}} \tag{10}$$

from which it is seen that the only determinant variables are the pressure area and the volume. If the airspring area is constant at all working heights we can simplify the natural frequency to:

$$f_n = \frac{1}{2\pi}\sqrt{\frac{\gamma g}{h_0}} \tag{11}$$

where h_0 is the working height. The above is linearization of the airspring. Any airspring or cushion considered to operate at a set working height which is near its linear spring range.

3.4.6. Shock limiting valve

The purpose of the shock limiting valve is to act during floor shocks by dumping overpressure air mass in the cushion through a pipe into the tank. The valve is mounted in the upper part of the cushion described as the buttock interface. It is designed that the valve will open at a set upward acceleration of the buttock interface. The accelerations at which the valve opens can be set from a lower limit of 5 m/s^2 up to 50m/s^2. This setting is changeable by adjusting a screw with a screwdriver, which tensions a spring. The spring holds the valve closed, counteracting a small mass which opens the valve during acceleration.

4. Analysis and Simulation

In this chapter the seated human body model on an air suspension cushion with special anti-resonance properties is considered. The human model used is taken from the literature and the analytical model of the cushion was derived from first principles. Simulink is used to simulate the system and predict a transmissibility curve from varying system parameters. The Simulink model is used for both a simple mass and a human dummy model from the literature on the cushion. The combination is for the designer to first verify the performance of his cushion with a single mass before incurring the expense of human subject testing.

4.1. Human Model:

The mechanical impedance of a seated human body is different from that of a single mass. In the literature section 2.3 several human models are mentioned. A human model with the following qualities is required:

- A model with z-axis only. Various in-field studies on off road forestry vehicles show that the human whole body vibration exposure is higher in the z-axis than in the x, or y axes. Multi-axis vdv is dominated by vibration inputs in the z-axis.
- A model that is internationally recognised by experts in suspension seat evaluation.
- A model that can be mathematically interfaced with the basic principles of multi degree of freedom spring mass damper systems.
- A model that is not overly complicated to simulate in Matlab / Simulink.
- A model that closely resembles the apparent mass of the human body when seated in an erect posture.
- A model which can be removed and replaced with a static mass to evaluate the dynamic properties of the air suspension cushion system.

Section 2.3 mentions a specific human model by Wei & Griffin (1998a). This model complies with all the qualities required earlier. In brief description of the model is shown in Figure 22 and Table 1 :

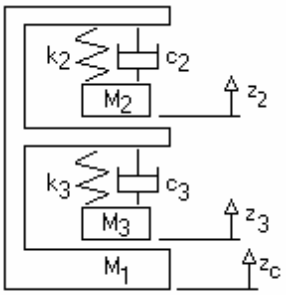

Figure 22 :- Model of the seated human body (Wei and Griffin 1998a)

Where k_2 and k_3 are spring coefficients, c_2 and c_3 are damping coefficients and M_1, M_2 andM_3 are masses in the model. The use of non-capital variables in the model does not indicate variation with time, as indicated in 4.2, but is used to match the model symbols in the literature.

Table 1 :- Parameters to simulate a seated human body according to Wei & Griffin (1998a)

Sitting Mass Scale (kg)	k_3 (N/m)	c_3 (Ns/m)	k_2 (N/m)	c_2 (Ns/m)	M_1 (kg)	M_3 (kg)	M_2 (kg)
40	27982	627	22728	281	604	27.7	6.0
50	34977	783	28410	352	8.0	34.6	7.4
60	41973	940	34092	422	9.6	41.5	8.9
70	48968	1096	39774	493	11.2	48.4	10.4
80	55965	1253	45432	564	12.8	55.3	11.9
90	62780	1404	51495	644	14.4	62.2	13.5

4.2. Air suspension cushion & tank definitions:

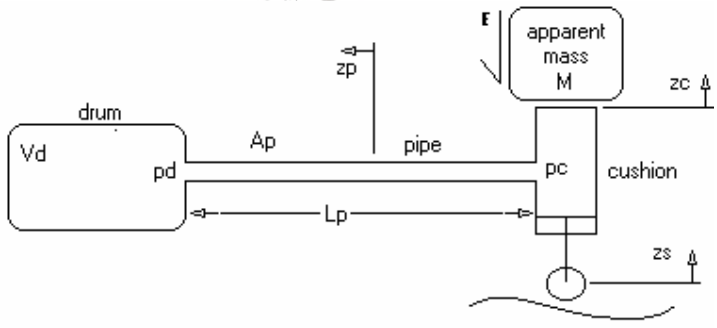

Figure 23 :- Schematic model of cushion with pipe and tank

Symbols by definition will be written in capitals if the variable parameter does not change with time. For example P_A and V_d. Variables that do change with time are written in small letters. Examples are z_c and p_c. Where the time variate (t) is omitted it is to unclutter the formulas, and have the same meaning for example $z_c(t)=z_c$; and $z_p(x)=z_p(x,t)$. The exceptions is g- gravitational acceleration and variables with Greek symbols where a small letter is used even though it does not vary with time. Lowercase 't' is used for time only and where uppercase 'T' varies with time, T(t) is used.

Displacement symbols:

All displacements, velocities and accelerations are absolute and not relative to another point on the system or vehicle.

z_s – displacement of the seat output and input to the cushion in the z-axis, normally measured on the cabin floor; units in meter

z_c – displacement of the cushion top and input to the human body in the z-axis; units in meter

z_p – displacement of the air "plug" in the pipe as measured where the pipe is attached to the cushion; units in meter

h_c – height of cushion $h_c = z_c - z_s$ in meter

Human model:

M_1 – mass one of the human model (kilogram)

M_2 – mass two of the human model (kilogram)

M_3 – mass three of the human model (kilogram)

K_2 – stiffness of the spring between masses one and two as per the human model (Newton/meter)

K_3 - stiffness of the spring between masses one and three as per the human model (Newton/meter)

C_2 – damping coefficient between masses one and two as per the human model (Newton seconds /meter)

C_3 – damping coefficient between masses one and three as per the human model (Newton seconds /meter)

z_2 – displacement of the second mass representing the human body (meter)

z_3 – displacement of the third mass representing the human body (meter)

Cushion parameters:

A_c – area cushion; units in square meter (m^2)

A_p – area pipe; units in square meter (m^2)

L_p, L – length of pipe; units in meter (m)

V_c - volume of cushion with the human body sitting and pressure in cushion is P_0 should the magnitude of this volume vary with time it is shown as $V_c(t)$ or lowercase v_c); units in cubic meter (m^3)

V_d – volume of tank with the human body sitting and pressure in cushion is P_0; units in cubic meter (m^3)

m_p – mass of the air in the pipe; units in kilogram (kg)

m_c – mass of the air in the cushion; units in kilogram (kg)

m_d – mass of the air in the tank; units in kilogram (kg)

T – temperature, T(t) indicates that temperature varies with time; units in Kelvin (K)

T_0 – average temperature; units in Kelvin (K)

P_A – atmospheric pressure; units in Pascal (Pa)

μ- friction of air in pipe; unitless

ρ – density; units in kilogram per cubic meter (kg/m^3)

P_0 – total static pressure inside cushion, pipe, and tank system, which is the sum of the atmospheric pressure and the added pressure due to the static weight of the human body on the cushion; units in Pascal (Pa)

$p_c = p_c(t)$ – pressure inside cushion which dynamically fluctuates around P_0 and can be positive or negative; units in Pascal (Pa)

$p_d = p_d(t)$ - pressure inside tank which dynamically fluctuates around P_0 and can be positive or negative. Differences between p_d and p_c propels the air mass in the pipe forwards and backwards; units in Pascal (Pa)

External forces:

F-any force acting on the mass m_1, should the magnitude of this force vary with time it is shown as lowercase f or f(t). units in Newton (N)

General symbols and constants:

g = gravitational acceleration normally 9.81 meter/second squared (m/s^2)

R = gas constant of dry air – normally 287 Joule/kilogram/Kelvin

π = ratio between a circle circumference and diameter (unitless)

γ = 1.4 is the specific heat ratio for diatomic gasses like O_2 an N_2 at ordinary temperatures. ; unitless

Energy and work:

E = energy; units in Joule (J)

W= work done; units in Joule (J)

4.3. Formulas and calculations:

Consider Newton's law on the piston mass in the cushion Figure 23:

$$0 = -P_A.A_c - M.(\ddot{h}_c(t) + \ddot{z}_s(t)) - f(t) + p_c(t).A_c - M.g$$

where M is the apparent mass of the object supported by the cushion and f(t) is a time dependent force working down on the mass. Rearranging we get:

$$\ddot{h}_c(t) = -\ddot{z}_s(t) - g - \frac{f(t) + P_A.A_c - p_c(t).A_c}{M} \tag{12}$$

We consider an adiabatic process of air flow through the pipe as no heat is added to or taken away from the closed system, therefore according to Daugherty and Franzini (1977):

$$p_c v_c^{\gamma} = \text{constant} \tag{13}$$

Derive the equations of motion for the various elements of the air suspension cushion system. Dynamic force balances are considered to produce variables for a state space linear system. Ensure that the wavelength of the acoustic pressure wave running in the pipe is more than 10 times longer than the pipe length itself. The pressure gradient is then close to linear and similar to the density. The average of the density in the cushion and that in the tank can therefore be used.

We need to determine the average system operating pressure to ensure that the system can be inflated with normal "filling station" air pressure. We determine the static pressure in the system when in rest. The gravitational force on the mass has the pressure. i.e.:

$$P_0 = P_A + \frac{M.g}{A_c}$$

where t=0 and normal atmospheric pressure P_A = 101325Pa

Therefore the density of the air in the system is dependant on the area of the cushion and the mass of the object that the cushion supports.

4.3.1. System condition equations

4.3.1.1. Constant mass rule

The mass of air in the system will remain constant:

$$m_c(t) + m_d(t) + m_p(t) = m_{system}$$

where m_{system} is constant

The initial condition:

$$m_{system} = \frac{P_0.v_{system}}{R.T_0} = \frac{P_0.(v_c + V_p + V_d)}{R.T_0} = \frac{P_0.(h_c(0).A_c + L._p A_p + V_d)}{R.T_0}$$

where P_0 =pressure in due to gravitation force on the mass supported by the cushion, T_0 is the system temperature equal to the ambient temperature if the system has been in equilibrium for a while. $h_c(t) = z_c(t) - z_s(t)$ is the working height of the cushion. The mass in the pipe is:

$$m_p = \frac{P_0.(h_c(0).A_c + L.A_p + V_d)}{R.T_0} - m_c - m_d \qquad (14)$$

Take the time derivative:

$$\dot{m}_p(t) = -(\dot{m}_c(t) + \dot{m}_d(t)) \qquad (15)$$

For each part of the system mass equals density times volume; $m = \rho v$ and similarly the time derivative is

$$\dot{m} = \dot{\rho} v + \rho \dot{v}$$

So we can write the mass equation as:

$$\dot{\rho}_c.v_c + \rho_c \dot{v}_c + \dot{\rho}_d V_d + \rho_d \dot{V}_d + \dot{\rho}_p V_p + \rho_p \dot{V}_p = 0$$

But since the volume of the tank and the volume of the pipe is constant, the time derivatives $\dot{V}_d = 0$ and $\dot{V}_p = 0$. The mass equation reduces to

$$\dot{\rho}_c.v_c + \rho_c \dot{v}_c + \dot{\rho}_d V_d + \dot{\rho}_p V_p = 0$$

We can write cushion volume in terms of the cushion area A_c and the working height of the cushion $h_c(t)$.

$$v_c(t) = A_c.h_c(t) \tag{16}$$

with its time derivative

$$\dot{v}_c(t) = A_c.\dot{h}_c(t)\,.$$

Similarly for the pipe the volume is related to the pipe area A_p and pipe length L_p.

$$V_p = A_p.L_p\ .$$

The tank and pipe volumes remain constant which we can measure experimentally. No derivative equation as the volume is constant.

The mass equation then becomes:

$$\dot{\rho}_c(t).A_c.h_c(t) + \rho_c(t)A_c\dot{h}_c(t) + \dot{\rho}_d(t).V_d + \dot{\rho}_p(t).A_p.L_p = 0 \tag{17}$$

Rearranging

$$\dot{\rho}_p(t).A_p.L_p = -\dot{\rho}_c(t).A_c.h_c(t) - \rho_c(t)A_c\dot{h}_c(t) - \dot{\rho}_d(t).V_d\,0$$

And

$$\dot{\rho}_p(t) = -\frac{\dot{\rho}_c(t).A_c.h_c(t) + \rho_c(t)A_c\dot{h}_c(t) + \dot{\rho}_d(t).V_d}{A_p.L_p} \tag{18}$$

4.3.1.2. System Status in each volume

For **adiabatic** condition in the system, the following apply:

$p(t).v^{\gamma}(t) = k$, from (13), where the specific heat ratio γ is 1.4 for **adiabatic** expansion of air, and k is constant over time

Taking the time derivative:

$$\dot{p}(t).v^{\gamma}(t) + p(t).\gamma.v^{\gamma-1}(t).\dot{v}(t) = 0 \tag{19}$$

Also for air behaving like an **Ideal Gas**:

$$p(t).v(t) = m(t).R.T(t) \tag{20}$$

With time derivative of:

$$\dot{p}(t).v(t) + p(t).\dot{v}(t) = \dot{m}(t).R.T(t) + m(t).R.\dot{T}(t) \tag{21}$$

But with

$$\rho(t) = \frac{m(t)}{v(t)}$$

We get

$$p(t) = \rho(t).R.T(t)$$

With a time derivative of

$$\dot{p}(t) = \dot{\rho}(t).R.T(t) + \rho(t).R.\dot{T}(t) \tag{22}$$

From (19)

$$\dot{p}(t) = -\frac{p(t).\gamma.v^{\gamma-1}(t).\dot{v}(t)}{v^{\gamma}(t)} = -\frac{p(t).\gamma.\dot{v}(t)}{v(t)} \tag{23}$$

Substitute into (21)

$$-\frac{p(t).\gamma.\dot{v}(t)}{v(t)}.v(t) + p(t).\dot{v}(t) = \dot{m}(t).R.T(t) + m(t).R.\dot{T}(t) \tag{24}$$

Rearrange

$$p(t).\dot{v}(t).(1-\gamma) = \dot{m}(t).R.T(t) + m(t).R.\dot{T}(t) \tag{25}$$

4.3.2. Dynamics of system elements

4.3.2.1. Force balance on air in pipe:

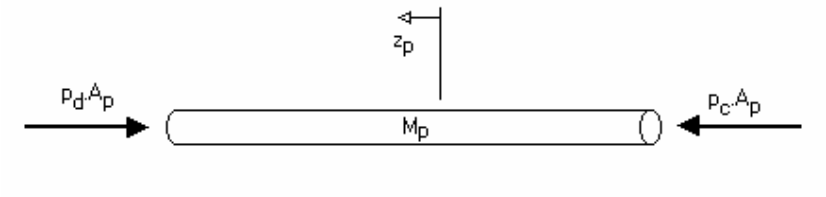

Figure 24 :- Force balance on air in pipe

Take the mass flow rate as $\dot{m}(t) = u(t)$ [kg/s] in the pipe in the direction of z_p. As air is compressible, the flow rate along the pipe may vary. Define therefore the distance x along the length of the pipe from the cushion to the tank. The mass flow rate at x is then u(x,t). We know that the density at the cushion $\rho_c(t)$ and at the tank $\rho_d(t)$ are not equal due to the difference in pressure between the tank and the pipe. Close to the cushion where x=0, the air has a velocity of

$$\dot{z}_p(0) = \frac{u(0,t)}{\rho_c.A_p}$$

and close to the tank where x = L

$$\dot{z}_p(L) = \frac{u(L,t)}{\rho_d.A_p}.$$

Which in general at position x along the pipe equates to:

$$\dot{z}_p(x,t) = \frac{u(x,t)}{\rho_p(x,t).A_p} \tag{26}$$

The time derivative will be

$$\ddot{z}_p(x,t) = \frac{\dot{u}(x,t).\rho_p(x,t) - u(x,t).\dot{\rho}_p(x,t)}{\rho_p^2(x,t).A_p}$$

Rewriting

$$\ddot{z}_p(x,t).\rho_p(x,t).A_p = \dot{u}(x,t) - \frac{u(x,t).\dot{\rho}_p(x,t)}{\rho_p(x,t)} \tag{27}$$

The airspeeds at the tank entrance and at the cushion entrance are not the same. As friction is dependent on speed, this speed variation will render friction variation along the pipe. As stated previously the wavelength of the acoustic pressure wave travelling in the pipe is substantially longer than the pipe length. We can therefore consider the pressure drop over the length of the pipe to be near linear. The density increase and the airspeed increase over the length of the pipe are therefore linear.

Ignoring friction for a moment, consider the force balance over a small length of pipe dx at distance x from the cushion end of the pipe:

$$-\rho_p(x,t).A_p.dx.\ddot{z}_p(x,t) + p_p(x,t).A_p - (p_p(x,t) + dp_x).A_p = 0 \tag{28}$$

where dp_x is the pressure variation over the small length dx and $p_p(x,t)$ is the pressure at any point x along the length of the pipe.

We suggested earlier that this pressure variation dp_x is linear i.e.:

$$dp_x = (p_d - p_c).\frac{dx}{L}$$

And for density

$$\rho_p(x,t) = (\rho_d(t) - \rho_c(t)).\frac{x}{L} + \rho_c(t)$$

With a time derivative of

$$\dot{\rho}_p(x,t) = (\dot{\rho}_d(t) - \dot{\rho}_c(t)).\frac{x}{L} + \dot{\rho}_c(t) \tag{29}$$

Substituting into the force balance equation ((28):

$$\dot{u}(x,t).dx. - \frac{u(x,t).[(\dot{\rho}_d - \dot{\rho}_c).\frac{x}{L} + \dot{\rho}_c]}{(\rho_d - \rho_c).\frac{x}{L} + \rho_c}.dx + (p_d - p_c).\frac{dx}{L} = 0$$

divide by dx

$$\dot{u}(x,t) = u(x,t)\frac{\dot{\rho}_d.x + \dot{\rho}_c(L-x)}{\rho_d.x + \rho_c(L-x)} + \frac{p_c - p_d}{L}$$

substitute x=0, the mass flow change is:

$$\ddot{m}_c(t) = \dot{u}(0,t) = \dot{m}_c(t).\frac{\dot{\rho}_c(t)}{\rho_c(t)} + \frac{p_c(t) - p_d(t)}{L} \tag{30}$$

And at the tank where x=L:

$$\ddot{m}_d(t) = \dot{u}(L,t) = \dot{m}_d(t).\frac{\dot{\rho}_d(t)}{\rho_d(t)} + \frac{p_c(t) - p_d(t)}{L} \tag{31}$$

But from equation (15)

$$\dot{m}_p(t) = -(\dot{m}_c(t) + \dot{m}_d(t))$$

With time derivative

$$\ddot{m}_p(t) = -(\ddot{m}_c(t) + \ddot{m}_d(t)) \tag{32}$$

$$\ddot{m}_p(t) = -\left[\dot{m}_c(t).\frac{\dot{\rho}_c(t)}{\rho_c(t)} + \dot{m}_d(t).\frac{\dot{\rho}_d(t)}{\rho_d(t)} + 2\times\frac{p_c(t) - p_d(t)}{L}\right] \tag{33}$$

To simplify we consider the mass in the pipe as a lump mass, the whole mass will move as a unit. We can say from above that:

$$u(t) = \dot{z}_p.\rho_p.A_p = \dot{z}_p.\frac{m_p}{V_p}.A_p = \dot{z}_p.\frac{m_p}{L_p.A_p}.A_p = \dot{z}_p.\frac{m_p}{L_p}$$

where $\dot{z}_p$ is the average speed (flow in pipe is simplified to laminar flow) over the length of the pipe and ρ_p is the average density over the length of the pipe.

Taking the time derivative:

$$\dot{u}(t) = \ddot{z}_p.\frac{m_p}{L} + \dot{z}_p.\frac{\dot{m}_p}{L} \tag{34}$$

This gives the relationship between the mass flow rate and the actual velocity of the air in the pipe.

4.3.2.2. Inertia of the air slug in the pipe

We have to take into consideration the inertia of the air mass in the pipe. According to Helmholtz principle the mass of the air will cause it to resonate with the spring created in both the tank and the cushion volumes. Taking pipe flow friction into account the force balance equation will be:

$$-m_p\ddot{z}_p + p_c A_p - p_d A_p - \mu.\dot{z}_p = 0 \tag{35}$$

Replacing $m_p.\ddot{z}_p = \dot{u}(t).L - \dot{z}_p.\dot{m}_p$ from equation (34)

$$-\dot{u}(t)L + \dot{z}_p\dot{m}_p + p_c A_p - p_d A_p - \mu.\dot{z}_p = 0 \tag{36}$$

Substituting $\dot{z}_p = u(t).\frac{L}{m_p}$

$$\dot{u}(t) = +\frac{u(t)}{m_p}(\dot{m}_p - \mu) + \frac{p_c A_p}{L} - \frac{p_d A_p}{L} \tag{37}$$

4.3.2.3. Equation of state regarding the change of mass flow rate in the pipe

But substituting $\dot{m}_p(t)$ from equation (15) and $u(t) = \dot{m}_d = -\dot{m}_c$:

$$\dot{u}(t) = -\frac{u(t)\mu}{m_p} + \frac{p_c A_p}{L} - \frac{p_d A_p}{L} \tag{38}$$

substituting equation (14)

$$\dot{u} = -u\left(\frac{\mu}{\frac{P_0(h_c(0).A_c + LA_p + V_d)}{R.T_0} - m_c - m_d}\right) + \frac{p_c.A_p}{L} - \frac{p_d.A_p}{L} \tag{39}$$

4.3.2.4. Force balance on Static Mass

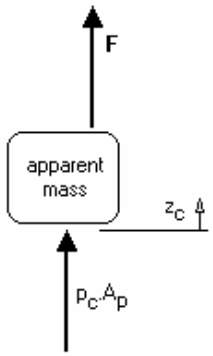

Figure 25 :- Force balance on apparent mass

Initially we assume the apparent mass (M) is a simple static mass with no inherent damping or multi degree of freedom characteristics.

F is any arbitrary static force that may do work on the mass M. If F = F(t) we define f= F(t) as the time varying force.

$$f + p_c.A_c - M.\ddot{z}_c = 0 \tag{40}$$

4.3.2.5. Pressure expansion balance on tank.

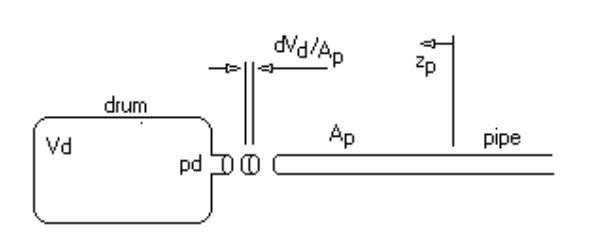

Figure 26 :- Pressure expansion balance on tank

Rearranging equation (13)

$$\dot{p}_d(t). = -\frac{p_d(t).\dot{v}_d(t)}{v_d(t)} + \frac{\dot{m}_d(t).R.T_d(t)}{v_d(t)} + \frac{m_d(t).R.\dot{T}_d(t)}{v_d(t)}$$

but the tank volume is constant with $\dot{v}_d = 0$, therefore:

$$\dot{p}_d(t). = \frac{\dot{m}_d(t).R.T_d(t)}{v_d(t)} + \frac{m_d(t).R.\dot{T}_d(t)}{v_d(t)}$$

replace RT with $p_d.v_d / m_d$ and $u(t) = \dot{m}_d(t)$ and rearrange:

$$\dot{p}_d(t) = u_d(t).\frac{p_d(t).}{m_d(t)} + \frac{m_d(t).R.\dot{T}_d(t)}{v_d(t)} \tag{41}$$

Which renders a relationship between the time derivative of the pressure in the tank and other state parameters, however the time derivative of the Temperature in the tank needs to be defined.

4.3.2.6. Energy balance on the tank

We consider the tank to be closed and isolated, so no energy can enter or leave the system by means of heat transfer.

The energy in the tank can be written as:

$$E(t) = m_d(t).c_v.T_d(t)$$

The change in the state of energy over time will be the time derivative:

$$\dot{E}(t) = \dot{m}_d(t).c_v.T_d(t) + m_d(t).c_v.\dot{T}_d(t)$$

The only occurrence of change in energy in the tank will be when there is mass flow between the tank and the pipe.

The work done on the air on the tank by the mass inflow is:

$$\dot{W}(t) = -\frac{p_d(t)}{\rho_d(t)}.\dot{m}(t)$$

Therefore the energy flow is

$$m_d(t).c_v.\dot{T}_d(t) + \dot{m}_d(t).c_v.T_d(t) = +\frac{p_d(t)}{\rho_d(t)}.\dot{m}_d(t) \tag{42}$$

This defines the time derivative of the temperature in the tank as:

$$\dot{T}_d(t) = \frac{\dot{m}_d(t)}{m_d(t)}.(\frac{p_d(t)}{\rho_d(t).c_v} - T_d(t)) \tag{43}$$

replace RT with P_d / ρ_d :

$$\dot{T}_d(t) = \frac{\dot{m}_d(t)}{m_d(t)}.(\frac{p_d(t)}{\rho_d(t).c_v} - \frac{p_d(t)}{\rho_d.R})$$

rearranging

$$\dot{T}_d(t) = \frac{\dot{m}_d(t).p_d(t)}{m_d(t).\rho_d(t)}.(\frac{1}{c_v} - \frac{1}{R})$$

Noting that the rate of mass flow from the pipe to the tank is $u(t) = \dot{m}_d(t)$ then

$$\dot{T}_d(t) = \frac{u(t).p_d(t)}{m_d(t).\rho_d(t)}.(\frac{1}{c_v} - \frac{1}{R}) \quad (44)$$

Or similarly replacing P_d / ρ_d with RT:

$$\dot{T}_d(t) = \frac{\dot{m}_d(t).T_d(t)}{m_d(t)}.(\frac{R.}{c_v} - 1)$$

Noting that the rate of mass flow from the pipe to the tank is $u(t) = \dot{m}_d(t)$ then

$$\dot{T}_d(t) = \frac{u(t).T_d(t)}{m_d(t)}.(\frac{R.}{c_v} - 1) \quad (45)$$

4.3.2.7. State equation for the pressure in the tank

We can now substitute equation (45) into equation (41) :

$$\dot{p}_d(t) = u(t).\frac{p_d(t).}{m_d(t)} + \frac{m_d(t).R.\frac{u(t).T_d(t)}{m_d(t)}.(\frac{R.}{c_v} - 1)}{v_d(t)}$$

rearranging and replacing with $p_d = \frac{m_d.RT_d}{v_d}$

$$\dot{p}_d(t) = u(t).\frac{p_d(t).}{m_d(t)} + \frac{u(t).p_d(t)}{m_d(t)}.(\frac{R.}{c_v} - 1)$$

Again

$$\dot{p}_d(t) = \frac{u(t).p_d(t).R}{m_d(t).c_v} \quad (46)$$

4.3.2.8. Pressure / Volume expansion balance in the cushion

As we defined the relationship between p_d and z_p for the tank, we can define the relationships amongst p_c, z_c, z_s, z_p.

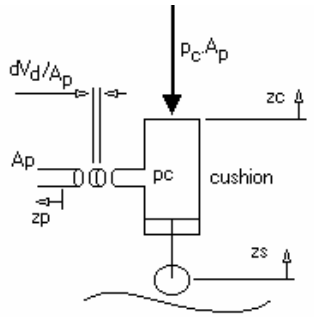

Figure 27 :- Pressure / volume expansion balance on the cushion

Apply equation (19) to the cushion:

$$\dot{p}_c(t).v_c^{\gamma}(t) + p_c(t).\gamma.v_c^{\gamma-1}(t).\dot{v}_c(t) = 0 \tag{47}$$

Multiply by cushion volume:

$$\dot{p}_c(t) + \frac{p_c(t).\gamma}{v_c(t)}.\dot{v}_c(t) = 0 \tag{48}$$

And from (16)

$$\dot{p}_c(t) = -\frac{p_c(t).\gamma}{A_c.h_c(t)}.A_c\dot{h}_c(t) = -\frac{p_c(t).\gamma}{h_c(t)}.\dot{h}_c(t) \tag{49}$$

This gives a relationship for the expansion of the air in the cushion only, and does not take into account the air that may flow into the pipe. This will be used in the Simulink model to compare to the system having zero pipe diameter and zero tank volume.

Apply equation (21) to the cushion

$$\dot{p}_c(t) = -\frac{p_c(t).\dot{v}_c(t)}{v_c(t)} + \frac{\dot{m}_c(t).R.T_c(t)}{v_c(t)} + \frac{m_c(t).R.\dot{T}_c(t)}{v_c(t)}$$

replace RT with $p_c.v_c / m_c$ and $u(t) = -\dot{m}_c(t)$ and $v_c(t) = A_c.h_c(t)$ and its derivative:

$$\dot{p}_c(t) = -\frac{p_c(t).\dot{h}_c(t)}{h_c(t)} - \frac{u(t).p_c(t)}{m_c(t)} + \frac{p_c(t).\dot{T}_c(t)}{T_c(t)} \tag{50}$$

Which renders a relationship between the time derivative of the pressure in the cushion and other state parameters, however the time derivative of the temperature in the tank needs to be defined.

4.3.2.9. Energy balance on the cushion

Consider the system to be closed and isolated, so no energy can enter or leave the system by means of heat transfer.

The energy in the system can be written as:

$$E(t) = m_c(t).c_v.T_c(t)$$

The change in the state of energy over time will be the time derivative:

$$\dot{E}(t) = \dot{m}_c(t).c_v.T_c(t) + m_c(t).c_v.\dot{T}_c(t)$$

There are only two occurrences of change in energy in the cushion, when there is work done on the air in the cushion by the mass flow $\dot{m}_c$ from the pipe to the cushion (similar to that in the tank), and secondly when work is done by the air in the cushion against an external force. The total work rate by the air is:

$$\dot{W}(t) = -\frac{p_c(t)}{\rho_c(t)}.\dot{m}_c(t) + A_c.p_c(t).\dot{h}(t)$$

So the energy change rate of the air in the cushion is:

$$m_c(t).c_v.\dot{T}_c(t) + \dot{m}_c(t).c_v.T_c(t) = +\frac{p_c(t)}{\rho_c(t)}.\dot{m}_c(t) - A_c.p_c(t).\dot{h}(t) \quad (51)$$

Noting that the rate of mass flow from the cushion to the pipe is $u(t) = -\dot{m}_c(t)$ then

$$m_c(t).c_v.\dot{T}_c(t) - u_c(t).c_v.T_c(t) = -\frac{p_c(t)}{\rho_c(t)}.u(t) - A_c.p_c(t).\dot{h}(t)$$

Replace P_c/ρ_c with R.T_c and rearrange

$$\dot{T}_c(t) = \frac{u_c(t).T_c(t)}{m_c(t)}.[1-\frac{R}{c_v}] - \frac{A_c.p_c(t).\dot{h}(t)}{m_c(t).c_v} \quad (52)$$

4.3.2.10. State equation for the pressure in the cushion

Substitute equation (52) into equation (50):

$$\dot{p}_c(t) = -\frac{p_c(t).\dot{h}_c(t)}{h_c(t)} - \frac{u(t).p_c(t)}{m_c(t)} + \frac{p_c(t).[\frac{u_c(t).T_c(t)}{m_c(t)}.(1-\frac{R}{c_v}) - \frac{A_c.p_c(t).\dot{h}(t)}{m_c(t).c_v}]}{T_c(t)}$$

rearrange after replacing $p_c = \frac{m_c.R.T_c}{v_c}$

$$\dot{p}_c(t) = -\frac{p_c.\dot{h}_c}{h_c} - \frac{u.p_c}{m_c} + p_c.[\frac{u_c}{m_c}(1-\frac{R}{c_v}) - \frac{A_c.p_c.\dot{h}}{c_v.m_c.T_c}]$$

now replace $\frac{A_c.p_c}{m_c.T_c} = \frac{R}{h_c}$ in the last part

$$\dot{p}_c(t) = -\frac{p_c.\dot{h}_c}{h_c} - \frac{u.p_c}{m_c} + p_c.[\frac{u_c}{m_c}(1-\frac{R}{c_v}) - \frac{R.\dot{h}}{c_v.h_c}]$$

Rearrange

$$\dot{p}_c(t) = -\frac{p_c(t).\dot{h}_c(t)}{h_c(t)}(1+\frac{R}{c_v}) - \frac{p_c(t).u_c(t)}{m_c(t)}\frac{R}{c_v} \tag{53}$$

From the gas laws of specific heat:

$$R = c_v - c_p \text{ and } \gamma = \frac{c_p}{c_v} \text{ therefore } \gamma = \frac{R}{c_v} + 1$$

And

$$\dot{p}_c(t) = -\frac{p_c(t).\dot{h}_c(t).\gamma}{h_c(t)} - \frac{p_c(t).u_c(t).(\gamma-1)}{m_c(t)} \tag{54}$$

4.4. Equations of State

The equations of state are therefore:

Pressure in the cushion:

$$\dot{p}_c(t) = -\frac{p_c(t).\dot{h}_c(t).\gamma}{h_c(t)} - \frac{p_c(t).u_c(t).(\gamma-1)}{m_c(t)}$$

Pressure in the tank:

$$\dot{p}_d(t) = \frac{u(t).p_d(t).R}{m_d(t).c_v}$$

Mass flow:

$$\dot{u} = -u(\frac{\mu}{\frac{P_0(h_c(0).A_c + LA_p + V_d)}{R.T_0} - m_c - m_d}) + \frac{p_c.A_p}{L} - \frac{p_d.A_p}{L}$$

Cushion height:

$$h_c(t) = z_c(t) - z_s(t) + z_c(0) - z_s(0)$$

4.5. Simulink model

From the equations of state, a Matlab Simulink model was created which is shown with a single solid mass in Figure 73. In an extended model, the solid mass is replaced with a human model. Simulation results from the extended model are shown in Figure 28 and Figure 29 without and with a resonator respectively. Both simulations are with a seated human model. Experimental verification of the model is done in the next chapter.

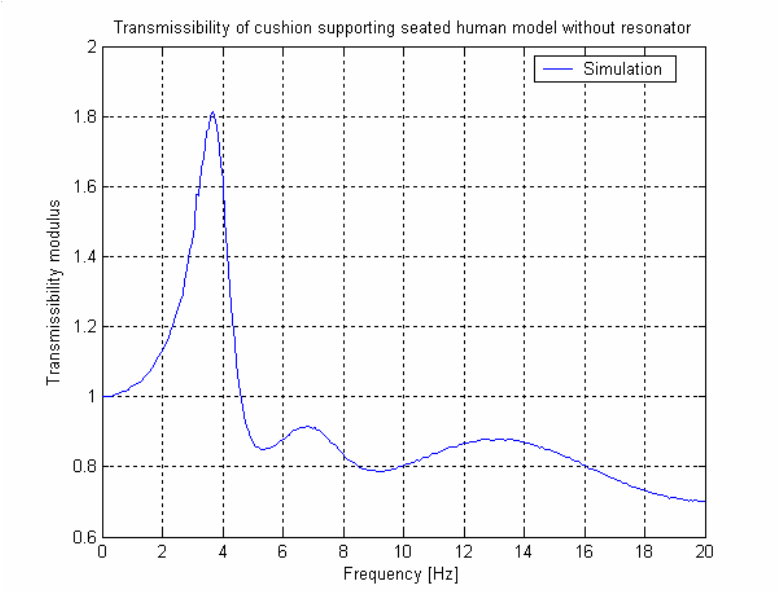

Figure 28 :- Transmissibility curve from model supporting seated human model without resonator

Figure 28 is a simulated transmissibility curve of a human model on a cushion similar to cushion type 2. The shape of the curve is similar to that found in measurements from the literature (Griffin 1990). The first, second and third resonances can be clearly distinguished. Ideally, a suspension seat would attempt to reduce the transmissibility curve to below one at all frequencies. If that were not fully achievable, a reduction of the first peak in both magnitude and frequency would be required.

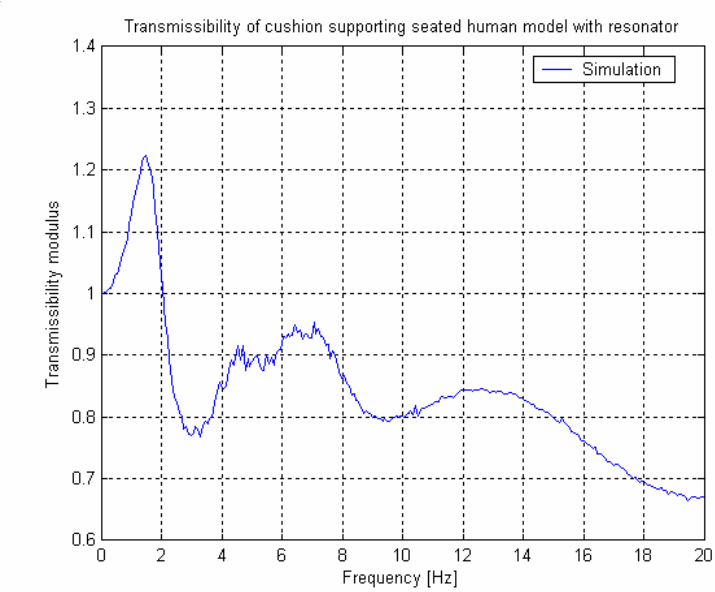

Figure 29 :- Transmissibility curve from model supporting seated human model with resonator

The resonator does not reduce the transmissibility curve to below one at all frequencies, but it does reduce both the frequency and the magnitude of the first peak. A pipe and tank configuration was chosen to demonstrate this effect. Figure 29 show that where the magnitude of the transmissibility curve at 4 Hz was 1.8, the resonator reduced it to less than 0.8. It therefore attenuates at 4Hz instead of amplify as the case with other seats. However, a peak still exists at 1.5Hz, but it is where the human body is less sensitive to vibration according to the ISO 2631 (1997) W_k weighting.

Alternative pipe and tank configurations can be chosen to change the frequency of the anti-resonance. Longer pipes with smaller diameters and larger tank volumes results in the anti-resonance moving towards the lower frequencies.

5. Experimentation

Experimentation is carried out to determine whether theories hold in practice. Often it is not cost effective to test in-field until a concept has been refined and is ready for implementation under real world conditions. This refinement phase is paramount in the development process. During the conceptual phase experimentation was carried out to refine several concepts. In-field tests were done to define the real world problem, and laboratory tests to verify the analytical model.

The conceptual phase suggested two concepts for refinement and testing under laboratory conditions. The torus in foam concept raised many initial questions regarding linearity and ability to isolate vibration as efficiently as the tube torus with constant pressure area. The latter concept was therefore used in experiments to understand the functionality of the pipe and tank resonator. This knowledge of the resonator could then be employed to refine the concept of the tube torus in a foam surround. The tube torus in foam was tested with solid mass and human subjects. From this point regard the 'tube torus in foam with pipe and tank' concept as 'the prototype'.

Similar test setups were used for both cushions except that for the torus with constant pressure area a self levelling control mechanism was used. For the prototype a constant pressure control mechanism was used to maintain working height. The experimental planning describes the various aspects addressed during experimentation and applies equally to both cushions. Supportive information gathered to assist in the concept refinement is mentioned.

The sequence in which this experimentation chapter is presented is not necessarily how it was carried out. It is intended to assist the reader to follow a thought process. The supportive information gathering is mentioned first as it is used in the later experimentation. Secondly various pipe and tank configurations were tested. Thirdly static and dynamic tests are used to determine the influence of varying prototype system parameters. Fourthly the dynamic performance of the prototype was tested with a solid mass and compared to the analytical model. Fifth and final phase of the experimentation was on human subjects to verify that the prototype proves the hypothesis.

5.1. Supportive information gathering

Leading up to the final evaluation of the air suspension cushion, certain sets of data were necessary to support the design process as well as the final evaluation. These included the gathering of actual in-field data to confirm the initial problem statement.

5.1.1. Three-wheeled logger tests

It was required to evaluate a three-wheeled logger to obtain the spectral input signal from below the seat during an in-field operation. Congruently the transmissibility of the existing seat was determined for later comparison with the air suspension cushion. In 2003 in-field tests were conducted on the three-wheeled logger in the Grabouw State Forestry area. The experimental results showed

extreme levels of vibration during stacking tasks and normal field road manoeuvring.

The vehicle is propelled by a hydraulic actuator system driven by a diesel engine pump. The diesel engine is set at constant revolutions during operation, which causes noticeable single frequency vibration. The power spectral density of the acceleration showed this behaviour below and above the seat cushion of the driver. Tests results from the diesel engine at idle revs also contained vibration peaks at certain frequencies. Appendix C contains a concise report on the in-field tests. Figure 30 shows the psd of one in-field run in comparison with the ISO7096 classification for earth moving equipment.

5.1.2. ISO 7096:2000 EM curves

Figure 30 compares the floor acceleration measured below the three-wheeled logger seat with the classes of floor input suggested by ISO 7096:2000. It is evident that the class EM 2 (scraper without axle or frame suspension) and class EM 3 (wheeled loader >4500kg) have frequency peaks closest to that measured on the logger. The resonator parameters chosen during the cushion design to reduce SEAT value on the logger. This could also be suitable for other class EM3 and possible class EM2 vehicles. The acceptance levels for a class EM3 suspension seat shall have a SEAT value of 1.0 or less. The standard also calls for the transmissibility curve at resonance to be less than 1.5 for these classes.

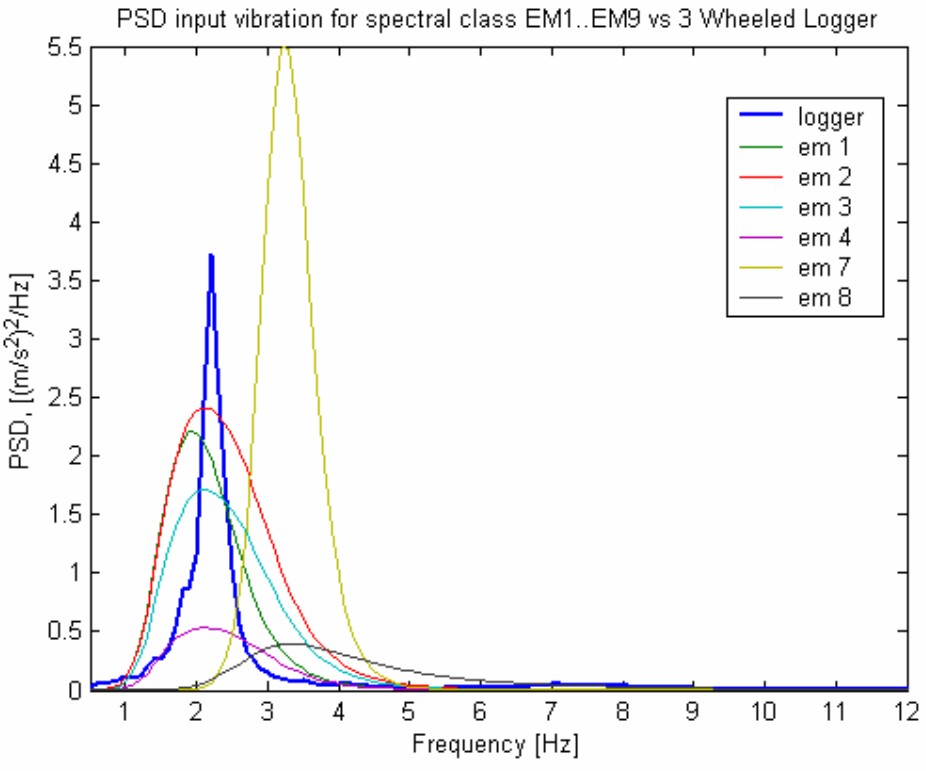

Figure 30 :- relevant ISO 7096 EM curves compared to the input acceleration, measured under the three-wheeled logger seat during in-field operations

5.2. Various pipe and tank configurations

Various pipe and tank configurations were tested with the round torus with constant pressure area supporting a solid mass. The complexities of the human impedance on the cushion and the expected non-linearity of the tube torus without constant pressure area were eliminated.

The round torus with constant pressure reached prototype phase as it was the first concept deemed to render workable results. Constant pressure area during vertical deflection was achieved through a rolling membrane. 40mm pipe connections on both the cushion and the tank were fitted to be easily reducible for smaller pipe diameters. The pipe length was adjusted by replacing the pipe with desired length of pipe. The tank was partly filled with water and the remaining air volume served as the resonator volume. A single mass was placed on the air suspension cushion to achieve a single degree of freedom spring mass system with attached resonator.

Laboratory experiments were carried out with various pipe and tank configurations. These included pipe lengths of 1, 2 and 4 m. Pipe diameters were 15mm, 25mm and 40mm. Tank volumes were 100l, 50l, 20l and 10l. Detail on the experimental procedure is given in appendix A. The obtained results were used as part of the conceptual refinement process and are not detailed here. However, one configuration is mentioned below as an example.

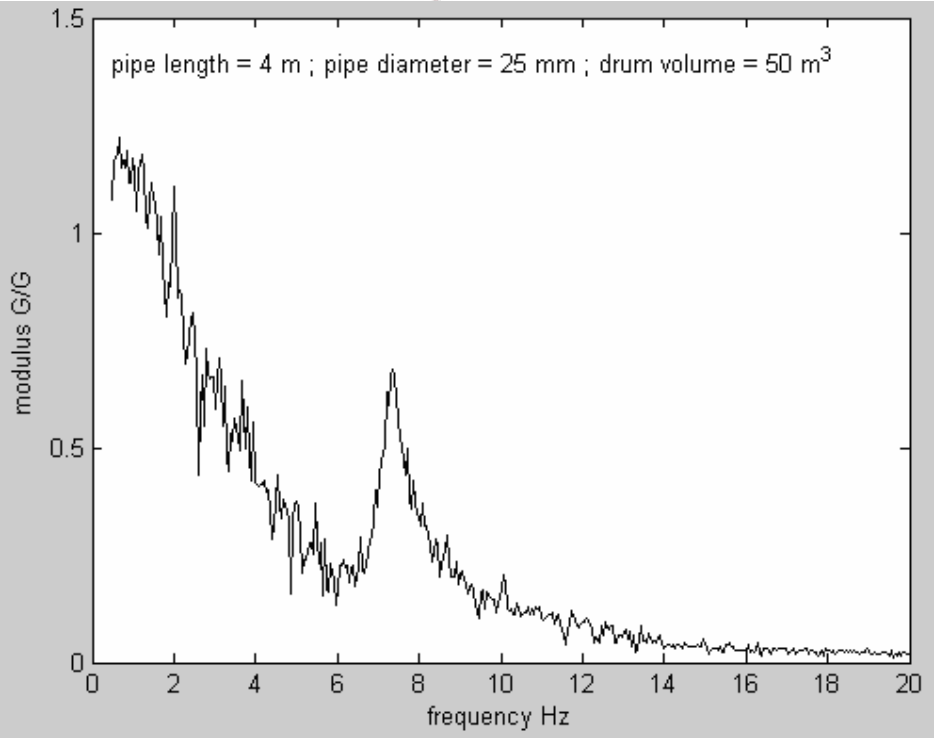

Figure 31 :- Transmissibility curve for steel cushion with static mass

Figure 31 shows the transmissibility curve of the round torus with constant pressure area and 4m long pipe with 25mm diameter and tank volume of 50l. Note the first peak at 1Hz and the second at 7.5Hz. Pipe diameter and length adjustment can be used to manipulate the frequency at which the second peak occurs. Tank volume

adjustment affects the frequency of the first peak slightly. The 25mm diameter pipe used has less friction than a 15mm pipe for the same air volume speed. The larger pipe diameter with less damping is expected to have a lower transmissibility curve modulus at the anti-resonance frequency. It is more suitable to isolate problem frequencies with narrow bandwidth.

It was found that the pipe diameter and length can be adjusted to move the second peak and preceding valley along the frequency axis. Tank volume mainly contributed to the position of the first peak on the frequency axis.

5.3. The influence of varying prototype system parameters

The prototype is a rubber tube of torus shape in a foam surround. No static or dynamic performance data is available on its use as a seat cushion. Spring stiffness is required at various loads, system pressure and pressure areas. It is essential to obtain these parameters to analytically describe the dynamics of the cushion.

A rubber tube torus is known to stretch when subjected to vertical and lateral forces. Its ability to service in motor vehicle wheels under high impact conditions indicates its reliability. In modelling the human airspring system it is required to quantify various parameters of the tube torus. The following relations were determined:

- Pressure area versus static load
- Stiffness coefficient versus load
- Roll resistance versus pressure
- Frequency response of single degree of freedom system versus pressure
- Frequency response of two degree of freedom system versus pressure

5.3.1. Pressure area versus static load

An increase in load on the round tube torus will require an increase in pressure or pressure-area or both. Upward acceleration of the supported mass is considered similar to an increase in load, and downward acceleration a decrease in load. This experiment determines the relationship between increases in load and pressure or pressure area.

The round tube torus is pressurised to an initial pressure where it is fully inflated but not to the extent of deformation due to overpressure. The torus is placed on a glass table after the contact area was sprayed with milk a photograph is taken from directly below the glass to determine the area of contact where the milk was spread. The pressure in the tube is noted using a H_2O manometer. A second photograph is taken from the side of the torus to capture the shape of the torus. Now a rigid wooden board (melamine covered pressed wood) is placed on the torus. Two slots in the board support two metric rulers to indicate the vertical displacement of the torus under load. The two cameras remain still and are triggered by infra red remote control to prevent movement between pictures. Four kilogram loads are added consecutively and the pressure in the torus recorded at the time of the photographs. The size of the pressure area and the shape of the torus under the

pressures are determined by digitising the respective photograph. The photograph is inserted in the background and the graphical plot of the torus outline scaled to fit.

Initially the round tube torus was considered to be not an option due to its shape and possible non-linearity. It was also seen as a solution with a problematic interface to a pipe and tank. Thorough refinement of this concept proved increasingly viable.

Figure 32 shows the digitised tube torus shape under pressure. The graph is scaled to the measurements on the rulers in the picture. The exact diameters are determined for contact outer diameter, contact inner diameter, tubes outer size diameter, and the tubes inner size diameter.

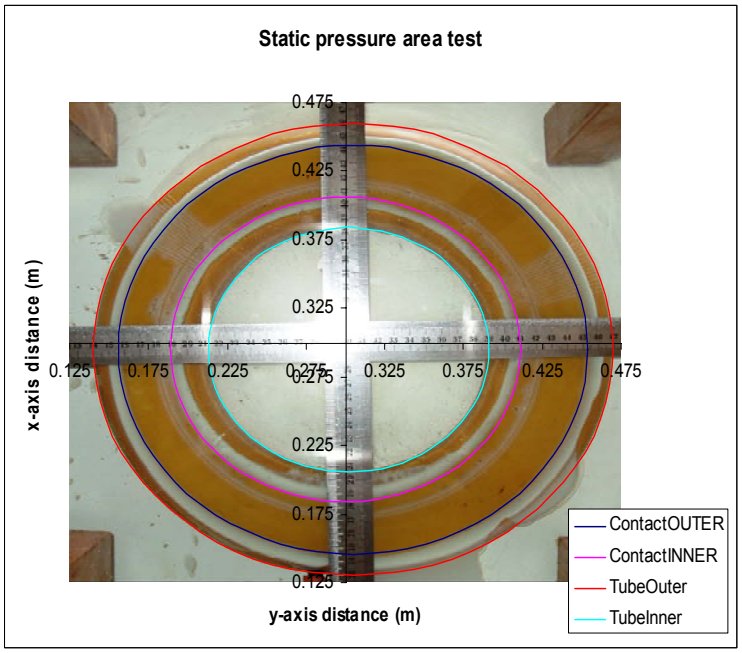

Figure 32 :- Tube torus (digitised) under static load

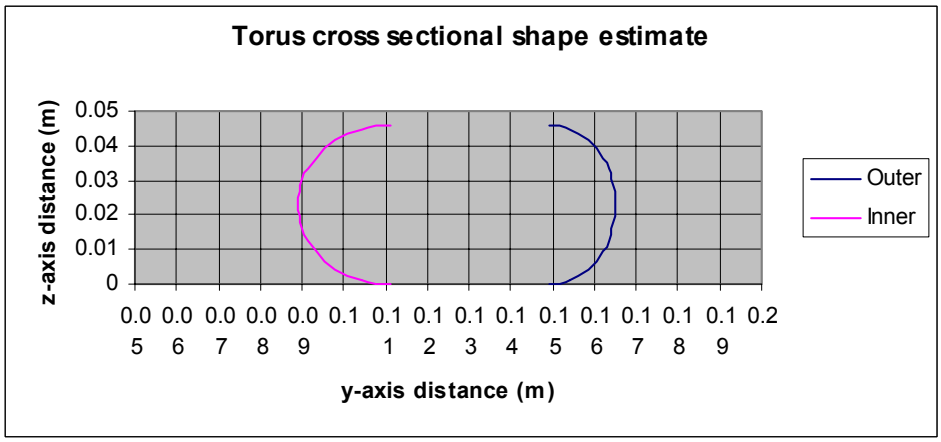

Figure 33 :- Digitised shape of cross sectional through tube torus under load

Figure 33 digitally estimates the cross sectional shape of the tube torus by using the diameters determined. It was found that the best curve fit is an ellipse with near circular shape. The outer circle is less rounded due to circumferal stretch perpendicular to the section. The volume of the torus is mathematically determined from the cross sectional information.

The graph in Figure 34 indicates that the increase in pressure can be approximated linear to the increase in load. It was determined from static measurements with varying loads on the tube torus. 5kPa was chosen as a starting as it relates to a final working pressure of 8 kPa under load of a seated subject. Similarly the pressure area increases almost linearly with the increase in load.

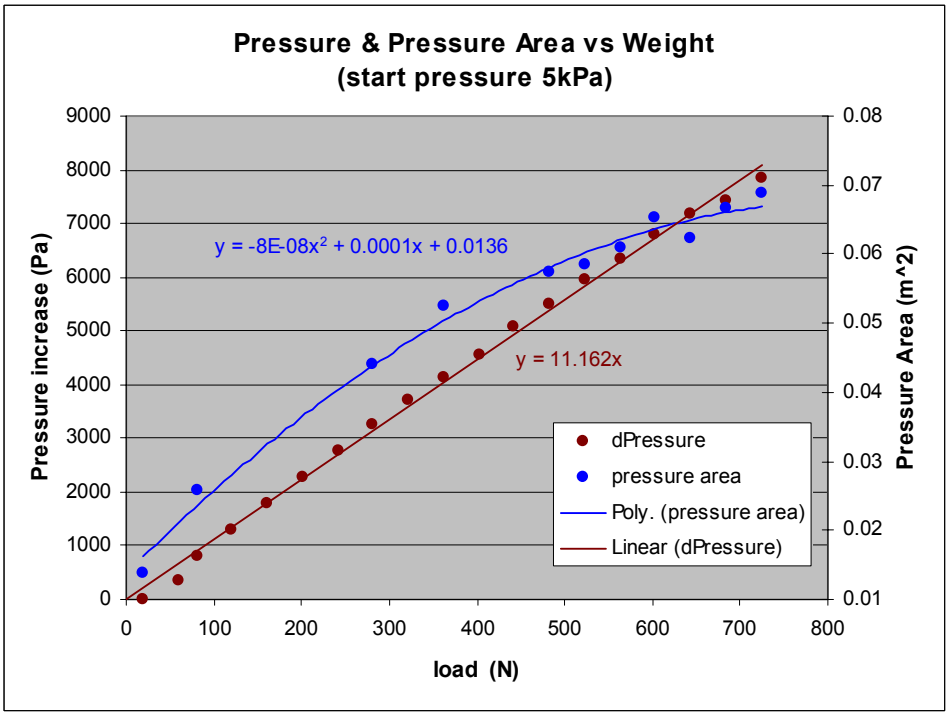

Figure 34 :- Pressure and pressure area increase versus load increase

For modelling the pressure in the cushion, the designer can ignore the increase in pressure area and consider only the linear relationship between pressure and load. Acceleration increase causes a linear increase in load and therefore in pressure.

5.3.2. Stiffness coefficient versus static load

In a linearised model, the stiffness coefficient (N/m) determined the systems' frequency response characteristics. The pressure line in Figure 34 indicated that the pressure versus acceleration relationship is linear. However, the pressure area does not remain constant. The increase in pressure area at higher loads means that the torus stiffness is likely to be higher at higher loads. Static and dynamic tests were used to determine the stiffness versus pressure relationship.

During the static test, the displacement is measured when increasing loads are placed on the tube torus. Tests on a tube torus results are in Figure 35. The dotted

line represented load force "F". The solid black curve is a polynomial curve fitted to "F". The increase in stiffness is evident in the steeper slope at the heavier loads.

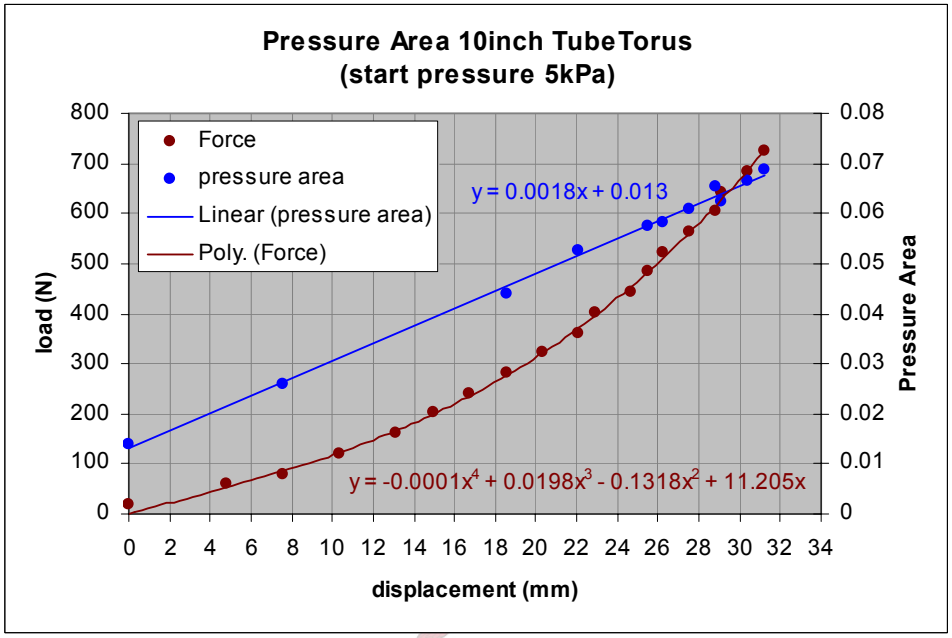

Figure 35 :- Stiffness versus load at starting pressure of 5kPa – static test

Dynamic stiffness is determined from the natural frequency of a single degree of freedom spring mass system. The simple setup in Figure 36 shows four masses equalling 62kg on a tube torus on a vertical vibration actuator. The load is varied by adding / removing masses each at approximately 15.4kg.

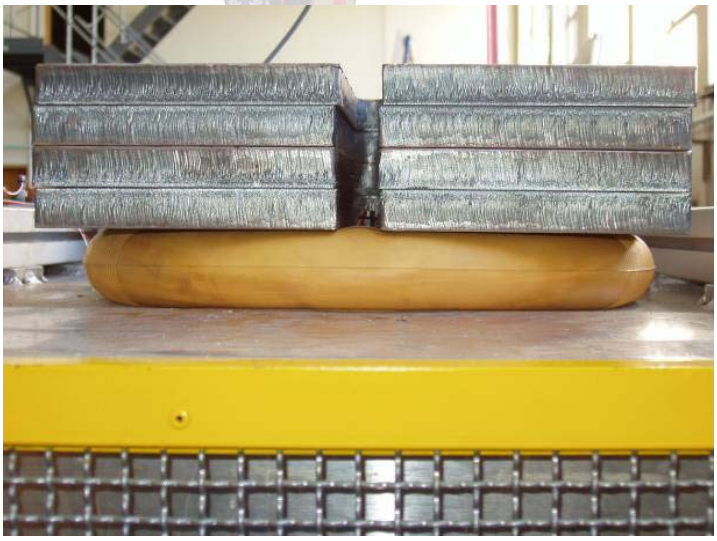

Figure 36 :- 62kg static mass on tube torus during dynamic testing

Various systems pressures were evaluated and the dynamic stiffness of the systems are presented in Figure 37. The lower mass of 15.42kg has a near linear increase in stiffness with increase in pressure. The larger heavier masses show a decrease of

stiffness on increase of pressures. (Note different tube torus is used in this test from the previous – characteristics between the tori differ).

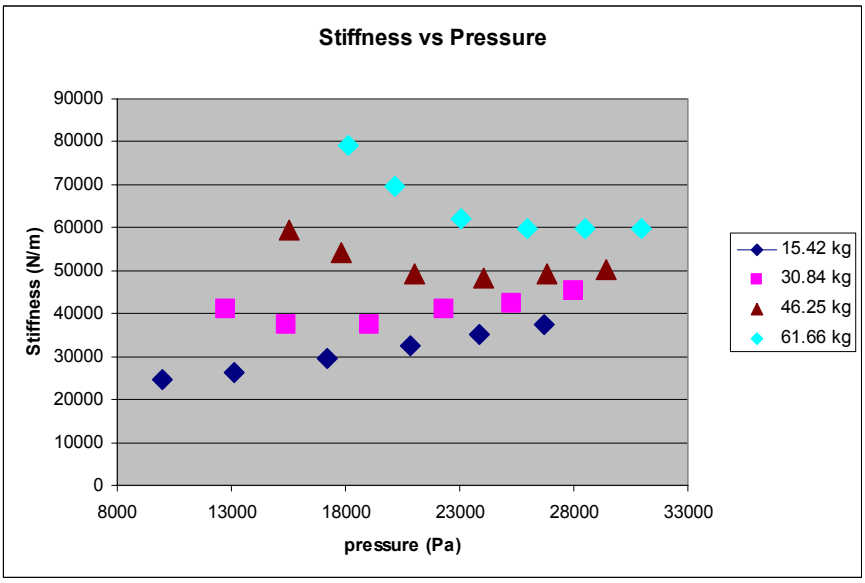

Figure 37 :- Stiffness versus pressure for various masses

Note the increase in stiffness at lower pressures. To investigate this, simplify equation (7) by setting V_0=A*h:

$$k = \frac{\gamma A P_0}{h} \tag{55}$$

Figure 38 shows that pressure area increase with increase in pressure. This suggests a relationship between pressure area and pressure. If the relationship is simplified to linear, equation (47) becomes:

$$k = \frac{\gamma x P_0^2}{h} \tag{56}$$

Where x is the linear ratio A / P.

Equation (48) suggests a quadratic relationship between the stiffness and the pressure in the system. This explains the parabolic shape of the stiffness curves in Figure 37. Therefore for each supported load there is an operating pressure where stiffness is at a minimum.

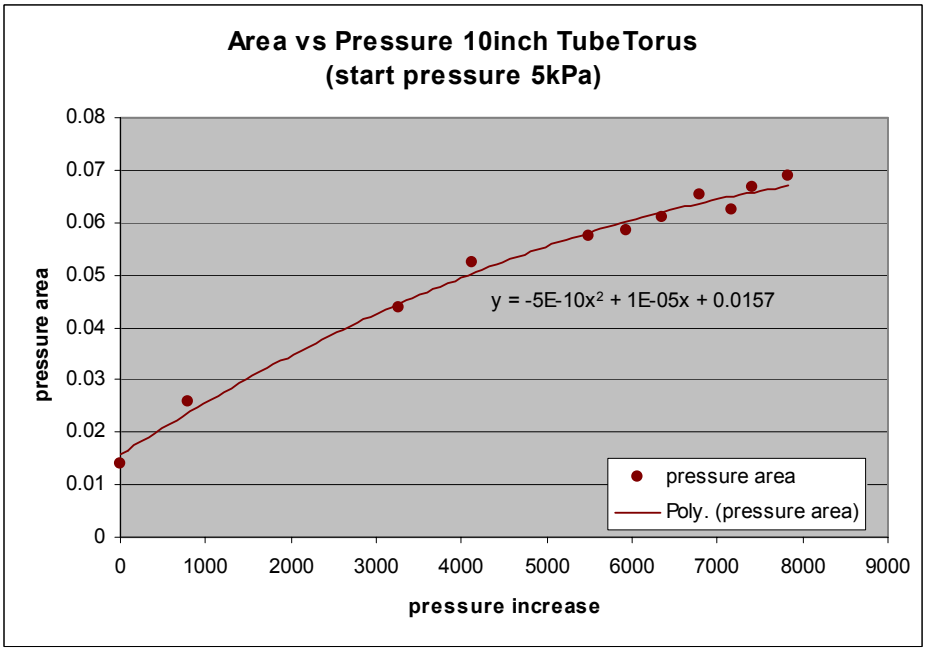

Figure 38 :- Pressure area versus pressure

5.3.3. Dynamic load – natural frequency versus pressure

From the above the starting pressure has an influence on the characteristics of the cushion. The natural frequency at which the peak occurs was recorded at various pressures for various masses in Figure 39. For light masses, the natural frequency increases with increasing pressure. This indicates a higher stiffness at higher pressure. Increased masses, however has the contrary effect. For the 31kg and 46kg masses, the natural frequency reduces with increase in pressure up to a point. After this point, the natural frequency increases again with increased pressure. The same is expected for the 62kg mass at higher pressures. An ideal working pressure is in the region of the lowest pressure.

The cushion designer could utilise this phenomenon to adjust the natural frequency for maximum vibration isolation. In general vibration isolation terms, lower natural frequency systems have better isolation properties. The challenge is to determine which mass to use when the cushion has to support a human body. The model of a human body indicates a multi degree of freedom system. Griffin (1990) suggests by definition of the apparent mass, this to be the most suitable.

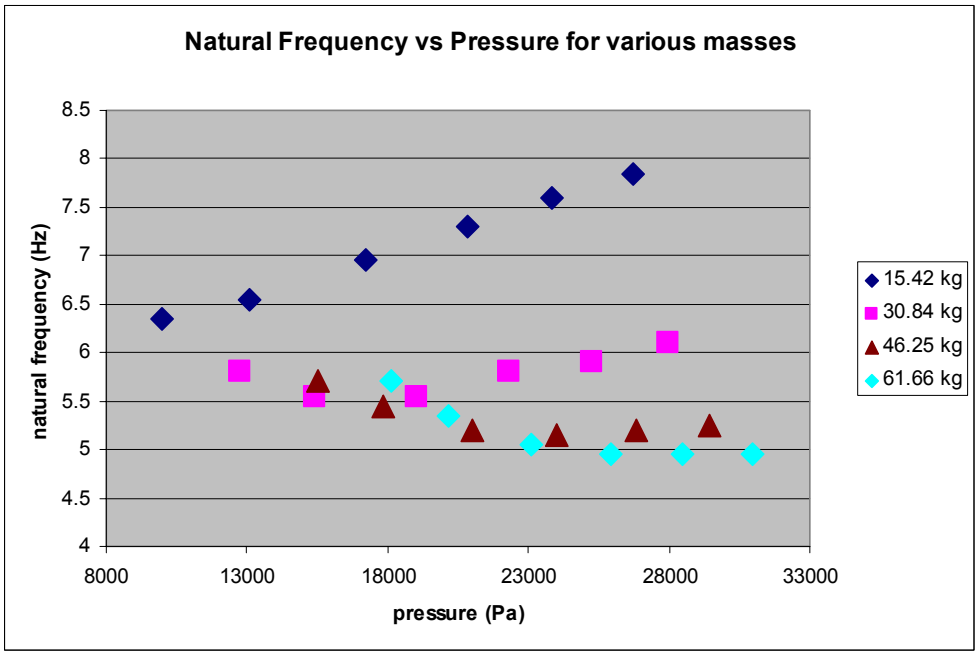

Figure 39 :- Natural frequency of spring mass system on air suspension cushion at various pressures

5.3.4. Static load – determine tilt resistance

During operation lateral forces on the upper body of the seated operator is caused by horizontal acceleration. A moment is created which tends to roll the body, and is compensated by applying a counter reaction. The operator can apply the counter force through hanging onto the hand controls, pushing against the seatback, pushing against the armrests, or rolling his hips to generate a moment on the seat base. The last mentioned action is investigated in this section – to determine its effect on the roll stiffness of the tube torus.

A hypothesis is that the torus would resist moment by enlargement of pressure area where higher force is applied and reduction in area on the lower force side. With the pressure in the tube equal, a moment is generated In Figure 40 the blue dashed line is the digitised outer contact perimeter and the red dashed line is the inner contact area perimeter. The Area between the lines is the actual contact area. As the lines are closer together on the left side of the picture, and farther apart on the right side, a difference in area exists. Pressure is the same in the tube therefore a force difference exists. This force difference is integrated over the total pressure area to determine the reaction moment.

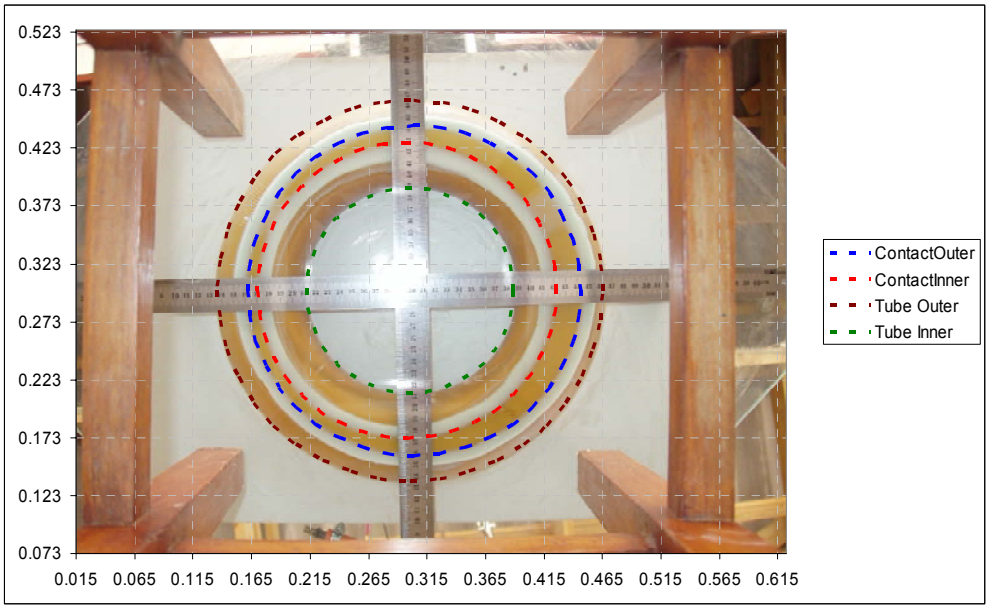

Figure 40 :- Bottom view of tube torus during angle tests (with digitize lines)

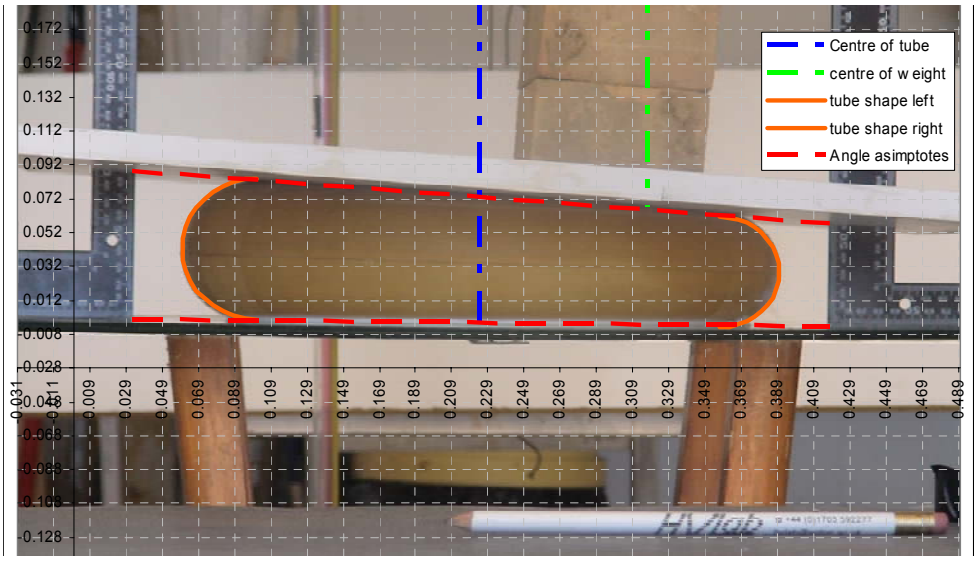

Figure 41 :- Side view of tube torus during angle tests (with digitise lines)

The static test conducted with an off centre mass on the cushion is in Figure 41. The blue line indicated the centre of the tube, the green line the centre of the mass, and the red dashed lines the angle approximation. The orange lines approximate the shape of the torus when under pressure. Six starting pressures and five masses where used in this test. The distance between the centre line of the tube and the position of the mass on the white plank is constant Calculations took into account the small increase in horizontal distance between the centre of the tube and the centre of the stacked weights due to the increased angle. Figure 42 shows the results of the moment versus angle tests at various starting pressures. At the lower starting pressures 6kPa and 9.8kPa, the tilt angles were greater at the same

moment. At all pressures above 15kPa the angular stiffness remained the same. Different torus diameters and masses of supported subjects will give different results.

In conclusion, the hypothesis holds at higher pressures. The tube torus counter acts roll by change of pressure area to create a moment force.

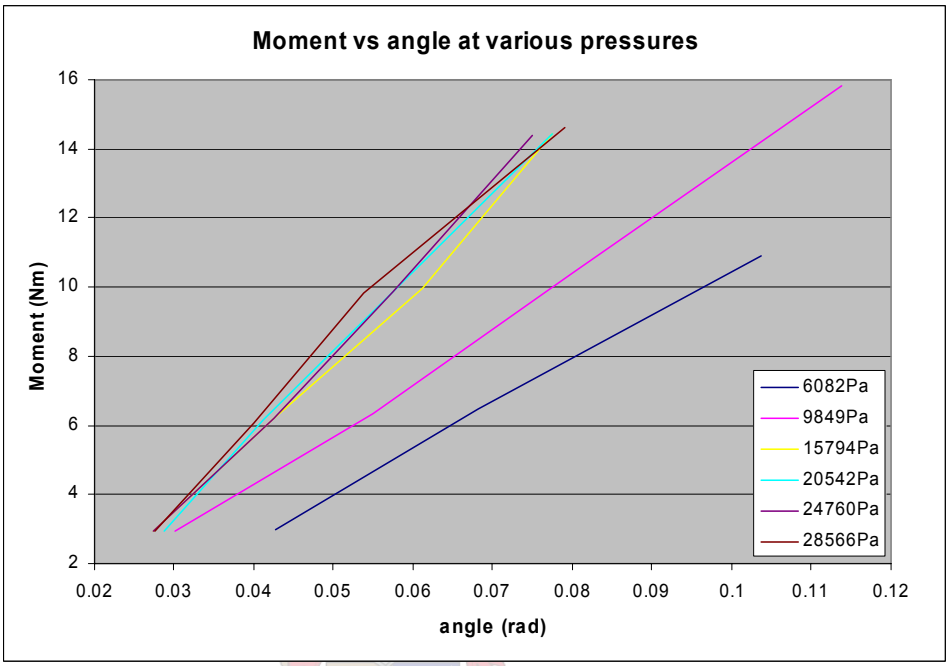

Figure 42 :- Angular stiffness of tube torus at various pressures

5.3.5. Determine the effect of pressure on the transmissibility curve

5.3.5.1. Tube torus without pipe and tank

A single 61kg mass was tested on a tube torus at a high pressure (close to the higher pressures previously tested) and at a low pressure (close to the lower pressures tested). At the higher pressure (red) in Figure 43, the natural frequency is lower than at lower pressure (green). At high pressure less "pressure area" is used to support the mass and higher volume results in lower stiffness of the single degree of freedom system. Consider the equation for stiffness of a simple air spring from the literature equation (10):

$$f_n = \frac{1}{2\pi}\sqrt{\frac{k}{M}} = \frac{1}{2\pi}\sqrt{\frac{\gamma A g}{V_0}} \tag{57}$$

A decrease of the area will result in a decrease of the natural frequency, and an increase of volume will decrease the natural frequency. In conclusion, the pressure can easily be manipulated to change the transmissibility curve to the designer's requirements.

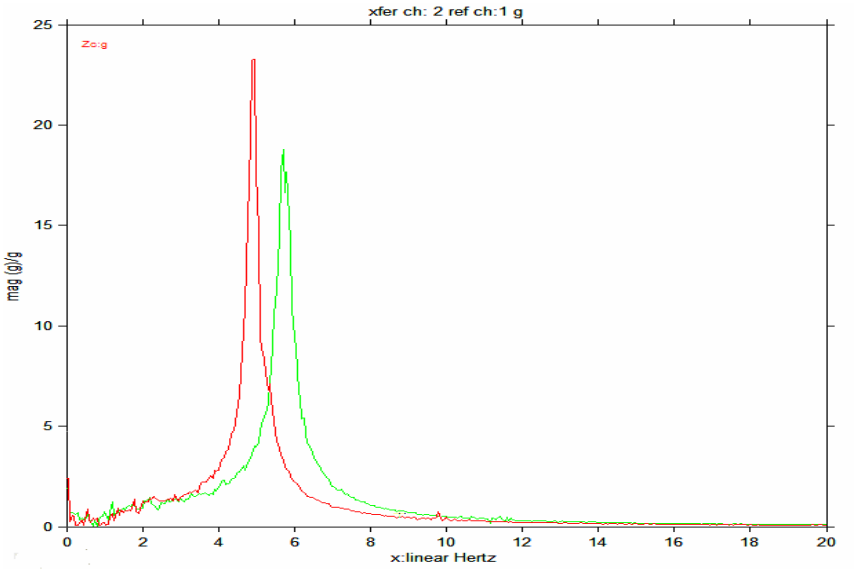

Figure 43 : - Higher & lower pressure without pipe & tank

5.3.5.2. Tube torus with pipe and tank

Pipe and tank parameters were chosen to create anti-resonance at the natural frequency of the system without the resonator. At the higher pressure (red) in Figure 44 the first peak is at a higher frequency than for the lower pressure (green), and the second peak at a lower frequency. The frequency increase of the first peak is different in behavior to that of the single degree of freedom system. The smaller pressure area (due to higher pressure) should result in a lower stiffness and resonating frequency, but does not. The difference is that the additional tank volume V_d is added to the cushion volume V_c, which changes the natural frequency equation to:

$$f_n = \frac{1}{2\pi}\sqrt{\frac{\gamma A_c g}{V_c + V_d}} \tag{58}$$

The larger volume V_d does not increase when the pressure increases and blows the cushion volume V_c up slightly. The increase in total volume is therefore small in comparison to the decrease cushion pressure area A_c. From section 5.3.3 can be seen that higher pressures increase the stiffness of a system. Typically in a two degree of freedom system increased stiffness of the primary spring would bring peaks closer, and lower stiffness push the peaks apart. It can be concluded that the system pressures in this test are higher than the ideal pressure suggested in section 5.3.3.

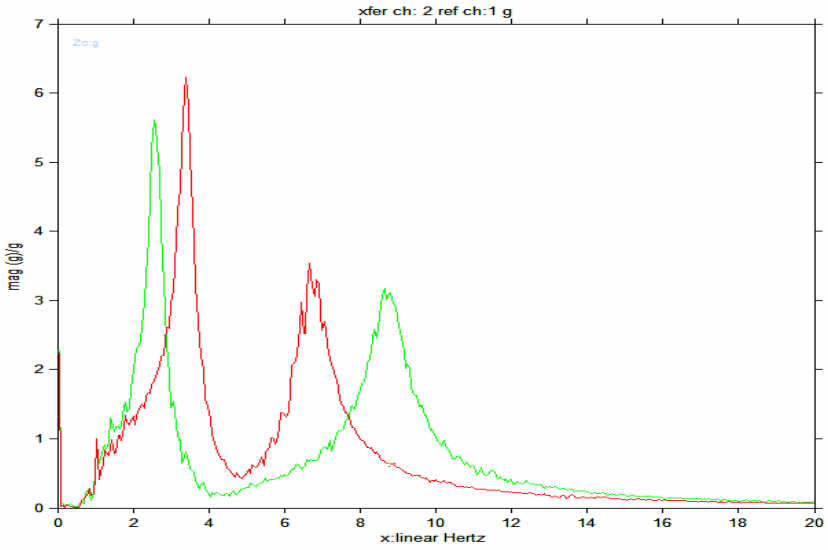

Figure 44 : - Higher & lower pressure with pipe & tank

5.4. Analytical model verification

A solid mass is used to verify the analytical model to the prototype. The equations of state are found earlier and modelled in Simulink Figure 73 to produce a theoretical transmissibility curve. This transmissibility curve is compared with that measure on the prototype under laboratory conditions. The verification of the model is done in three steps; Step 1 verifies the cushion only without pipe and tank to allow detail model adjustment of cushion volume and pressure area. Due to the non-linearity of the air suspension cushion stiffness, the magnitude of experimentation is selected at this stage and should be kept constant for all tests. Step 2 verifies tank and pipe pressure resonance where minor adjustments are made to inaccurate pipe diameter and pipe length. Step 3 verifies the complete system.

For all experimentation in the laboratory, a standard method was used to quantify the vibration transmissibility curves of seat cushions. Varying conditions were that of supported mass, pressure, input acceleration magnitude and cushion type. Cushion type distinguishes between any two cushions with any of the following parameters unequal: Tube size, tube make, foam design, foam characteristics, pipe length, pipe diameter, tank volume, or any other dimensional parameter. Experimental setup and analysis detail are given in appendix A.

5.4.1. Step 1 – verification of the cushion without pipe and tank

An input acceleration magnitude of 1m/s^2 rms is selected as it is the closest to the data measured in-field on the seat. The cushion's dimensional parameters that were used are in Table 2:

Table 2 :- Cushion dimensional parameters used during experimentation

Parameter	Quantity	Unit	Symbol
Pressure Area	0.068	m^2	Ac
Cushion Volume	0.009	m^3	Vc
Atmospheric pressure	101325	Pa	Pa
Mass	62	kg	M
Specific heat ratio – adiabatic	1.4		γ
Specific heat ration - isothermal	1		k

In simplified terms the natural frequency of this single degree of freedom spring mass system is represented by equation:

$$f_n = \frac{\sqrt{\frac{K}{M}}}{2\pi}$$

where

$$K = \frac{A_c^{\,2}.\gamma.(P_a + \frac{Mg}{A_c})}{V_c}$$

With parameters from Table 2 this calculates to a natural frequency of 5.92Hz. Alternatively, a Simulink model can be based on the first part of equation (54). The second part equals zero as mass flow u(t) in the absence of a pipe is nil.:

$$\dot{p}_c(t) = -\frac{p_c(t).\dot{h}_c(t)}{h_c(t)}\gamma$$

The Simulink model is shown in Figure 45, and the model results in Figure 46. Laboratory results of the transmissibility curve at three excitations are shown on the same graph. The natural frequency calculated earlier, closest represents the curve at the lowest excitation. As the excitation magnitude increased, damping became more significant and decreased the natural frequency and the magnitude of the peak.

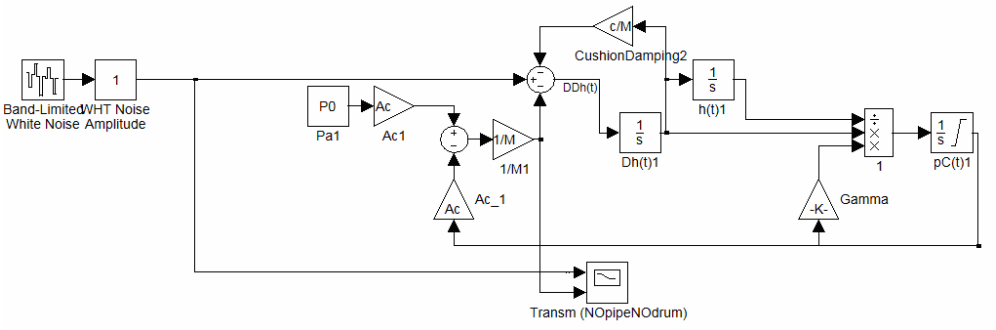

Figure 45 :- Simulink model of cushion without resonator

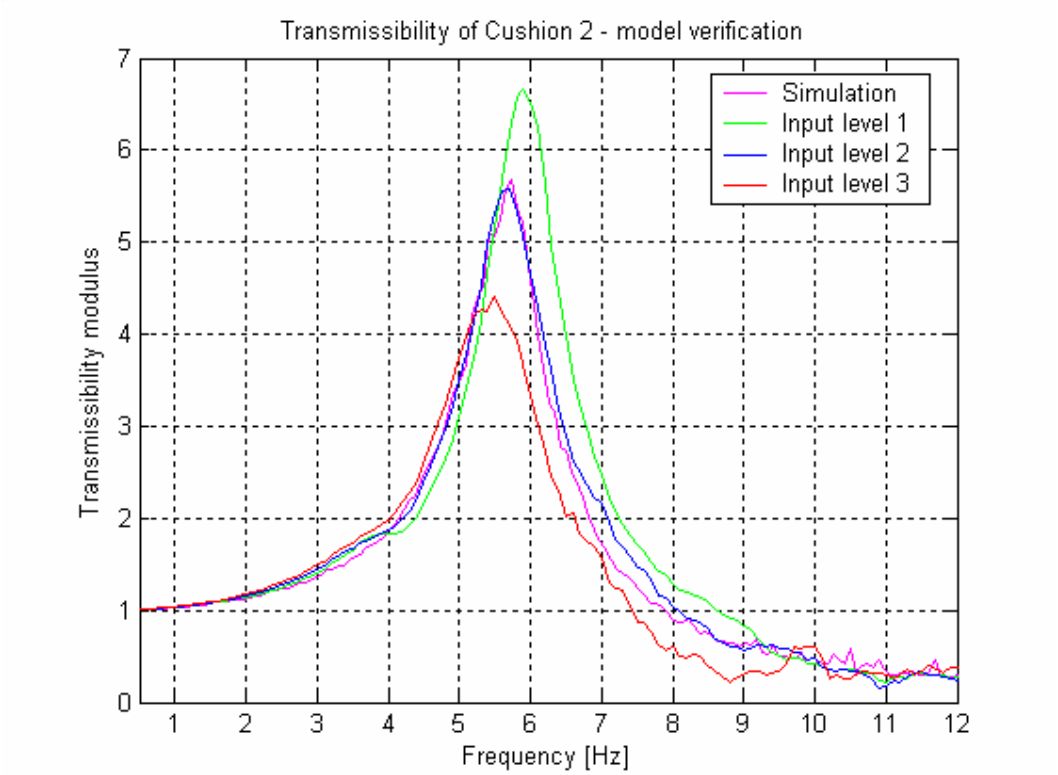

Figure 46 :- Transmissibility curve for cushion 2 without resonator – model verification

5.4.2. Step 2 – Pipe and tank pressure resonance

According to the Helmholtz principle; when the air in the pipe is excited by a varying pressure in the cushion, the air will oscillate sinusoidally. In this section are assessed the parameters affecting the resonator frequency and magnitude. Table 3 gives the parameters of the pipe, used in experimentation and verification of the Simulink model.

The cushion designer uses a simple formula to calculate natural frequency for the Helmholtz resonator:

$$f_h = \frac{c}{2\pi}\sqrt{\frac{A_p}{V_d L_p}}$$

From the parameters in Table 3 this equates to a natural frequency of 1.62Hz. Running the Simulink model in Figure 73 with marginal floor input and nil friction in the pipe resulted in a natural frequency of 1.49Hz. The difference was found due to the stiffness of the air in the cushion. As a rule half of the cushion volume should be added to the tank volume to achieve more accurate results.

Table 3 :- Pipe and tank dimensional parameters used during experimentation

Parameter	Quantity	Unit	Symbol
Length of pipe	22.3	meter	L_p
Volume of tank	25	litre	V_d
Diameter of pipe	0.025	m	d_p
Speed of sound in air	343	m/s	c
Friction of air in pipe factor	0.032[1]		μ

$$f_h = \frac{c}{2\pi}\sqrt{\frac{A_p}{(V_d + {}^{V_c}\!/_{2})L_p}} \tag{59}$$

Substituting the parameters again into equation (59) equals 1.50Hz, is a more reliable initial estimate.

A spectral response is used to determine the natural frequency from the measured data. The pressure ratio is determined as a transmissibility curve, with the pressure in the tank as the response and the pressure in the cushion the reference pressure. For comparison with the results measured in the laboratory, the pipe friction is increased to the quantity in Table 3, and shown in Figure 47.

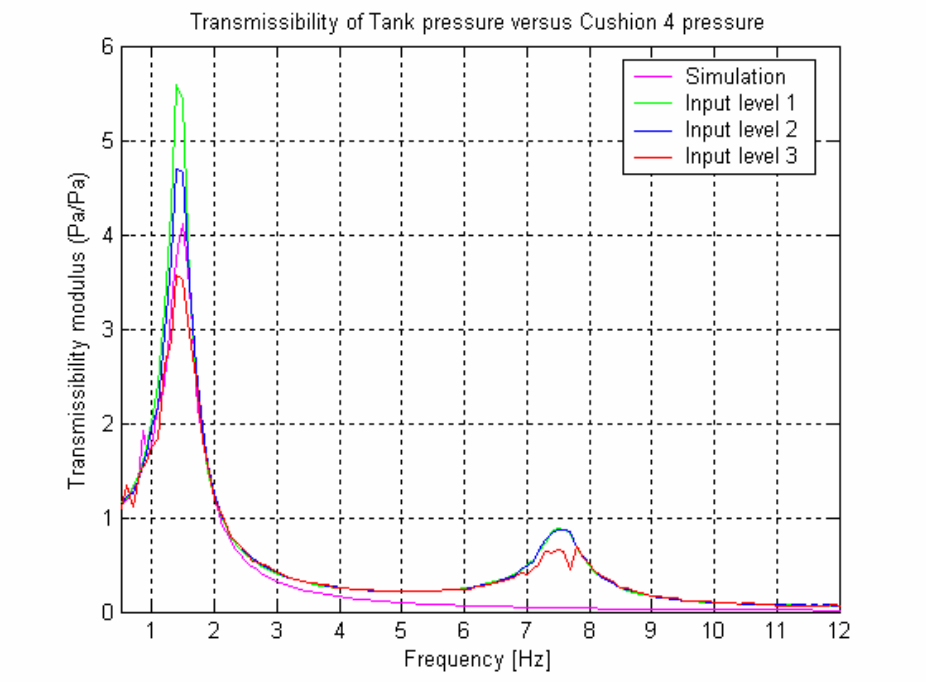

Figure 47 :- Pressure ratio in system for cushion 4 compared to model

[1] The friction of the air in the pipe was determined iteratively until the magnitude at resonance of the simulation equals the magnitude of the prototype.

The small peak between 7 and 8Hz on the measured pressure transmissibility curve is due to the pipe resonance harmonics of the air. The shorter pipe used in cushion 3 does not show this resonance. Compared with cushion 4 in Figure 52 the acceleration transmissibility curve actually reduces at these frequencies as shown in Figure 52. This peak is not on the simulation, as it does not calculate pipe harmonics.

5.4.3. Step 3 – Compare the transmissibility of the complete cushion 4

In the previous steps all the dimensional parameters of the system are confirmed. The transmissibility of the model can then be compared with the transmissibility curve, measured in the laboratory. Factors that may vary slightly are damping and mechanical coupling between the cushion and the pipe. Figure 48 shows the transmissibility of the model, in comparison with that of three measurements from the laboratory. The laboratory measurements were done at various levels of excitation. It was found that 20% higher damping was required in the model with the pipe and tank, in comparison with the model without the pipe and tank. All other parameters are equal to those stated in the previous steps.

In Figure 48 at 2.25Hz the effect of the resonator can be noted. Below 2.25Hz the curve is slightly higher than without the resonator as seem in Figure 46. The valley created by the resonator in the transmissibility curve, is at a frequency higher than the resonance frequency. For initial estimation, a ratio of 1.425 was found empirically. The frequency at which the effective valley occurs would therefore be 1.425 times the frequency of the resonator. Without damping this factor is closer to 1.41.

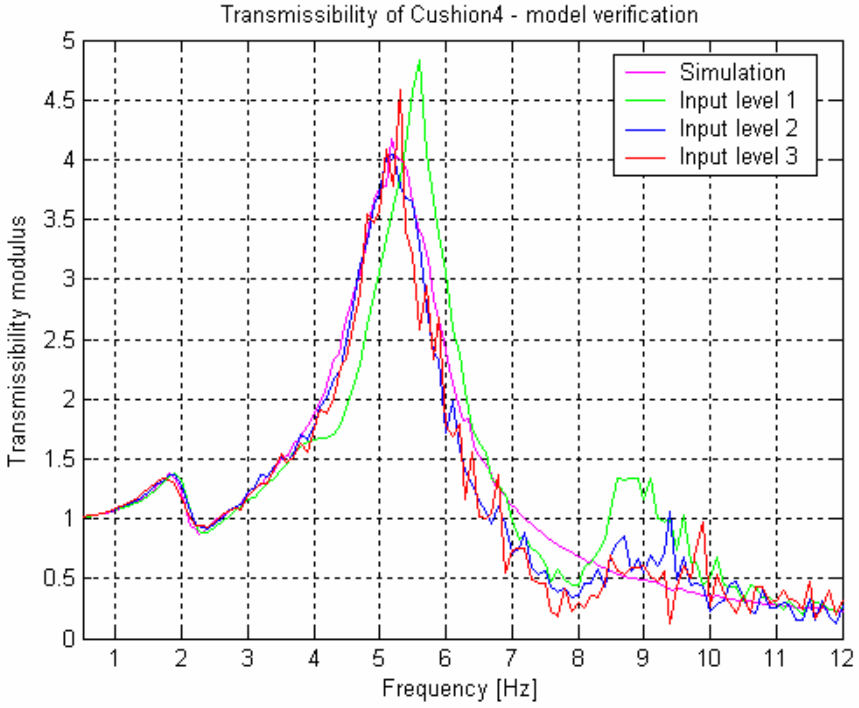

Figure 48 :- Transmissibility of cushion 4 - model verification

5.5. Prototype testing

It is required to evaluate whether the prototype indeed proves the hypothesis true. The SEAT value for the cushion during an in-field run is to be at least 20% lower than that measured during the in-field tests. A foam cushion represents the foam seat base currently installed in the vehicle. Human subjects were used to evaluate four cushions under varying conditions.

A documented safety methodology for experimentation using human subjects was followed. The vibration test platform and control system conform to ISO 13090-1:1998 Mechanical vibration and shock -- Guidance on safety aspects of tests and experiments with people -- Part 1: Exposure to whole-body mechanical vibration and repeated shock (1998). Subjects were briefed about the goals of the experiment, the safety measures in place and instructed that they may terminate the experiment at any time by pressing an emergency stop button convenient placed next to the seat. The fact that the published results will not include their personal identity, that the testing was not compulsory and that they terminate their participation without any consequences to them was also impressed on all the subjects before any testing commenced.

5.5.1. Description of cushions:

- Cushion 1 - A 530mm x 480mm x 100mm open cell foam cushion of density 30kg/m^3 and hardness factor 20 as used commercially by foam manufacturers.
- Cushion 2 - The tube torus cushion in Figure 49 is of the same outer dimensions as in cushion 1 but with a 10inch vehicle tyre inner tube fitted inside a cut-out of the foam (of similar hardness and density as cushion 1). A 16mm pressed wood seat board on the tube spreads the force at the interface with the buttocks. An extension of the board under the legs prevents cut of blood flow, which could occur when seated directly on the tube. The foam is shaped for lateral and roll support.
- Cushion 3 - A 20mm inner diameter pipe of 2m length is fitted to cushion 2 and connected to an auxiliary volume of 5liter. The volume has rigid sides to minimise change of volume when subject to pressure variations.
- Cushion 4 - A 25mm inner diameter pipe of 22.3m length is fitted to cushion 2 and connected to an auxiliary volume of 25liter. The volume has rigid sides to minimise change of volume when subject to pressure variations.

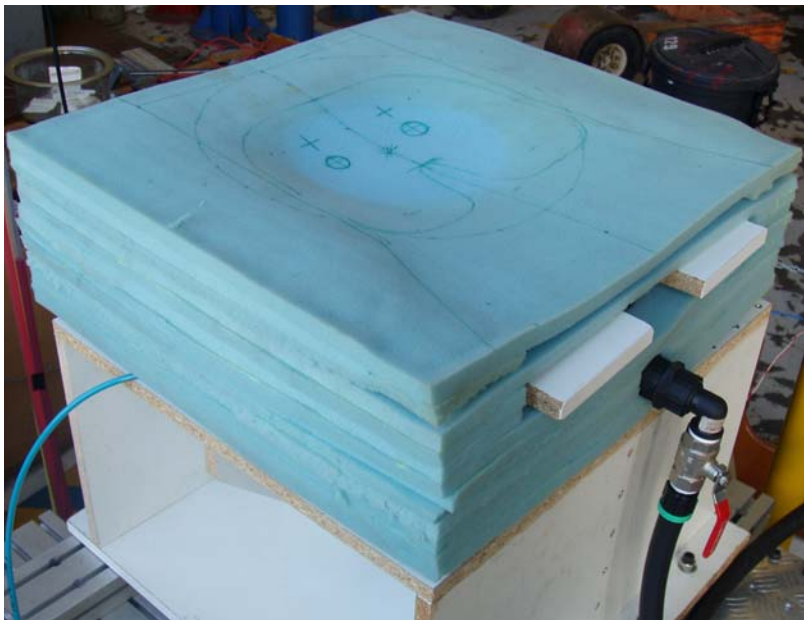

Figure 49 :- Prototype in laboratory

5.5.2. Varying conditions:

The human subjects are 5 healthy adult males between the ages of 20- and 50 years. The group has a mass distribution in accordance with the known South African male population. Each subject is wearing light working clothes. Standing and seated masses are determined with a calibrated bathroom type scale. Standing mass range was between 61kg and 102 kg.

Table 4 :- Test subject mass and height

Person	Mass (kg)	Height (m)
1	61	1.65
2	66	1.72
3	72	1.69
4	86	1.78
5	102	1.89

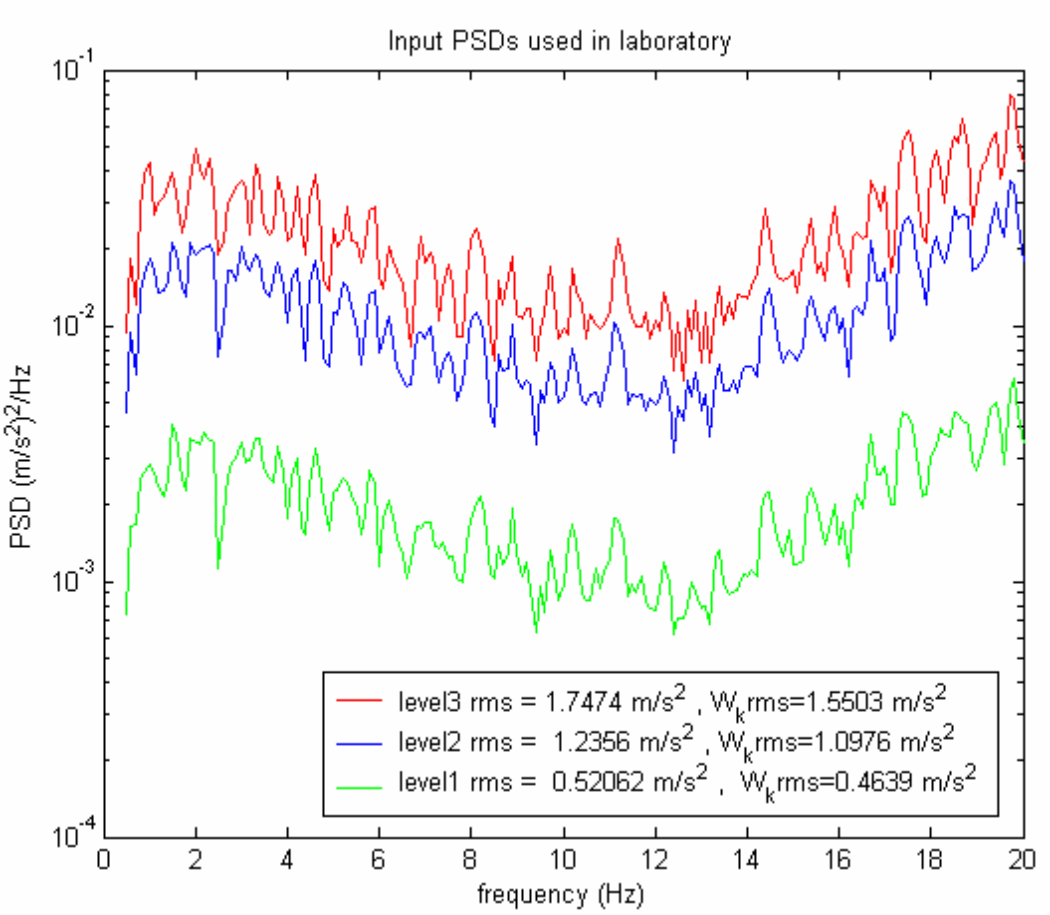

Figure 50 :- Input acceleration psds measured in laboratory

Three magnitude levels of un-weighted acceleration are used to assess the characteristics of the cushions. Floor acceleration is calculated from the input accelerometer in the frequency domain is presented in Figure 50 and below:

- Level 1 rms 0.5 m/s^2 (~ approximately W_k weighted rms 0.46 m/s^2)
- Level 2 rms 1.2 m/s^2 (~ approximately W_k weighted rms 1.10 m/s^2)
- Level 3 rms 1.7 m/s^2 (~ approximately W_k weighted rms 1.55 m/s^2)

The PID controller on the vibration actuator interprets its excitation signal as a displacement signal. A typical pink noise signal (equally distributed in the frequency domain) used as input to the controller does not give enough amplitude in the low frequencies. A signal which equally accelerate the actuator at all frequencies is required. This signal was created from a random signal integrated twice in the time domain and then bandpass Butterworth filtered between 0.5Hz and 20Hz. A modified 0.1Hz Hanning window was applied to the time domain signal for soft start and end conditions. The signal played back continuously through the analyser output generator. Refer to the appendices for more detail on he input signals.

System pressure will be according to the supported mass to maintain constant working height. At constant working height, greater mass results a slight increase in the pressure area, because of the stretch of the rubber torus. Due to the area increase, a non-linear relationship exists between mass and pressure. Pressure for subject 5 is approximately 7880Pa (0.0788bar), but will vary between subjects in order to maintain constant working height. Absolute system pressure is measured in both the cushion and in the tank.

Working height influences the pressure area of the cushion and the natural frequency of the single degree of freedom system. It is kept constant for all subjects at approximately 60mm.

5.5.3. Results

The results obtained from the tests are firstly considered for spectral content of the transmissibility curves and then evaluated with respect to the input signal obtained in-field on the three-wheeled logger. The ISO 7096 EM curves will also be applied to determine the suitability of each cushion for each type of vehicle.

In Figure 51 the experimental results show all subjects tested on each of the cushion types at the three levels of excitation. Refer to section 5.5.1 for cushion descriptions. The inter-subject differences are the lowest between 5 and 10Hz for cushion 4. The tube without the pipe and tank (cushion 2) and the foam cushion (cushion 1) show the typical second peak between 5 and 10Hz. Cushion 3 with 2m long 20mm pipe and 5litre tank is suitable for applications with a dominant frequency around 7.8Hz, but is of little value for isolating the vibration in the logger. Above 10Hz the inter subject variation is the greatest for cushion 1 and cushion 3. Cushions 2 and 4 have the least inter subject differences at the higher frequencies.

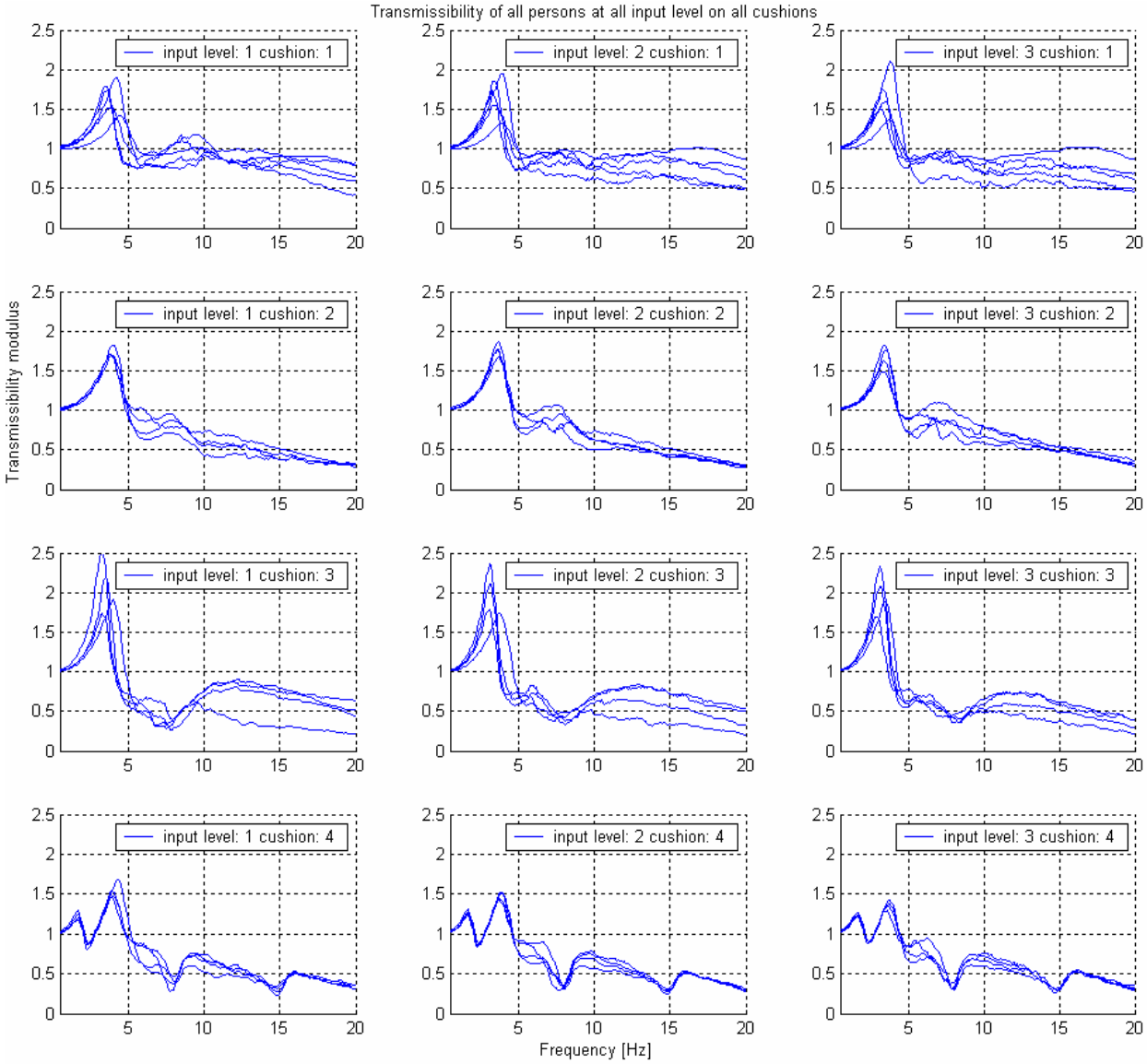

Figure 51 :- Transmissibility of all subjects on all cushions at all input levels

Differences in the transmissibility curves between cushions are shown in Figure 52. Cushion 3 has the highest peak for all levels of excitation, but provides the best general isolation between 4Hz and 10Hz. The foam cushion 3 has the second lowest peak, but due to high damping, is the worst at frequencies above 6Hz. The cushion without resonator has the second highest peak, but provides the best isolation at higher frequencies. Cushion 4 with the resonator, tuned for best isolation at 2.2Hz, also has the lowest peak overall.

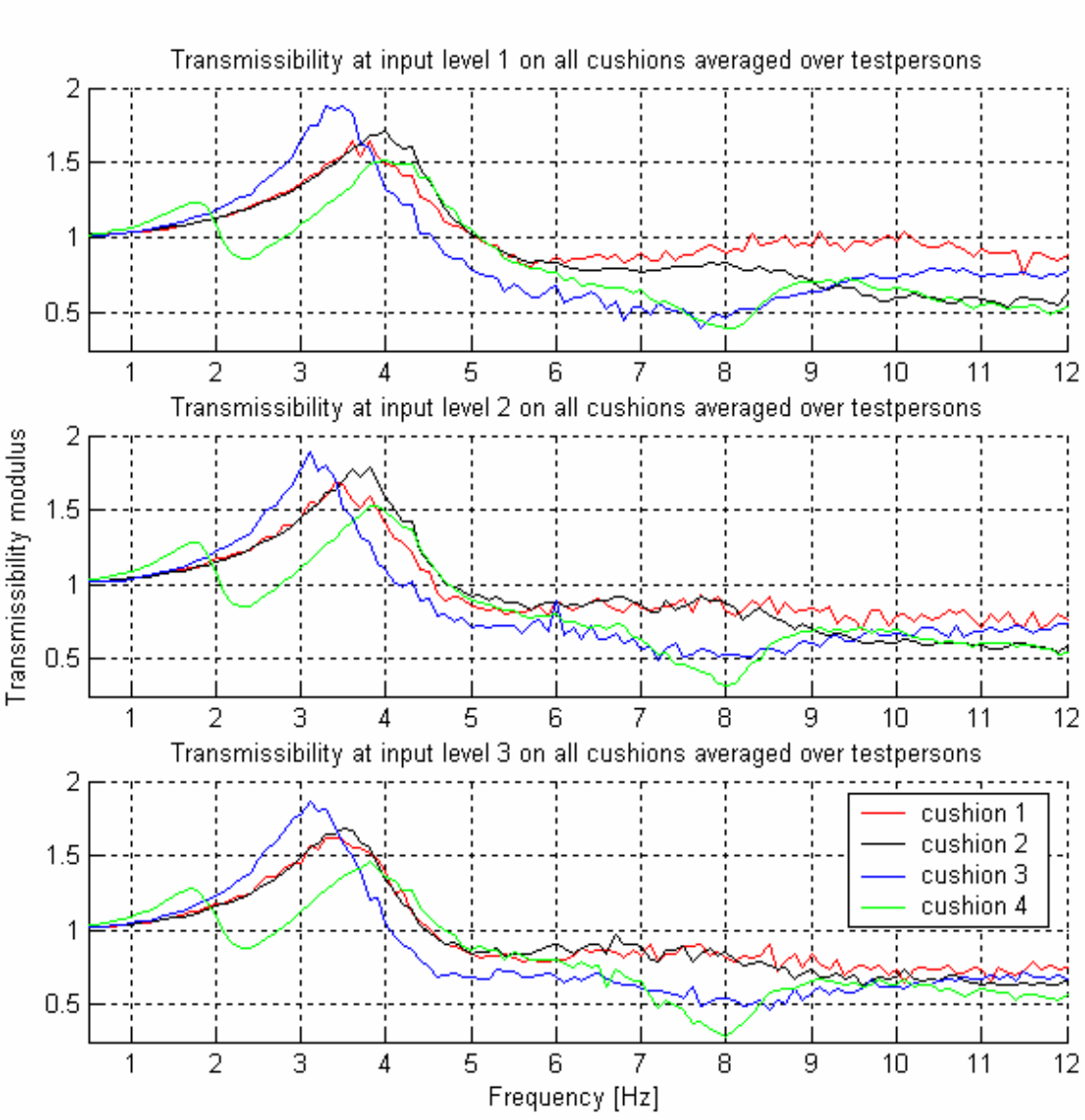

Figure 52 :- Transmissibility curve averaged overall human subjects for three input levels

Few suspension systems are linear with respect to excitation magnitude. Figure 53 compares the transmissibility curves for each cushion at various excitation levels. Cushion 4 shows that no significant different exists between the levels at the anti-resonance frequency. At 4 Hz more influence is noted. At the highest excitation level the peak appears at a lower frequency than for the lowest excitation level.

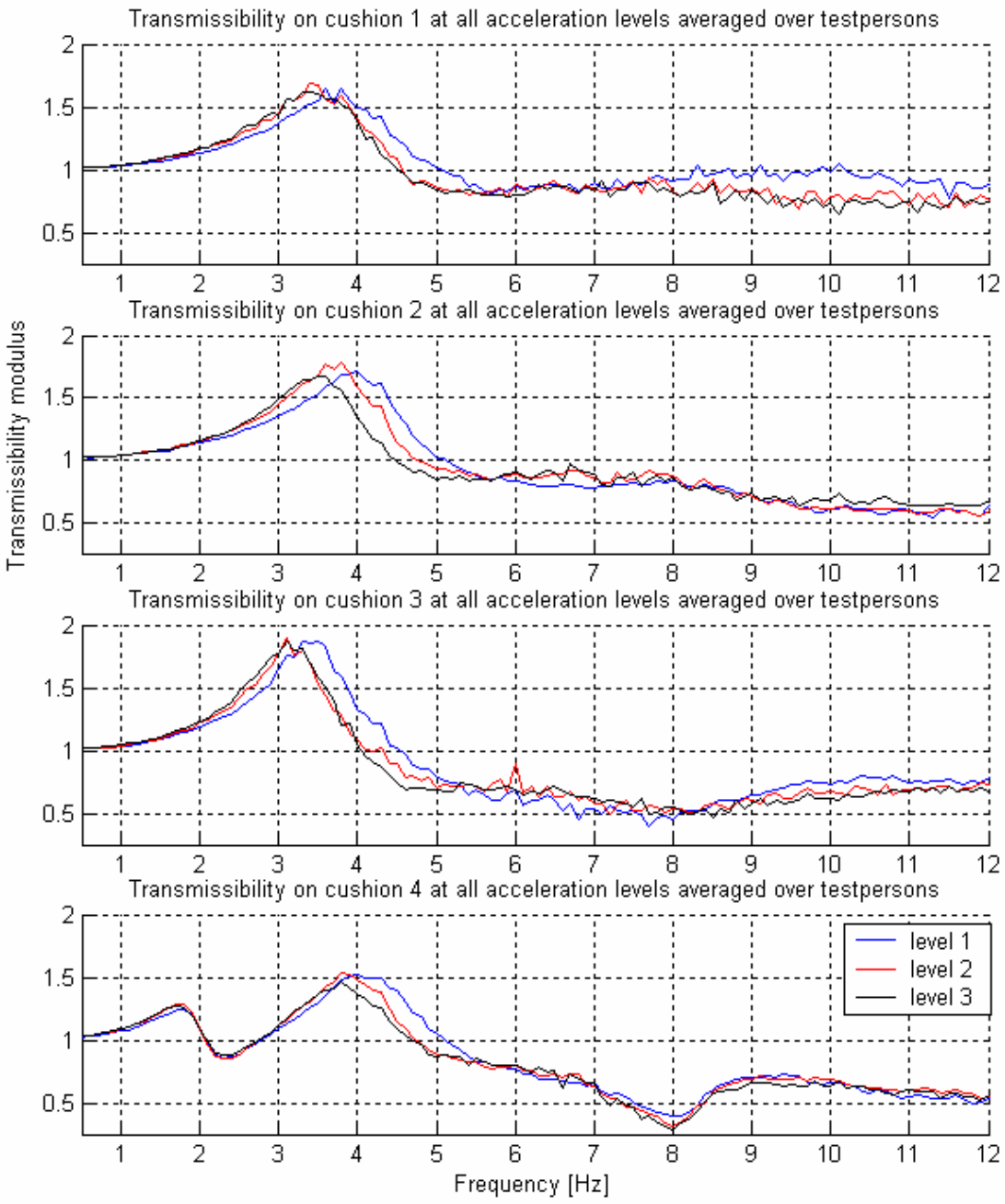

Figure 53 :- Comparing transmissibility curves at various excitation levels

It is concluded that the anti-resonance is not influenced by supported mass impedance or by excitation magnitude.

6. Results & Discussion

The purpose of the experimentation was to evaluate the validity of the analytical and simulated model and to verify the practical use of the air suspension cushion. The validation of the analytical model is more accurately done with a known solid mass, which eliminates the inter- and intra-variations of human subjects. Subsequent verification of the cushion's ability to reduce narrow band vibration was done with human subjects. The effect of different pipe lengths, diameters and tank volumes had to be clarified. Also important, was to establish whether inter subject differences such as weight and damping would affect the resonator frequency and efficiency. Finally, to test whether it reduces vibration on the logger and other vehicles.
The model experimental verification provided a tool to determine which cushion and resonator parameters to use in the prototype testing. The prototype was assessed for inter subject variability. Thirdly the prototype's ability to isolate vibration on the logger is discussed. Finally the air suspension cushion prototype's ability to reduce vibration on ISO7096 classed vehicles is calculated.

6.1. Validating the model

The model predicts the actual measurement data with adequate accuracy to design a cushion for a specific input acceleration (Figure 48). Various system parameters can be adjusted to create anti-resonance in the cushion transmissibility curve. The tuning of the pipe and tank resonance is important in determining the frequency at which the transmissibility curve will be reduced. The pipe friction factor is the only parameter affecting the damping and should be minimised to obtain a deep valley in the transmissibility curve. If a wider valley is required to counter broader band of peaks in the input psd, the damping can be increased. Daugherty and Franzini (1984) provided details on how to determine pipe friction for different flow conditions. The most important to note is that friction is inversely proportional to hydraulic radius of the pipe. Larger diameter pipes therefore, have less friction.

The cushion designer can use short thin pipes at shorter length to achieve the same resonator frequency, as with larger diameter longer pipes. A rule of thumb found during this research is that a 20mm pipe gives predictable results. The designer can use this as a starting point for iteration. At tank volumes smaller than twice the cushion volume, the resonator performance became less predictable.

6.2. Transmissibility – effect of inter-subject variation

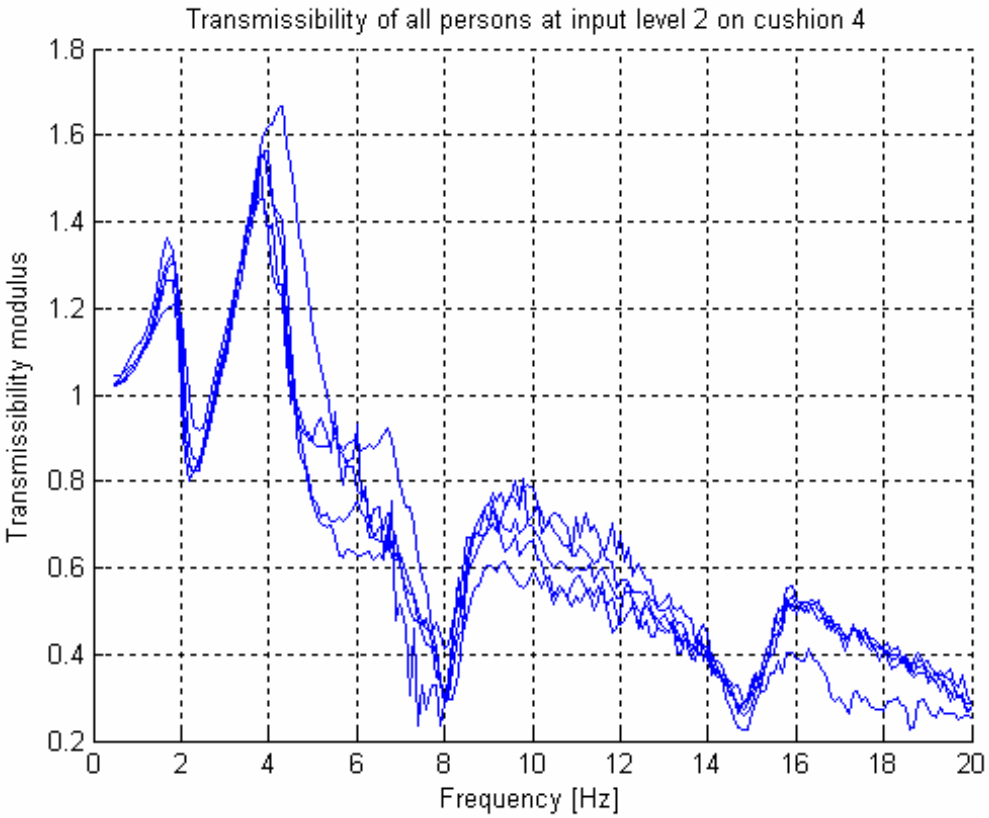

Figure 54 :- Inter-subject variability for cushion 4

Inter-subject variation on cushion 4 subjected to vibration excitation level two is illustrated in Figure 54. Below 4.5Hz, the variation is less than at higher frequencies. For heavier subjects, the valleys are deeper and the peaks higher than for the lighter subjects. This is due to the lower damping to mass ratio for heavier persons. Valley occurrences at 8Hz and 15Hz are due to harmonics of the resonator. These contribute to a reduction of the transmissibility curve and output acceleration psd.

Mathematical analysis in section 3.4.5 showed that mass variance does not affect the natural frequency of the system if assumed linear and with constant working height. The natural frequency of the seated human subject is normally around 4Hz according to the literature (Griffin, 1990 p395). Both statements support the results obtained above. Additionally the Helmholtz resonator mathematical model in equation (4) is not affected by pressure or by change in cushion parameters. The resonator frequency is dependent on pipe and tank parameters. The consistent position of the valley at 2.25Hz supports this theory.

The air suspension cushion can therefore be designed vehicle specific. It will reduce input vibration for different human operators.

6.3. Vibration reduction on the three wheeled logger

The resonator fitted to the prototype air-suspension cushion was designed to be the most suitable for the three-wheeled logger. The average transmissibility curve of five human subjects was used to evaluate the cushion performance. Figure 55 shows the transmissibility curves for the foam cushion and the prototype measured at vibration excitation level two. The air suspension cushion performed very similar with a relatively high transmissibility peak near 4Hz in both cases.

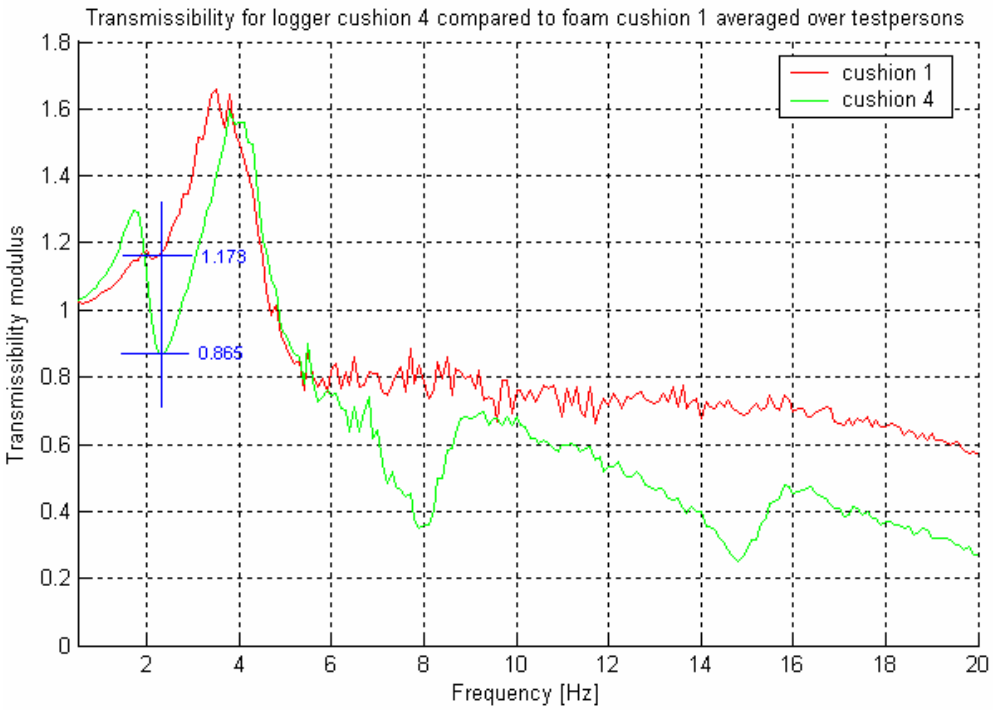

Figure 55 :- Transmissibility of foam cushion compared with prototype

The real hurdle with the logger is its high input acceleration psd peak at 2.25Hz. See figure Figure 30. The transmissibility curve should therefore be less than unity at this frequency to reduce the vibration transfer to the human subject. The resonator is therefore designed not to reduce the natural frequency peak at 4Hz, but to minimize the input acceleration psd peak at 2.25Hz. Laboratory results show the transmissibility curve magnitudes at 2.25Hz for the foam cushion is 117.3% and for the air suspension cushion 86.5% in Figure 55. This is an improvement of 30.8% at this frequency. An improvement in the SEAT value can therefore also be expected.

Table 5 :- SEAT values averaged for all subjects during all in-field runs in percentage

Input Level	Cushion1	Cushion2	Cushion3	Cushion4
Level 1	117	117	125	92
Level 2	118	120	127	93
Level 3	119	121	128	95

Calculated[2] estimates of the real SEAT values are presented in Table 5. The averaged SEAT value for all human subjects at input excitation level 2 on the foam cushion is 118% and for the air suspension cushion 93%; an improvement of 25%.

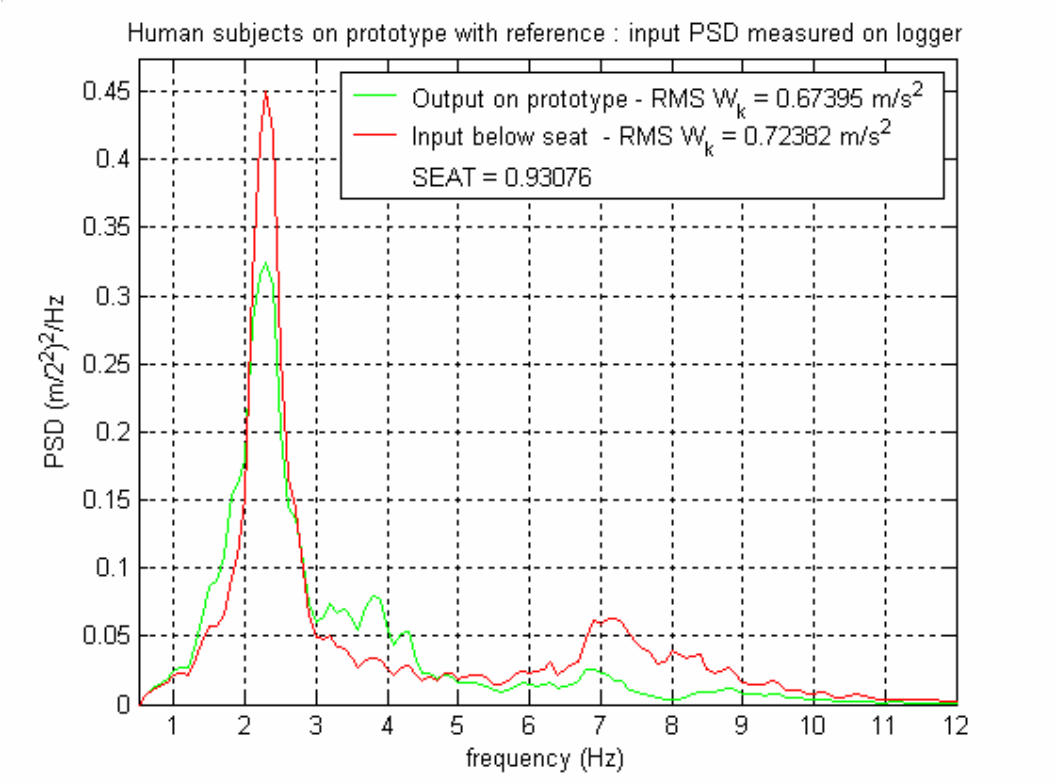

Figure 56 :- Input and output acceleration psds for prototype on logger

The input and estimated output acceleration psds in Figure 56 show the improvement at 2.25. Note the frequencies where the output psd is higher than the input psd. This is due to new peaks that appear at frequencies immediately below and immediately above the new valley on the transmissibility curve in Figure 55. The cushion designer should take care that these new peaks do not coincide with peaks on the input psd. For weighted input psds with peaks at many frequencies it is recommended to determine the lowest SEAT value through iteration.

6.4. Vibration reduction on ISO 7096 (2000) classed vehicles

ISO7096 (2000) provides guidelines to suspension seat manufacturers on how to assess the performance of their product. It allows certification of suspension seats to nine vehicle classes. Although not designed specifically for the EM class three wheeled loader>4500kg, the prototype is compared with this specification. ISO7096

[2] The real SEAT value is calculated from the ISO 2631 W_k weighted time domain data. For laboratory comparison purposes the estimated SEAT values are calculated with equation (3) from the frequency domain psd of the field measured input acceleration and transmissibility curves of the prototype determined in the laboratory. This assumes linearity of the system between the excitation magnitudes of in-field and laboratory tests.

(2000) standard suggests that to test for the EM3 class suspension seat, the input psd used in laboratory tests to be that of the EM3 curve in Figure 30. The laboratory input psd used in this study is uniform over the frequency spectrum and has comparable maximum energy at the relevant frequencies 0.89Hz to 11.22Hz. The input psd used therefore conforms to the required input psd.

The estimated output acceleration psd is compared to the input acceleration in Figure 57. The SEAT value is 1.133, which is above unity. This indicates that the air suspension cushion prototype cannot be considered a suspension seat according to ISO7096 for EM class 3.

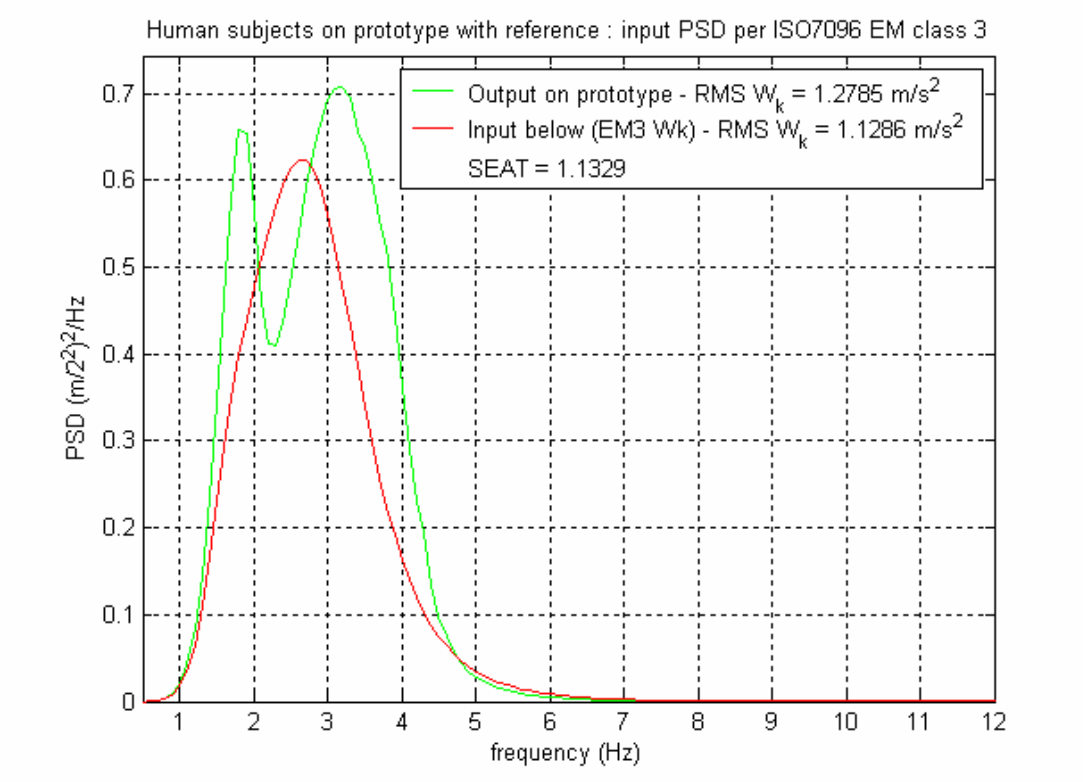

Figure 57 :- Input and output acceleration psds for prototype on EM class 3

It is estimated that the prototype would reduce the SEAT value on the logger by 25% to below unity. However, it does not reduce the SEAT value on the EM3 class vehicles to below unity. In fact, the input psd peak on the logger at 2.25Hz is higher than that of the EM3 class vehicle at 2.65Hz. The main difference is the width of the peak, which is narrower in the case of the logger. In the final design section (7.3), an improvement of the prototype is discussed as a case study. It is shown that by changing the system parameters pipe length and tank volume the SEAT value can be reduced to below unity.

7. Final design

In engineering it is often frowned upon when a simple device provides an acceptable solution. Throughout the conceptual design phase a complex linear air suspension solution was envisaged. The outcome, however pointed to a simple solution; a round rubber tube set in a stable surround. The rubber tube however has to adhere to certain parameters to suit the design specification, but it is an easily obtainable item that is both reliable and at low cost. The interface between the rubber tube and the pipe will have to be reliable. The same will apply to the interface from the pipe to tank; and for that matter the pipe and tank.

It is however, not as simple as that, a tube in foam surround and connected to a tank will isolate vibration under all circumstances. By adjusting the pipe length and diameter and also the tank volume, the cushion can be optimised for a certain vehicle. Working backwards from an ideal SEAT value and known input acceleration psd $G_{ff}(f)$, the ideal transmissibility curve $H_c(f)$ can be calculated for a given vehicle and operation.

In this final design phase a generic method of design could be applied to any whole body vibration problem with a specific example for the three-wheeled logger. The product design specifications defined what the end user would expect from the cushion. Static design considerations could affect dynamic performance of the cushion and should be weighed up. A mathematical formulation of the ideal transmissibility curve is included in the dynamic cushion design procedure. The simulation model predicts the transmissibility curve expected for a set of system parameters. Ideally the simulation would iterate through different system parameters to narrow down to the most suitable.

An air suspension cushion for a wheeled loader >4500kg (EM class 3) is designed to demonstrate the procedure.

7.1. Final product design specifications:

- Cushion - The cushion consists of four parts; the tube torus, seat plate, foam surround and skin:

  - Tube torus - A 300mm (10 inch) diameter by 145mm standard car tyre tube is used.

- Seat plate - The pressure supporting the buttocks should be distributed similar to a normal seat cushion. High-pressure areas normally exist below the ischial tuberosities and lower pressure under the legs. The tube torus will apply even pressure across the interface and due to its shape result in higher pressure under the legs than normal. To prevent blood flow cut-off to the legs a rigid seat plate is introduced which normalises the buttock support pressure. This plate is shaped similar to the pressure distribution outline found in the literature.

- Foam surround - The foam surround contains the tube torus and positions the seat plate. It provides lateral and fore-aft stability during x- and y-axis acceleration.

- Skin - The purpose of the skin is to enclose the other parts, provides an interface with the human body, and interface with the vehicle, and be self extinguishing in case of fire.

- Pipe - Any bends in the pipe should be of hydraulic radius larger than that of the average pipe diameter.

- Tank - The tank side walls will be rigid to withstand dynamic pressure variations. Maximum pressure rating of the tank will be 1 bar or higher. No tank dimension will exceed 1 meter. Tank volume will be empty and not used for storage. Tank capacity will be 25liter or as otherwise specified by specific design.

- Cushion to pipe interface - A 20mm inner diameter tank adapter with flange is vulcanised onto the rubber tube membrane and strengthened with a second layer of rubber membrane on the outside of the adapter flange. The adapter fixation is tested by multiple repetitions of pull and twist force on the adapter to simulate normal use.

- Pipe to tank interface - A 20mm inner diameter tank adapter is flush mounted to the inner surface of the tank. Care is taken to minimise tank adapter flow losses.

7.2. Dynamic cushion design procedure

An air suspension cushion design is vehicle specific. Suspension seat systems that cater for all vehicles types won't effectively isolate all problem frequency vibrations for a specific vehicle and unlikely economically viable to use in the vehicle.

For ergonomical, maintenance, practical, economical and of course vibration isolation, issues have to be considered for the design of a seat cushion. Ergonomically, the cushion has to be comfortable, sweat inhibiting, providing an even pressure interface, supporting a range of body masses and be aesthetically pleasing. Low maintenance would be expected, for example a fabric with at least crip5 and 50000 rubs resistance and air chambers that are sealed to maintain pressure. Practically, the cushion has to fit into the operator's seating space and must be easy to re-inflate. Economically viable to be manufactured, installed, and replaced in event of failure. Vibration isolation, should in comparison, be better than the existing cushion to justify substitution.

The dimensions of the cushion are limited by the space available at the operator's seat area inside the vehicle. In vehicles fitted with seats that are adjustable for fore-aft and height, may keep such mechanism and only remove the seat base and foam cushion. An adaptive interface plate may be necessary to support the new air suspension cushion. The backrest of the seat may be left intact.

Suspension seats reduce shock by allowing movement of the buttock interface relative to the seat base. Such movement requires more vertical distance, than a non-suspension seat. Due to the increase in thickness (and effective seated height) when a suspension cushion is installed, it might be necessary to lower the seat base, or provide a higher footplate for the operator. The pedals still have to be reachable. As a design indicator, a typical suspension cushion has a thickness of 100mm.

The width of a cushion is dictated by the operator population and an extra few centimetres are normally added for lateral stability and anti roll support. Typically a width of 530mm is a good starting point.

The cushion depth is often determined by the amount of leg support the respective operator would require. Long distance driving at relatively constant pedal position would require more leg support. Short distance driving and vehicle manoeuvring require more frequent pedal control and freedom. Too much leg support might inhibit the ability of a short subject to effectively depress the foot pedals. A design indicator is typically a fore-aft length of 480mm. Care should be taken, that blood flow to the legs is not cut off by excessive pressure supporting the legs.

During its typical operating tasks each vehicle has its unique response to path induced acceleration input $G_{ff}(f)$. As the operating task varies, the road conditions change the path input acceleration. In addition, the vehicle power pack often produces peak vibration at one or more frequencies. Load handling vehicles where the power pack drives a hydraulic pump which in turn drives the wheels and material handling arms often exhibit this phenomenon. The power pack, when set at constant operating revolutions per minute, produces vibration of the vehicle at a specific frequency, often undampened by the suspension system. The input acceleration frequency spectrum of the vehicle plays a major role when considering the vibration isolation performance of a suspension seat or cushion. Consider the equation to calculate the single SEAT value which the industry uses to compare suspension interfaces:

$$SEAT = \sqrt{\frac{\int_{0.5}^{80} H_c^2(f).G_{ff}(f).W_k^2(f).df}{\int_{0.5}^{80} G_{ff}(f).W_k^2(f).df}} \qquad (60)$$

where

$G_{ff}(f)$ = power spectral density of the floor acceleration spectrum input in $(m/s^2)^2/Hz$

$W_k(f)$ = ISO 2631 W_k weighting spectrum in Hertz

$H_c(f)$ = transmissibility of the suspension interface with the human operator seated

$G_{ss}(f)$ = power spectral density of the acceleration spectrum output at the buttock interface in $(m/s^2)^2/Hz$

The last part of the equation (60) use the input psd $G_{ff}(f)$ above and below the line. The weighting spectrum W_k is suggested by ISO 2631(1997) for vertical whole body vibration. The only designer adjustable variable is the suspension interface transmissibility curve $H_c(f)$. The seat suspension designer can only manipulate $H_c(f)$ to minimise the numerator integral to achieve a lower SEAT value. The method assumes linearity of the system between vibration excitation levels in the design and the intended use.

Important to the designer is that the denominator of the equation is merely a scalar equal to the rms of the W_k weighted input vibration $G_{ff}(f)^{0.5}$. The SEAT value is a scalar as well. The numerator is the rms of the $W_k(f)$ weighted output signal $G_{ss}(f)$ on

top of the cushion. This is the part of the equation that the seat designer aims to minimize by reducing $H_c(f)$. However, the product of $H_c(f)^2$, $G_{ff}(f)$ and $W_k(f)^2$ is integrated over the frequency spectrum to equate the numerator. At frequencies where the product of $G_{ff}(f)$ and $W_k(f)^2$ is large, a low $H_c(f)^2$ is required. This reasoning can therefore be used to determine a rough estimate of the shape of the goal transmissibility curve $H_{max}(f)$ from:

$$H_{\max}(f) = (G_{ff}(f).W_k^2(f))^{-0.5}.SEAT.\sqrt{\int_{0.5}^{80} G_{ff}(f).W_k^2(f).df} \qquad (61)$$

$H_{max}(f)$ is a frequency domain array of the maximum transmissibility curve occurrence at each frequency and is shown as a graph in Figure 58. ISO 7096 (2000) EM class 3 is used as an excitation psd. The graph is indicative of where on the frequency axis the anti-resonance should be located. This technique makes the assumption that the output psd $G_{ss}(f)$ is equal at all frequencies, which is not accurate in practice. The magnitude of the $H_{max}(f)$ curve is therefore not correct, however a good indicator of the starting point in the iteration. If the suspension seat can be designed with a transmissibility curve below the blue curve at all frequencies it will conform to EM class 3. If any part of the transmissibility curve exceeds the blue curve, the SEAT value should be calculated with equation (61).

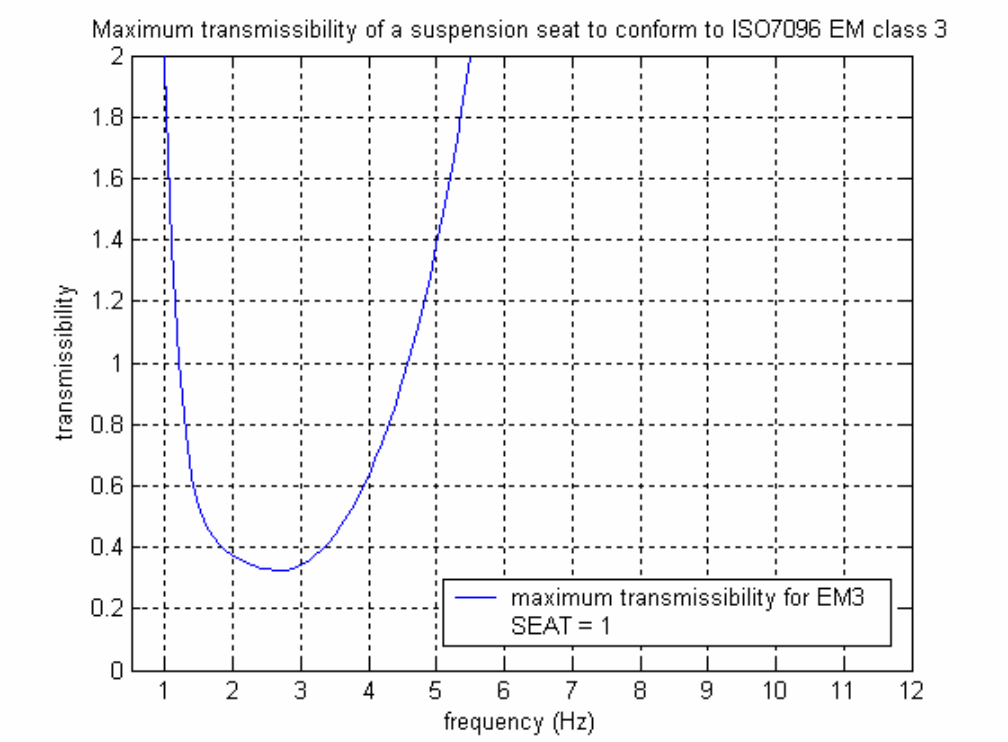

Figure 58 :- Maximum transmissibility curve to conform to EM class 3

In summary, follow these steps to design an air suspension cushion with pipe and tank resonator:

- Step 1: determine the dimensions of the cushion

The width (x-axis) and the depth (y-axis) of the cushion should be small enough to fit inside the operator's seat area, yet large enough to provide lateral and anti-roll support. As a guide, use 530mm width and 480 mm fore-aft length. The thickness of the cushion is determined by the height of the seat base off the floor (or footrest). A thickness of less than 50mm is normally undesirable as it could bottom out during peak accelerations. Also, a thick cushion could have less anti-roll and lateral support and may require a larger width and length.

- Step 2: Vehicle floor vibration spectrum

  The vehicle floor vibration acceleration can be obtained in two manners. Firstly by measuring the vehicles input acceleration spectrum during a typical operation, or by using industry standard curves for the type of vehicle concerned. The former will be vehicle and condition specific and not generally applicable where the latter method would be more suitable.

- Step 3: Create a transmissibility goal curve

  Determine what SEAT value would economically justify the development of this air suspension cushion. Calculate the maximum transmissibility curve $H_{max}(f)$ according to the method above.

- Step 4: Select the cushion, pipe and tank parameters

  Select the system parameters such that the predicted transmissibility $H_{cp}(f)$ curve approach the goal transmissibility $H_{max}(f)$. The frequency at which the anti-resonance valley occurs is determined by the tank and pipe parameters. A larger tank volume will lower this frequency.

  Small tank volumes restrict the amount of air flow into the tank during cushion compression. When the cushion bottoms out nearly all air in the cushion is forced into the tank. If the tank size is equal to that of the cushion, the pressure in the system will double due to the volume decrease. Double pressure equates to acceleration of 1G. Simplified if a maximum acceleration peak of 0.2G is expected, the tank volume should be five times that of the cushion volume. Tank volumes larger than ten times the cushion volume do not further increase the resonator efficiency.

  A pipe with longer length and smaller diameter will normally lower the frequency. Smaller diameter pipes may require shorter length, but has more friction and more damping. Where low damping (i.e. deep isolation valley) is required a larger diameter longer pipe will be required. The modified Helmholtz formula is a good indicator of the expected anti-resonance frequency for pipe, tank and cushion parameters:

$$f_{antiresonance} = 1.425 * F_{helmholtz(\text{mod})} = \frac{c}{2\pi}\sqrt{\frac{A_p}{(V_c + V_d) * l_p}} \qquad (62)$$

  Where

  c = speed of sound in the system normally 343m/s

  A_p = area of the pipe cross section

l_p = length of the pipe between the cushion and the tank

V_c = volume of the cushion at working height

V_d = volume of the tank

The 1.425 multiplier was determined empirically. Use 1.414 for systems with less damping.

- Step 5: Run the Simulink model with a static mass

  Ensure the correct pipe and tank dimensional parameters were chosen to produce a valley on the transmissibility curve at problem frequencies measured in step 2. Iterate until valley frequency is exact.

- Step 6: Run the Simulink model with a human model

  Determine the cushion transmissibility curve H_c in the Simulink model.

- Step 7: calculate the SEAT value

  Calculate SEAT value for the cushion using the transmissibility curve Hc from step 6 and the input signal from step 2. Compare this SEAT value with the desired value from step 3.

- Step 8: re-iterate

  To improve the SEAT value, re-iterate the development process from step 3 using the SEAT value calculated in step 7. Increase the pipe friction in the model to obtain shallower, wider valleys

  Note that it is helpful to determine peak on the estimated acceleration psd on the cushion $G_{ccw}=G_{ffw}*H_c$.

  Use Matlab function: $f = find(G_{ffw}.*Hc.\text{^}2>=max(G_{ffw}.*Hc.\text{^}2)/10)$ *to return the spectrum of frequencies where* G_{ccw} *dominates the cushion rms value.*

- Step 9: Construct the cushion with pipe and tank

- Step 10: Determine the cushion transmissibility curve H_c in the vibration laboratory.

  Ensure that the floor acceleration psd represents all frequencies and has equal energy to that measured in step 2. Narrow band rms values should be compared for problem frequencies.

- Step 12: Re – iterate if SEAT value above economically justified SEAT value

- Step 13: Manufacture the cushion

As an example an air suspension cushion for a wheeler loader >4.500kg per EM class 3 is considered:

7.3. Case study: improvement of the prototype to conform to EM class 3

Earlier the prototype's performance was evaluated against two input spectra i.e. the three-wheeled logger and an EM class 3 wheeler loader > 4.500kg (ISO7096, 2000). Figure 59 shows the power spectral densities of the two input psd spectra weighted by ISO 2631 (1997) W_k filter. Note that the EM 3 curve in Figure 59 has a peak frequency higher than in Figure 30 and the magnitude lower. This is due to the W_k weighing applied. Ideally, the EM3 wheeled loader will require a resonator tuned to the peak frequency of 2.65Hz on the EM3 psd.

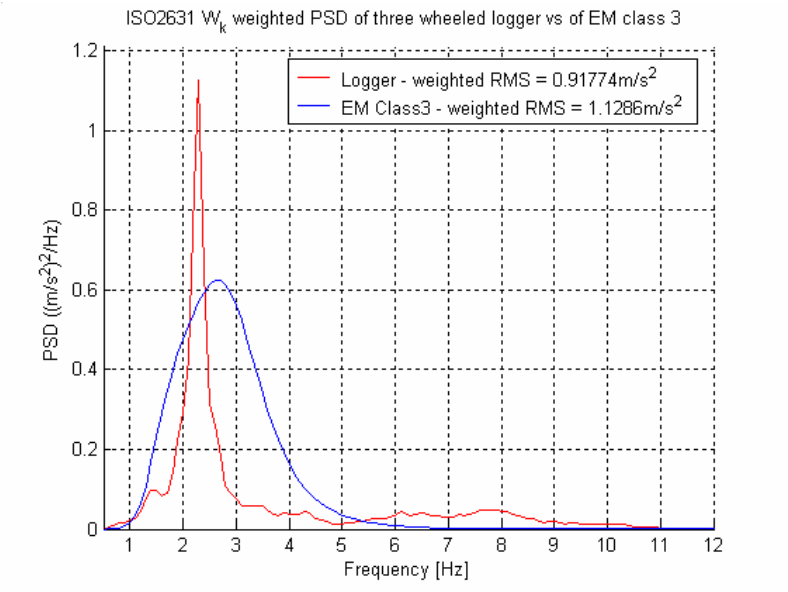

Figure 59 :- Weighted psd of input acceleration for logger and EM class 3

The cushion parameters remain as in Table 2 and the resonator parameters change to that in Table 6. It was found earlier that the best resonator for the logger has a natural frequency of 1.5Hz. Similarly, it can be shown that the best cushion configuration for the EM3 curve requires a resonator with natural frequency at 1.91Hz, which creates a valley in the transmissibility curve at 2.68Hz.

Table 6 :- Pipe and tank dimensional parameters used during experimentation

Parameter	Quantity	Unit	Symbol
Length of pipe	6.5	meter	L_p
Volume of tank	50	litre	V_d
Diameter of pipe	0.025	m	d_p
Speed of sound in air	343	m/s	c
Friction of air in pipe factor	0.02[3]		μ

[3] The friction of the air in the pipe was determined iteratively until the magnitude at resonance of the simulation equals the magnitude of the prototype.

The improved model generated the transmissibility curve in Figure 60. The resultant psd on the cushion is shown in Figure 61 together with the W_k weighted EM class 3 input psd. The SEAT value of less than 100% suggests that this air suspension cushion can qualify as a suspension seat according to the ISO7096 standard EM class 3.

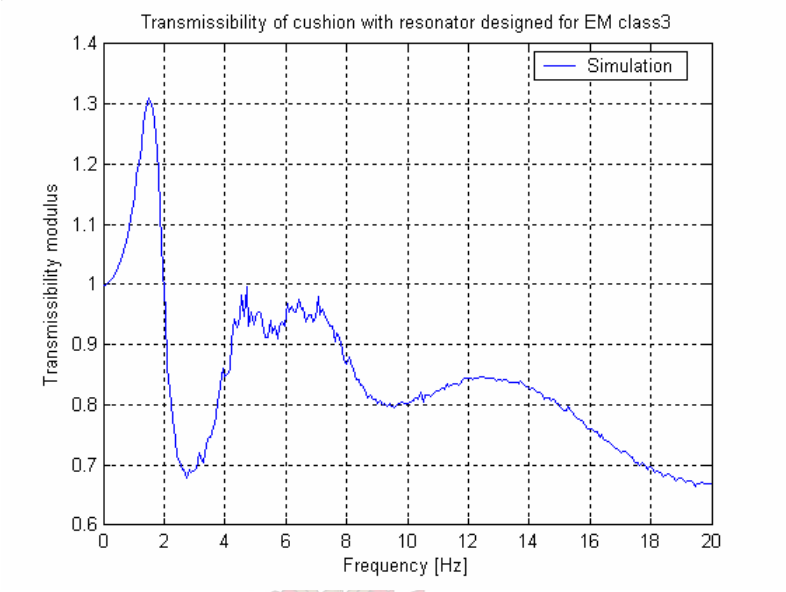

Figure 60 :- Transmissibility from model to achieve EM class 3

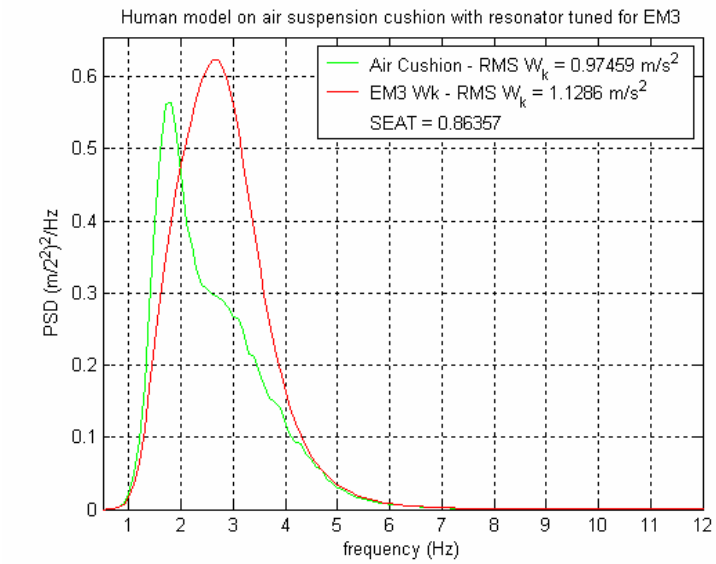

Figure 61 :- Weighted psd of input and output signal for EM3 cushion

8. Conclusions & Recommendations

An air suspension cushion prototype was developed and tested in the laboratory. Through conceptual evaluation and refinement a cushion was found to consist of a tube torus set in a foam surround. The tube torus is fitted with a pipe which is in turn connected to a tank. The pipe and tank system act as a resonator. Verification of the prototype was done in the laboratory on a human rated vibration actuator. In-field input data measured on a three wheeled logger was used for the prototype design. Calculations indicated a significant improvement in the estimated SEAT value. The resonator was tuned to provide anti-resonance in the transmissibility curve at the first resonance peak of the logger. System linearity was assumed. The following conclusions and recommendations can be made:

Major conclusions:

- A pipe connection between the cushion and the auxiliary tank creates an anti-resonance on the transmissibility curve.
- Changes in the tank volume, pipe length and pipe diameter cause the natural frequency of the resonator to change
- The air suspension cushion's natural frequency is not affected by the supported mass.

Minor conclusions:

- Auxiliary tank volume increase the anti-resonance effect
- Long pipe lengths cause pipe resonance
- Increased pipe damping broadens the anti-resonance but decreases the magnitude
- The tube torus has certain inherent anti-roll characteristics

A pipe connection between the air suspension cushion and an auxiliary volume (tank) acts as a resonator. The mass of the air in the pipe together with the spring character of the air in the tank create a single degree of freedom resonator. The transmissibility curve of the cushion with the resonator exhibits a definite valley at a frequency just higher than the natural frequency of the resonator. This anti-resonance can be tuned to be at frequencies higher and lower than the natural frequency of the initial system. Other research on air suspension with auxiliary volumes made use of an orifice to control damping. Some controlled the damping actively by variation of the orifice aperture size. The orifice technique was found not to reduce the transmissibility curve below unity. However, the anti-resonance created by the prototype in this study does reduce the transmissibility curve to below unity at the tuned frequency. Consequently, a peak appears on either side of the anti-resonance frequency. This is typical of a dynamic absorber added to a sdof mechanical system.

Adjusting the pipe length and pipe diameter cause the frequency of the resonator to change. These changes follow the Helmholtz formula. Higher resonator frequencies are achieved with larger pipe diameter and shorter pipe lengths. Larger tank volumes result in lower resonator frequencies.

The natural frequency of the air suspension cushion without the resonator is unaffected by the mass it supports if the working height remains constant. The resonator's natural frequency is also unaffected by system pressure. Therefore the air suspension cushion with resonator will perform equally with different supported masses. Changes of interface

impedance will however affect the transmissibility curve. Laboratory tests on human subjects showed little inter subject difference to the transmissibility curve at the frequency of anti-resonance.

Increase in auxiliary tank volume tends to increase the magnitude of the anti-resonance valley on the transmissibility curve. It was found iteratively that the resonator is more effective at tank volumes larger than three times cushion volume and smaller than ten times cushion volume.

Long pipes were found to generate pipe resonance. Expert opinion stated that the pipe length should ideally be less that one tenth of the resonance wave length. Increased pipe length also increases pipe damping, which broadens the anti-resonance valley but reduces the anti-resonance magnitude.

Anti roll stability was set as one of the important ergonomic specifications for the cushion. Inherently to the shape of the tube torus is its anti roll resistance. During roll the force on the one side of the cushion is increased and decreased on the other. The contact pressure between the torus and the base remains constant but the pressure area increase to resist the higher force on that side. Similarly the pressure area decreases on the other side to generate the opposing force moment.

Recommendations:

- A resonator design is to be vehicle specific
- The pipe and tank sizes have to be reduced

Future work:

- Reduce the sizes of the tank and pipe
- Use multiple resonators for broad band anti-resonance
- Test an improved prototype under in-field condition
- Subjective opinion

The highest vibration isolation efficiency will be achieved if the cushion resonator is designed vehicle specific. Vehicle input acceleration measurements during a typical operational task is required for the design. The resonator is tuned to provide anti-resonance at the specific resonance peaks in the vehicles characteristic input psd. This is possible on retrofit designs where the vehicle has been in operation and is well run in. For new vehicles that are not available for testing the ISO7096 (2000) specification could be used as input acceleration psd.

The prototype requires a large tank and a long pipe to effectively reduce the transmissibility curve through anti-resonance. Low frequency resonances and input psd peaks in typical off road vehicles require low resonator frequencies. The air in the pipe has low mass and therefore a low airspring stiffness in the tank is needed. This requires a large tank volume. One idea is to increase the mass of the inertial slug in the pipe. This means a higher stiffness spring requiring a smaller tank and a shorter pipe. A liquid slug could be considered to replace the air slug. Water is a thousand times denser than air, but at full cushion deflection, the air movement amplitude in the pipe could exceed the pipe length. A liquid slug would be pushed into the tank which could cause the resonator to change characteristic. Using a liquid the pipe friction is also expected to increase considerably.

Multiple smaller resonators of equal dimensional parameters are expected to work together and provide similar anti-resonance to a single large volume and long pipe. This

should be investigated in further research. Additionally an array of resonators with unequal dimensions could be considered for broadband anti-resonance.

Further research could also be done to determine the subjective opinion of vehicle operators. Ergonomic, operational and retrofit issues should be addressed. This would ideally be done in parallel to an in-field evaluation of the cushion under real operating conditions.

Finally it can be concluded that the air suspension cushion fitted with a correctly tuned resonator does reduce vibration at the seat interface, which allows an increase of the allowable operator exposure hours. If the size of the tank and length of the pipe can be reduced, this air suspension cushion makes an attractive commercial business case.

References

1. Allen GR (1976) **Progress on a specification for human tolerance of repeated shocks.** Proceedings of the United Kingdom Informal Group meeting of Human Response to Vibration, The Royal Military College of Science, Shrivenham, Swindon, UK

2. Allen GR (1977) **Human tolerance of repeated shocks.** Proceedings of the European Symposium on Life Science Research in Space, Cologne, ESA SP-130, 343-349.

3. Allen GR (1979**) Part I: The use of the spinal analogue to compare human tolerance of repeated shocks with tolerance of vibration. Part II: A critical look at biodynamic modelling in relation to specifications for human tolerance of vibration and shock**. AGARD Conference Proceedings CP-253. Models and Analogues for the evaluation of Human Biodynamic Response, Performance and protection, Paris, 6-10 November 1978 (H.E. von Gierke, ed.), paper A25. Advisory Group for Aerospace Research and Development, Neuilly-sur-Seine.

4. Amirouche FML, Xie M, Patwardhan A (1994) **Optimisation of the contact damping and stiffness coefficients to minimise human body vibration.** Journal of Biomechanical Engineering, 116 (4) 413-420.

5. Bekesy G von (1939) **"About the vibration feeling"**. Akustishe Zeitschrift, 4, 316 - 360.

6. Belytschko T and Privitzer E (1979) **A three-dimensional discrete element dynamism model of the spine head and torso.** AGARD Conference Proceedings CP-253: Models and analogues for the evaluation of human biodynamic Response, performance and protection, Paris, 6-10 November 1978 (H.E. von Gierke, ed.), paper A9. Advisory Group for Aerospace Research and Development, Neuilly-sur-Seine.

7. Boileau PE and Rakheja S (1998) **Whole-body vertical biodynamic response characteristics of the seated vehicle driver Measurement and model development.** International Journal of Industrial Ergonomics 22 (6) 449.

8. Boileau PE, Rakheja S and Wu X (2002) **A body mass dependent mechanical impedance model for applications in vibration seat testing.** Journal of sound and vibration 253 (1) 243-264

9. Boileau PE, Rakheja S Yang X and Stiharu I (1997) **Comparison of biodynamic response characteristics of various human body models as applied to seated vehicle drivers.** Noise and Vibration Worldwide, 28 (9) 7-15.

10. British standard institution (1987) **Measurement and evaluation of human exposure to whole body mechanical vibration and repeated shock**. BS 6841, Britain.

11. Bueche F (1979) **College Physics** McGraw Hill Book Company

12. Cho Y, Yoon YS (2001) **Biomechanical model of human on seat with backrest for evaluating ride quality.** International Journal of Industrial Ergonomics, 27 (5) 331-345
13. Coermann R (1940) **Investigation into the effect of vibration on the human body.** Luftfahrtmedizin, 4, 73-117. Translated into English in 1947 by Shirley W, Royal Aircraft establishment, Farnborough, RAE
14. Coermann RR (1962) **The mechanical impedance of the human body in sitting and standing position at low frequencies**. Human Factors, 4, 227-253.
15. Corbridge C and Griffin MJ (1986) **Vibration and comfort: vertical and lateral motion in the range 0.5 to 5.0 Hz**. Ergonomics, 29, 249-272
16. Daugherty RL and Franzini JB (1984) **Fluid Mechanics with Engineering Applications.** 272-273, McGraw-Hill
17. Demic M (1991) **Contribution to optimization of vehicle seats.** International Journal of Vehicle Design, 12, 5-6.
18. Du Plooy NF and Heyns PS (2001) **The development of a tuned vibration absorber for a pneumatic rock-drill handle**. Proceedings of the IX International Symposium on Dynamic Problems of Mechanics DINAME IX, Florianopolis, Brazil. 5-9 March, 531-536.
19. Ebe K and Griffin MJ (2001) **Factors affecting static seat cushion comfort.** Ergonomics, 44 (10) 901-921.
20. European Union Directive 2002/44/EC of the European Parliament and the Council of 25 June 2002 on the minimum health and safety requirements regarding the exposure of workers to the risks arising from physical agents (vibration).. "**On the Minimum Health and Safety Requirements Regarding the Exposure of Workers to the Risks Arising from Physical Agents: Vibration**." [16th Individual Directive Within the Meaning of Article 16(1)] of Directive 89/391/EEC. Brussels, Belgium.
21. Fairley TE (1990) **Predicting the transmissibility of a suspension seat.** Ergonomics, 33 (2) 121-135
22. Fairley TE and Griffin MJ (1989) **The Apparent Mass of the Seated Human Body: Vertical Vibration**. Journal of Biomechanics, 22 (2), 81-85.
23. Gouw GJ, Rakheja S, Sankar S, AfeworkY (1990) **Increased comfort and safety of drivers of off-highway vehicles using optimal seat suspension.** SAE Technical Paper Series, International Off-Highway and Powerplant Congress and Exposition
24. Griffin MJ (1990) **Handbook of Human vibration.** Academic Press Limited, London
25. Guignard JC (1965) **Vibration** In: A textbook of aviation physiology, Gilles JA ed Chap 29, 813-894 New York: Pergamon
26. Gyi DE, **Porter** JM and Robertson **NK (1998) Seat pressure measurement technologies: considerations for their evaluation** Applied Ergonomics, 29 (2), 85-91

27. Gyi DE and **Porter JM(1999) Interface pressure and the prediction of car seat discomfort** Applied Ergonomics 30 (2), 99-107

28. Helmholtz HLF von (1863) **On the Sensation of Tone As a Physiological Basis for the Theory of Music**. Germany

29. Hosten I (2004) **Analysis of seating during low frequency vibration exposure.** PhD thesis, Katholieke Universiteit Leuven, #606.

30. International Organisation for Standardisation (1998) **Mechanical vibration and shock -- Guidance on safety aspects of tests and experiments with people -- Part 1: Exposure to whole-body mechanical vibration and repeated shock** . International Standard, ISO 13090-1.

31. International Organisation for Standardisation (1997) **Mechanical vibration and shock – Evaluation of human exposure to whole body vibration – Part 1: General requirements**. International Standard, ISO 2631-1.

32. International Organisation for Standardisation (2004) **Mechanical vibration and shock – Evaluation of human exposure to whole body vibration – Part 5:** Method for evaluation of vibration containing multiple shocks addresses specific mechanical shock in the horizontal and vertical direction. International Standard, ISO 2631-5.

33. International Organisation for Standardisation (2000) **Earth-moving machinery – laboratory evaluation of operator seat vibration.** International Standard, ISO7096.

34. Jones R (1975) **Flight evaluation of helicopter rotor isolation system.** Karman Aerospace Corporation, Bloomfield, Connecticut.

35. Kashani R (2004) **Fluidic vibration controllers.** www.deicon.com

36. Kitazaki S and Griffin MJ (1998) **Resonance behaviour of the seated human body and effects of posture.** Journal of Biomechanics, 31 (2) 143-149

37. Kornhauser AA (1994) **Dynamic modelling of gas springs.** Transactions of the ASME, 116, 414 - 417

38. Lee J and Ferraiuolo P (1993) **Measuring seat comfort**. Automotive Engineering 101 (Jul1993),.25-30.

39. Liu LQ, Craggs MD, Nicholson GP, Knight SL, Chelvarajah R, Bycroft J, Middleton FRI, Ferguson-Pell M (2004) **Pressure changes under the ischial tuberosities of seated individuals during sacral nerve root stimulation.** 9th Annual conference of the International FES Society, Bournemouth, UK

40. Mallock A (1902) **Report on vibration.** Central London Railway. Appendix 1, p5. London HM stationary Office.

41. Mansfield NJ and Griffin MJ (2002) **Effects of posture and vibration magnitude on apparent mass and pelvis rotation during exposure to whole-body vertical vibration.** 2nd International Conference on Whole-Body Vibration Injuries Conference, Siena, Italy.

42. Mertens H (1978) **Non-linear behaviour of sitting humans under increasing gravity**. Aviation, Space and environmental Medicine 287-298.

43. Mohring (1999) consultation of an expert in the field of Helmholtz resonators. The issue of pipe length affecting the resonator performance was addressed. *Dr. J. Mohring Institut für Techno- und Wirtschaftsmathematik Erwin-Schrödinger-Straße D-67663 Kaiserslautern Tel: 0631/205-3886 Fax: 0631/205-4139*

44. Muller EA (1939) **Die wirkung sinusformiger verticalschwingunngen auf den sitzenden un stehenden menschen**. Arbeitsphysiologie, 10, 459-476.

45. Nashash H, Qassem W, Zabin A and Othman M (1996) **ECG response of the human body subjected to vibrations.** J Medical Engineering & Technology, 20 (1) 2-10.

46. Nell S and Steyn JL (1994) **Experimental evaluation of an unsophisticated two state damper. Journal of terramechanics**, 31 (4), 227-238

47. Nishiyama S, Uesugi N, Takeshima T, Kano Y and Togii H (2000) **Research on vibration characteristics between human body and seat, steering wheel, and pedals (effects of seat position on ride comfort)**. Journal of Sound and Vibration, Academic Press, London, England.

48. Paddan GS and Griffin MJ (2002) **Effect of seating on exposures to whole-body vibration in vehicles.** 2nd International Conference on Whole-Body Vibration Injuries, Siena, Italy.

49. Patil M K, Palanichamy M S and Ghista D N (1980) **Response of Human Body to tractor vibrations and its minimization by provision of relaxation suspensions to both wheels and seat at the plane of centre gravity**. Journal Medical & Biological Engineering & Computation 18, 554-562

50. Patten WN, Pang J (1998) **Validation of a non-linear automotive seat cushion vibration model**. Vehicle System Dynamics, 30 (1) 55-68.

51. Payne PR (1976) **On quantising ride comfort and allowable accelerations.** American Institute of Aeronautics and Astronautics and Society of Naval Architects and Marine Engineers, AIAA/ SNAME, Advanced Marine Vehicle Conference, Arlington, Virginia.

52. Payne PR (1978) **A method to quantify ride comfort and allowable accelerations.** Aviation, Space and environmental medicine 49, 262-269

53. Porter JM, Gyi DE and Tait HA (2003) **Interface pressure data and the prediction of driver discomfort in road trials** Applied Ergonomics, 34 (3), *207-214*

54. Qassem W (1996) **Model prediction of vibration effects on human subject seated on various cushions**. Butterworth-Heinemann Ltd, Oxford, England

55. Qassem W, Othman MO and Abdul-Majeed S (1993) **Effects of vertical and horizontal vibrations on the human body**. Butterworth-Heinemann Ltd, London, England

56. Quaglia G and Sorli M (2001) **Air suspension Dimensionless Analysis and Design Procedure.** Vehicle System Dynamics, 35 (6), 443- 475.

57. Rakheja S, Afework Y and Sankar S (1994) **Analytical and experimental investigation of the driver-seat-suspension system**. Vehicle System Dynamics, 23 (7) 501-524.

58. Rakheja S, Stiharu I and Boileau PE (2002) **Seated occupant apparent mass characteristics under automotive postures and vertical vibration.** 2nd International Conference on Whole-Body Vibration Injuries, Siena, Italy.

59. Rittweger J, Beller G and Felsenberg D (1999) **Acute physiological effects of exhaustive whole-body vibration exercise in man.** Clinical Physiology 20 (2), 134 – 142.

60. Rosen J and Arcan M (2003) **Modelling the human body/seat system in a vibration environment**. Journal of Biomechanical Engineering, American Society of Mechanical Engineers.

61. Safetyline Institute (2006) **Evaluation of human exposure to whole body vibration**. www.safetyline.wa.gov.au.

62. Schomer PD and Neathammer RD (1987) **The role of helicopter noise-induced vibration and rattle in human response.** Journal Acoustic Society of America. 81 (4), 966-976.

63. Selamet A, Dickey NS and Novak JM (1995) **Theoretical, computational and experimental investigation of helmholtz resonators with fixed volume lumped versus distributed analysis.** Journal of sound and vibration, 187 (2), 358-367

64. Strydom JPD, Heyns PS and Van Niekerk JL (2002) **Development of a vibration absorbing handle for rock drills.** Journal of the Institute of Mining and Metallurgy, 102 (3), 167-172.

65. Toyofuku K, Yamada C, Kagawa T and Fujita T (1999) **Study on dynamic characteristic analysis of air spring with auxiliary chamber**. JSAE review 20 p349-355

66. Ullman DG (2003) **The mechanical design process.** McGraw Hill, New York.

67. Van der Merwe AF (1989) **The effects of vibration and noise on human performance**. Masters thesis, University of Stellenbosch

68. Van Niekerk JL, Heyns PS and Heyns M (2000) **Human vibration levels in the South African mining industry**. Journal of the South African Institute of Mining and Metallurgy, 100 (4), 235-242.

69. Van Niekerk JL, Pielemeier WJ and Greenberg JA (2000) **The use of Seat Effective Amplitude Transmissibility (SEAT) values to predict dynamic seat comfort.** 35th Group meeting on Human Response to Vibration. Southampton, England.

70. Village J and Morrison JB (1989) **Whole body vibration in underground load haul dump vehicles.** Ergonomics, 32, (10), 1167-1183

71. Vogt HL, Coermann RR, and Fust HD (1968) **Mechanical impedance of the sitting human under sustained acceleration.** Aerospace Medicine 39, 675-679.

72. Wan Y, Schimmels JM, (1997) **Optimal seat suspension design based on minimum 'simulated subjective response'**. Journal of Biomechanics, English Translation ASME, 119 (4), 409-416.

73. Wei L and Griffin MJ (1998a) **Mathematical model for the mechanical impedance of the seated human body exposed to vertical vibration.** Journal of Sound and Vibration 212 (5), 855-874

74. Wei L and Griffin MJ (1998b) **The prediction of seat transmissibility from measures of seat impedance.** Journal of Sound and Vibration, 214 (1), 121-137.

75. Wei L and Griffin MJ (2000) **Effect of subject weight on predictions of seat cushion transmissibility.** 35th Group meeting on Human Response to Vibration, Southampton, England.

76. Wu X, Rakheja S and Boileau PE (1999) **Study of human-seat interface pressure distribution under vertical vibration**. International Journal of Industrial Ergonomics 21 (6), 433-449.

Appendix A - Experimental setup in laboratory

The same experimental setup was used to test the tube torus with constant pressure area as well as the prototype. This appendix provides details of the experimentation for reference purposes.

A.1. Equipment:

A.1.1 Vibration Actuator

An MTS 407 PID controller is used with a hydraulic floor vibration actuator, capable of 200mm travel. The actuator will move 12.6mm per Volt into the controller. The actuator is rated safe for human testing.

A.1.2 Analyzer

The Siglab DSP system provides Analogue to Digital input and Digital to analogue output simultaneously at frequencies from 0 to 20kHz. Two modules connected, enables 8 channels input setup to various DC, AC and ICP(AC) input configurations.

- Siglab Module serial number #11684 used for channel 1 to 4 and output
- Siglab Module serial number #11347 used for channel 5 to 7

The Siglab channel setup is captured in Figure 62. Column 2 indicates the full scale setting for the A/D converter in the Siglab; colom4 the DC offset; column 6, 7& 8 the engineering units.

On/Off	Full Scale	Coupling	Offset	Label	Engineering Units		Invert	0 dB Vref
Ch 1	±0.625 V	AC	0	d2Z_seat/	106.2	m/s2	/Volt	1e-005
Ch 2	±0.625 V	AC	0	d2Z_cush/	98.841	m/s2	/Volt	1e-005
Ch 3	±10.0 V	DC	0	Zseat	-12.78	mm	/Volt	1e-005
Ch 4	±10.0 V	DC	0	P_cush	1999	Pa	/Volt	1e-005
Ch 5	±10.0 V	DC	-0.003	P_tank	1986	Pa	/Volt	1e-005
Ch 6	±10.0 V	DC	0.008	Pcush-Pta	201	Pa	/Volt	1e-005
Ch 7	±10.0 V	DC	-3.97	Zcush-Zse	-59.5	mm	/Volt	1e-005

Figure 62 :- Siglab channels setup

A.1.3 Acceleration - Sensors & signal conditioning

Z input - under air suspension cushion – Channel # 1

PCB acceleration sensor 352C67 ICP serial #14976 sensitivity 106.2 m/s^2/Volt 2

Z output – on air suspension cushion – Channel # 2

PCB tri-axial acceleration sensor 356B40 serial #21385 z-axis sensitivity 98.841 m/s^2/Volt

A.1.4 Pressure - Sensors & signal conditioning

Pressure in cushion – Channel # 4

HBM differential pressure transducer PD1 (5 kHz inductive) serial# 5685 sensitivity 10kPa FSD @ 8mV/V

HBM bridge amplifier serial# 66557 sensitivity 10mV/V and output U_B = 5V

Pressure in tank – Channel # 5

HBM differential pressure transducer PD1 (5 kHz inductive) serial# 25022 sensitivity 10kPa FSD @ 8mV/V

HBM bridge amplifier serial# 94899 sensitivity 10mV/V and output U_B = 5V

Pressure in cushion – pressure in tank – Channel # 6

HBM differential pressure transducer PD1 (5 kHz inductive) serial# 29444 sensitivity 1.0kPa FSD @ 8mV/V

HBM bridge amplifier serial# 66558 sensitivity 20mV/V and output U_B = 5V

A.1.5 Displacement - Sensors & signal conditioning

Displacement of actuator Z input (Z_{floor}) relative to earth

Displacement sensor sensitivity 12.58mm/V

Connected to feedback output on PID controller

Displacement of Z output ($Z_{cushion}$) relative to Z input (Z_{floor})

Displacement sensor sensitivity 60mm/V

HBM bridge amplifier serial# 74231 sensitivity 20mV/V and output U_B = 1V

A.1.6 Calibration

All sensors have calibration certificates, and were crosschecked before experimentation commented and after experimentation concluded.

A.1.7 Other

- Purpose made tank in Figure 63 with pressure release valve at 100kPa and tank connector at top and bottom. A dial pressure gauge was fitted to monitor tank pressure
- Compressed air with variable pressure controller valve set to just higher than operating pressure P_0.
- For the round torus with constant pressure area concept a working height control system was used. It consisted of a normally open magnetically sensitive reed valve and magnet to control working height. The magnet was mounted on top of the cushion, and the reed valve at a set height above the magnet. When the pressure drops and the magnet lowers, the reed valve opens circuit and through at 12V x 220V relay switches, an air valve allows air into the tank.
- Electrical air valve, relay and 12VDC power supply

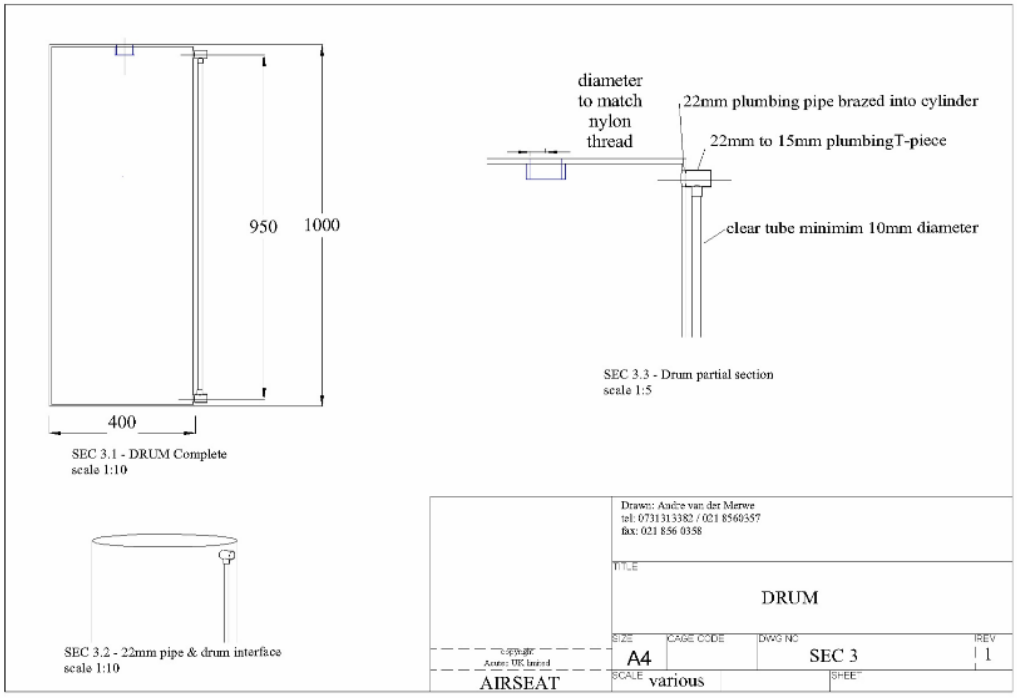

Figure 63 :- Steel tank with rigid sides (volume130 litre) – assembly drawing

A.2. Resource data:

The actuator PID controller requires a displacement signal to generate movement of the table. During in-field experimentation on the three-wheeled logger an acceleration signal was recorded from the accelerometers. It is therefore necessary to convert the acceleration signal in the time domain to a displacement signal in the time domain. The Siglab routines do this integration in the frequency domain for a capture window of time domain data, but have no way to export displacement signal back to the time domain. A dedicated routine was developed in Matlab to do this conversion in the time domain without conversion to the frequency domain. Time domain filtering was applied to eliminate unwanted low and high frequency data, and to generate a displacement data signal friendly to the PID controller.
For development details please refer to Appendix B of this document. Note that the routines were later modified to apply to a random signal instead of the in-field measured signal. The routine however apply equally to both.

A.3. Data capture procedure:

- in-field using SIGLAB VCAP to capture 8 channels of vibration data ; 8 runs stacking operation; 2 runs driving on field road
- in lab on vibration actuator capturing SIGLAB .vna Spectrum Analyser - Different pipe length, pipe diameter, tank volume and input signal amplitudes were used. Normally five repeats of each configuration were captured. The actuator's PID controller (displacement feedback) received a signal (PLAYSIGNALfs) which was generated from a random signal integrated twice to ensure that the acceleration output signal had near equal energy in the frequency range 0.5Hz to 20Hz (Butterworth bandpass filter applied to the time domain signal).

A.4. Supportive test methods:

A.4.1 Mass determination:

- Weigh each subject twice and take the average as his standing mass.
- Sit the subject on a bench with height such that the bench plus the scale height equals the loaded height of the cushion. The subject sits with his hands loosely on his legs and his back erect and vertical.

A.4.2 Pressure measurement:

Static system pressure is measured with a H_2O manometer before and after each test run. Pressure sensors recorded real-time pressure variation on channels 4 to 6 of the data logger.

A.4.3 Transmissibility measurement:

Siglab VNA routine determines the transmissibility curve of each seat cushion. A single axis PCB accelerometer measures the z-axis floor input acceleration and records it to the Siglab channel 1. A tri-axial seat pad accelerometer

measures the z-axis acceleration on top of the seat cushion and records it to the Siglab channel 2.

The Siglab VNA routine is set to average 50 measurement windows with 50% overlap at a sample rate of 51.2Hz. The average of the 'xfer' with unit 'mag' is saved as a single test for a cushion under specific conditions of mass and magnitude. A Hanning window is used and signal window length is 512 samples.

A.5. Data analysis process

A.5.1 Captured data:

A.1.5.1 in-field data using SIGLAB VCAP to capture 8 channels of vibration data

- 8 runs stacking operation
- 2 runs driving on field road

A.1.5.2 in lab on vibration actuator capturing SIGLAB VNA Spectrum Analyser

The actuator's PID controller (displacement feedback) received a signal (PLAYSIGNALfs).

A.5.2 Data analysis method:

A.2.5.1 In-field data;

- 'Data_Analysis.m' converted from 'vca' file to 'mat' and adjusted to calibration and engineering units. This routine called another routine 'Data_Analysis_Test[x].m' for each run [x]. The first stored data in file 'FIELDTEST[x]_ANALYSED' for each run
- 'psd_analysis.m' loads data stored above. It calculates a psd for the 3 Zfloor inputs channels #1,#4,#5 and the Zseat channel #8. Frequency limits of 0.5Hz and 80Hz are applied. The Zfloor channels are averaged to obtain one Zfloor psd for each of the 10 runs. ISO2621 W_k weighing filter in applied in the frequency domain and SEAT is calculated for the existing seat during each run. Data is stored in 'Bell' structure variable in file 'BellLoggerInFieldpsd_analysesResults.mat'.
- The SEAT values for the stacking operation and field road run are averaged mathematically to compare with the same SEAT values from the improved air suspension cushion.

A.2.5.2 Lab data;

- A Matlab routine called "AIRSEATANALYSE" hosts the various analyses steps. For reference the routine is added in the appendices.
- Step 1 – load the experimental parameters into variable LABPLAN. This will control and load appropriate Siglab *.vna files into memory for analyses.

Load the transmissibility curve Hc(f) for each cushion, subject and acceleration level.

- Step 2 – define frequency domain vector "w" with increment dF = 0.1Hz. Set frequency domain bandwidth limits of interest from 0.5Hz to 20Hz. Frequency domain data outside of these limits are discarded after power spectral density calculation.
- Step 3 – calculate ISO 7096 EM curves for frequency vector "w". For calibration purposes determine rms value between the frequencies limits set in the standard.
- Step 4 – load the time domain data measured on the there wheeled logger. Set limit to the time domain data to be analysed eliminating start, and end spikes and other erratic data points found. Multiply time domain data with engineering unit conversions for each sensor. Calculate rms_t from time domain data for each channel. Calculate the psd for each channel using maximum overlap and Hanning window. Calculate rms_f from frequency domain data to calibrate against rms_t . Select only frequency domain data related to vector "w".
- Step 5 – create ISO 2631 W_k frequency domain vector to "w" for use in frequency domain filtering.
- Step 6 – calculate $G_{ssw}(f)$ from input channels data, weighted to W_k filter for each in-field run psd, and each EM class psd. Calculate $G_{ccw}(f)$ for each combination of cushion condition $H_c(f)$ and input spectrum $G_{ssw}(f)$.
- Step 7 & 8 -- Calculate the SEAT value for each of the combinations in step 6
- Step 9 – Determine the lowest SEAT value for the logger input data, and the lowest SEAT value for the EM curves.
- Step 10 – Plot the transmissibility curves for the cushion with the lowest SEAT for the EM curves.
- Step 11 -- Plot the transmissibility curves for the cushion with the lowest SEAT for the logger runs.
- Step 12 – Plot the plot the transmissibility curves for all human subjects on one figure for each cushion and input level.
- Step 13 -- plot the transmissibility curves for each human subject versus input level for cushion 4 only.
- Step 14 - -plot the transmissibility curves for each human subject versus cushion at highest input level 3 only.
- Determine the average transmissibility curve of all human subjects for each cushion to compare at each level.

A.2.5.3 Statistical analyses:

- The SEAT values calculated from the above and below the seat during all the in-field runs are averaged to obtain a SEAT value for the chair currently installed in the logger.
- Cushion to replace the existing seat in the logger: Average the SEAT values calculated for each cushion at level 2 for all of the infield runs. Also determine standard deviation amongst each set of obtained SEAT values. Assess the range of the SEAT values from best to worst, and determine the significance of the results.
- Compare chair currently in Three-wheeled Logger with performance of cushion suggested.

Appendix B - Vibration actuator floor input signal

A.1. VIBRATION ACTUATOR INPUT SIGNAL DESIGN

A.5.3 Background & Aim:

A randomly generated displacement input signal to the vibration renders an acceleration signal which has inadequate energy in the low frequencies to evaluate the transmissibility of the AIRSEAT cushion. An input signal is required which produce a near equal distribution of energy at all frequencies from 0.5 to 20Hz.

A.5.4 Method:

Set up 3 channels on Siglab to measure the following:

1. Actuator Input in Volts – displacement
2. Actuator Output in g's - Acceleration (Cushion Input)
3. Actuator Feedback in Volts - displacement

Capture 40 seconds of time domain data at SampleRate of 51.2Hz. Store in Siglab vna files all possible cross channel data.
Analyse data and determine the coherence between the Actuator Feedback and Input. Similar for Actuator acceleration output and displacement Input.
Prepare Matlab subroutines to apply filtering, signal conditioning and integration to the Output Acceleration signal.
Integrate the Acceleration signal twice to achieve the new Actuator Input signal in Volts (called PLAYSIGNAL).
Filter the PLAYSIGNAL to a 4^{th} order Butterworth bandpass filter between 0.1 and 20Hz.
Apply Start and End conditions to the PLAYSIGNALf to eliminate high frequency, high amplitude shocks.
Evaluate the time domain signal PLAYSIGNALfs for spectral content.

A.5.5 Results and Analysis:

The graph below shows the spectral content of the three measured channels:

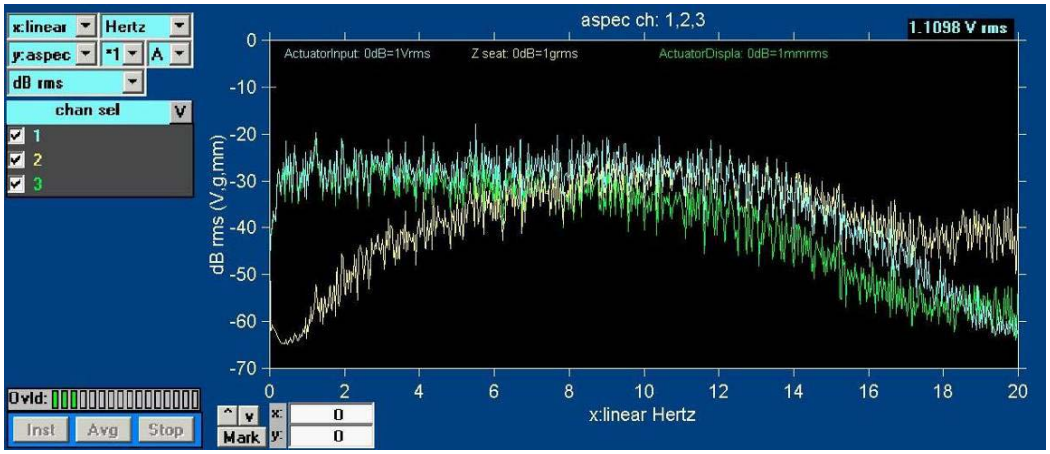

Figure 64 :- Spectrum Measured Data - INPUT Volts(blue), OUTPUT acceleration (yellow), FEEDBACK Displacement,(green) ,

Coherence of the OUTPUT and FEEDBACK signals are shown in graph below. It is evident that the coherence of the Acceleration signal reduces at the low frequencies. This is due to less amplitude at the low frequencies and therefore the signal reduces into the noise of the accelerometer output. Our interest extends down to 0.5Hz.

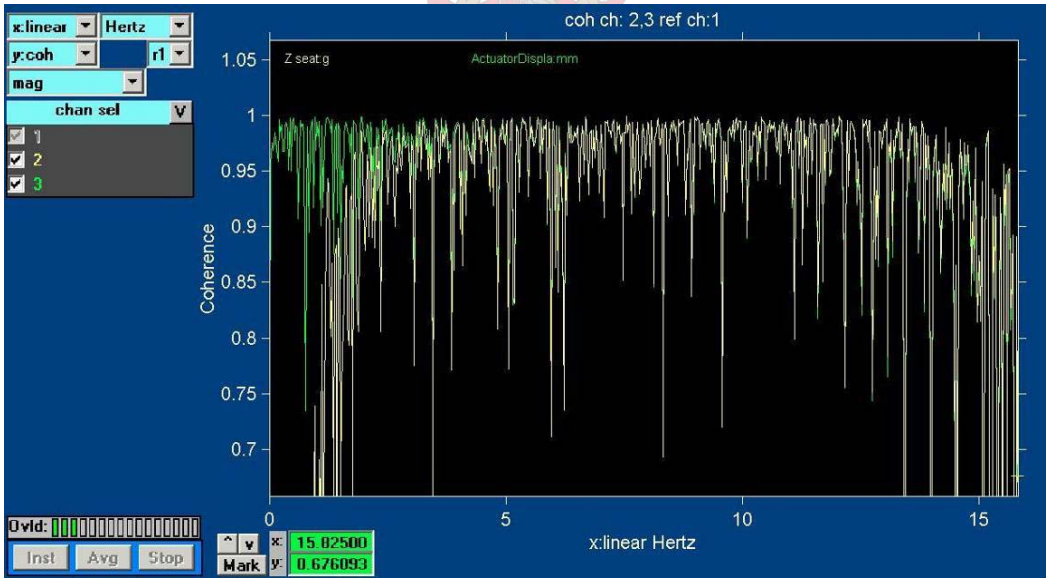

Figure 65 :- Coherence of measured data

The data was stored in Siglab VNA file format named run07.vna

Four Matlab subroutines were developed:

1. SIMP.m – to integrate according to Simpson rule

2. INTEGRAL.m and INTEGRALDOUBLE.m to employ progressive integration to the input signal
3. playsignalanalysis.m – to load, manage and display the data
4. ActuatorInputSignalCreator.m – to design and check bandpass filters, and apply forward and reverse FFT's in order to generate a time domain signal to use as input to the actuator

The results of the 'playsignalanalysis.m' subroutine are in the time and frequency domain signals below. The following sequence of signal processing is used to ensure usable end result:

1. generate random signal using Matlab randn function
2. filter using a 4th order Butterworth bandpass between 0.1 and 20Hz
3. apply a 0.1Hz modified Hanning window and the start and the end of the data
4. integrate the resultant time domain signal twice using a Simpson rule
5. apply a shift correction to centre the mean of the time signal on zero
6. filter the data again as above
7. apply the start and end window again
8. evaluate the time and frequency domain content on a graph below

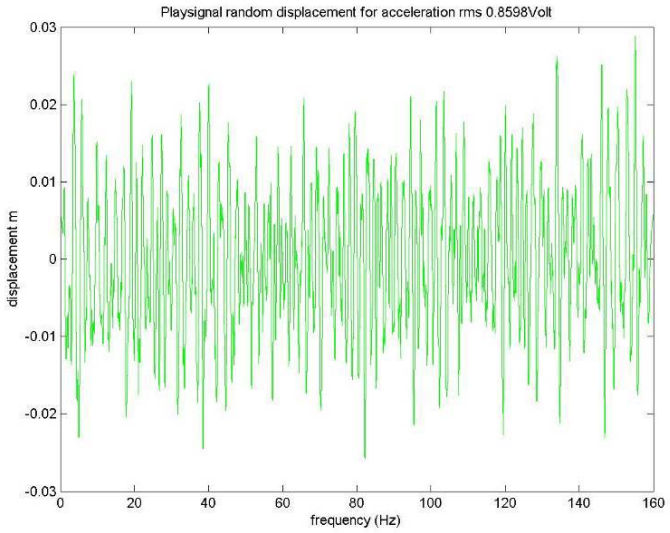

Figure 66 :- Actuator displacement signal under seat

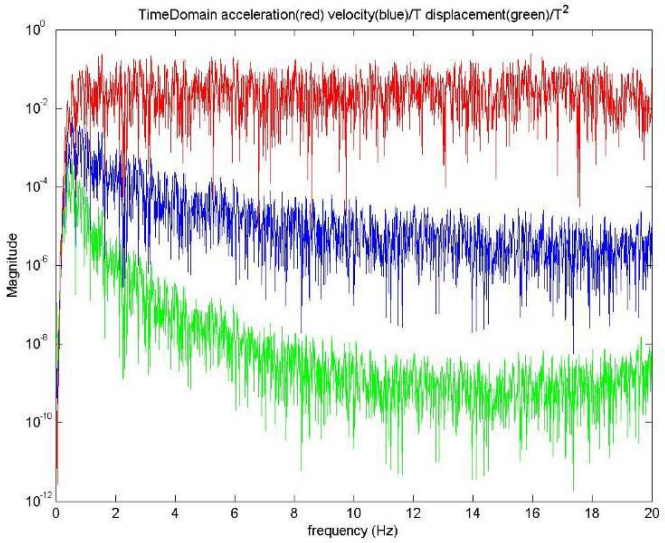

Figure 67 :- Power spectral density distribution of actuator input signal

Displacement is the green curve, velocity the blue and acceleration the red. The PLAYSIGNAL.vca containing the displacement in the time domain can now be played via the SIGLAB VFG (using the arbitrary function) into the actuator for the next cycle of iteration (if further iteration is required).

A.5.6 The Matlab code - included for reference:

```
% Generate playsignal_random_number.vca file for spectral content
% calculate 51.2Hz acceleration signal for 80 seconds from matlab 'randn' function
% integrate twice and save time domain displacement signal in SIGLAB vca file format
% graph is drawn to show sgnal psd in frequency domain
% author: AF van der Merwe
% 11 04 06
df = 0.01 % resolution of the frequency vector used for psd
max_freq=20; % maximum frequency of interest in the psd
Fs=51.2;
NFFT=Fs/df;
signaltime=160; %seconds
Playsignal.t=1/Fs:1/Fs:signaltime;
%Playsignal.t=Playsignal.t;
%filter the time signal using a Butterworth bandpass 0.5 to 20Hz
%the following filter can be used for 51.2Hz Sampling Rate
num = [0.3656 0 -1.4623 0 2.1934 0 -1.4623 0 0.3656];
den = [1.0000 -1.6317 -0.8753 1.6332 1.1343 -1.0202 -0.5911 0.2172 0.1337];%the spectral graphs are compared
Playsignal.acceleration=filter(num,den,randn(1,length(Playsignal.t)));
%Create end conditions - modified Hanning window with 0.2Hz high pass Smooth Start and Stop
Fw=0.2 %frequency of the start and stop hanning window
Start=sin(Fw/2*pi*Playsignal.t(1:round(Fs/Fw))).^2;
Stop=fliplr(Start);
Fill= ones(1,length(Playsignal.t)-length([Start Stop]));
StartStop=[Start Fill Stop];
Playsignal.acceleration=Playsignal.acceleration.*StartStop;
Playsignal.RMS.acceleration=sqrt(mean(Playsignal.acceleration.^2));
%Playsignal.acceleration=sqrt(2)*sin(Playsignal.t);
figure; plot(Playsignal.t,Playsignal.acceleration);
% integrate
%Playsignal.data=integraldoubl(Playsignal.t,Playsignal.acceleration,0,0,1);
Playsignal.data=integral(Playsignal.t,Playsignal.acceleration,0,1)
Playsignal.velocity=Playsignal.data'.*StartStop';
```

```
Playsignal.RMS.velocity=sqrt(mean(Playsignal.velocity.^2))
%Playsignal.velocity=Playsignal.velocity-mean(Playsignal.velocity);
Playsignal.data=integral(Playsignal.t,Playsignal.velocity,0,1);
Playsignal.displacement=Playsignal.data.*StartStop;
Playsignal.RMS.displacement=sqrt(mean(Playsignal.displacement.^2));
%psd acceleration
[P,w_psd]=psd(Playsignal.acceleration,NFFT,Fs);
Playsignal.psd.acceleration=P(1:(round(max_freq/w_psd(2))+1))./Fs*2; % only data up to max evaluation frequency
%psd velocity
[P,w_psd]=psd(Playsignal.velocity,NFFT,Fs);
Playsignal.psd.velocity=P(1:(round(max_freq/w_psd(2))+1))./Fs*2;
%psd displacement
[P,w_psd]=psd(Playsignal.displacement,NFFT,Fs);
Playsignal.psd.displacement=P(1:(round(max_freq/w_psd(2))+1))./Fs*2;
Playsignal.w=w_psd(1:(round(max_freq/w_psd(2))+1));
figure;
semilogy(Playsignal.w,Playsignal.psd.displacement,'-g',Playsignal.w,Playsignal.psd.velocity,'-
b',Playsignal.w,Playsignal.psd.acceleration,'-r');
  title('psd acceleration(red) velocity(blue)/T displacement(green)/T^2');
  xlabel('frequency (Hz)');
  ylabel('Magnitude');
hold off
save playsignal_random Playsignal Fs df NFFT;
plot(Playsignal.t,Playsignal.acceleration,'-r',Playsignal.t,Playsignal.displacement,'-g');
Playsignal.displacement=Playsignal.displacement.*9.5./max(Playsignal.displacement); %adjust to maximum 9.5V for use in VFG set
on 10V max actuator
mat2vca(Playsignal.displacement',Fs,'playsignal_random_number.vca')
Playsignal.RMS
%plot the time domain signal of the displacement
plot(Playsignal.t,Playsignal.displacement,'-g');
ylabel('Volts');
xlabel('time (sec)');
title('TimeDomain displacement(green)');

function OUTPUT=integral(x,INPUT,CONSTANT,PLOT);
%OUTPUT=integraldoubl(x,INPUT,CONSTANT1,CONSTANT2,PLOT);
%returns the INTEGRAL of INPUT with respect to vector x
%if the last parameter PLOT has to be larger than zero to get a plot
%by Andre van der Merwe - ACUTEC Acoustic & Digital Consulting engineers
n=length(INPUT);
dx=x(2)-x(1);
for i=2:n
  OUTPUT(i)=simp(x(1:i),INPUT(1:i));
end;
OUTPUT(1)=INPUT(1)*dx;
SHIFT = mean(OUTPUT)
OUTPUT=OUTPUT-SHIFT+CONSTANT;
size(OUTPUT)
RMS_INPUT=sqrt(mean(INPUT.^2))
MAX_OUTPUT=max(OUTPUT)
MIN_OUTPUT=min(OUTPUT)
RMS_OUTPUT=sqrt(mean(OUTPUT.^2))
RMS_INPUT/RMS_OUTPUT
if nargin < 4, PLOT = 0; end;
if PLOT > 0
  figure;plot(x,INPUT,'-b',x,OUTPUT,'-g');
  title('signal (blue) and integral (green)');
  xlabel('time (sec)');
  ylabel('Magnitude');
end
OUTPUT=[OUTPUT];
```

Appendix C - In-field tests on Bell logger

TEST REPORT

Three-wheeled logger in-field human vibration tests

Test date: 11 July 2003

Author: Andre van der Merwe

High levels of whole body vibration are common in vehicles operating in off highway conditions. The Bell logger has only the suspension of the inflated tyres and therefore offers minimum suspension against vertical shock and vibration. This test report is to assess the actual values of the vertical vibration the operator experiences during normal in-field logging operation.
The results evaluated to the British Standard 6841 show that on average the driver reaches the recommended maximum dose for a 4 hour work shift within 2 hours 17min of operation. Should the operator be exposed for more than 2hour 17min hours within a 4 hour work shift, medical problems are likely to appear, and claims may be made by the operator.
To assess the vibration acceleration levels induced on the operator of a Bell three-wheeled logger tractor during normal operating conditions. Vertical vibration results and recommendations are made available to Bell for their engineering and product development. Raw data and acceleration information are used at the Stellenbosch University on a research project titled 'An air suspension cushion to reduce human exposure to vibration'.

C.1. Measurement and Analysis Method

The tests were carried out at a forestry location south of Grabouw in the Western Cape. Typical infield conditions existed as trees were being fell. The 3 wheeler tractor was manufactured by Bell Equipment and had seen at least 5 years of service.

Vibration was measured at four positions of the operators seat; Firstly on top of the seat using a tri-axial seat accelerometer, Secondly a tri-axial accelerometer on the floor to the front right below the seat, thirdly a single axis vertical accelerometer on the floor to the right rear of the seat, and finally a single axis accelerometer on the floor to the left rear of the seat.
The accelerometers were all of the ICP type and recently calibrated. Accelerometer output was a voltage signal which was measured at rate of 256Hz by two modules of Siglab hardware. The Siglab hardware modules were connected to a Dell laptop computer which controlled the Matlab based acquisition process and stored to data onto hard disk. The Siglab hardware were mounted on the Three-wheeled logger and supplied by a 40Ah 12V deep cycle battery. The Dell computer ran in a screen off mode on two Dell module batteries.
Another computer was used as a terminal to control the Dell through a remote desktop software package over an Ethernet network link. The second computer was powered by an inverter from the 12V supply in the back of a Land Rover vehicle used as the base station. The network link was a long cable which was unplugged before every test. The network cable was plugged in when the logger stopped at the base to access the Dell computer and the Siglab hardware.
Test #1 through #10 data records were captured in a VCA format for each test. The VCA data files were cropped to 5 minute runs to eliminate start and stop data. A Matlab routine developed by the author was used to calibrate and filter the raw data according to the BS 6841 frequency weighting standard whilst in the time domain. Weighted Vibration Dose Value (vdv), Root mean Square (RMS), Crest Factor (CF) and estimated Vibration Dose Values (evdv) were calculated and tabled for each of the vertical vibration channels. International vibration standard ISO 2631-1 may be used to render similar results.
A Matlab routine 'SPtool' was used to do frequency spectral analysis of the weighted test data to obtain a visible representation of the frequency content of the vibration signals. Frequency spectrum curves presented herein were cut and paste from the SPtool screen display.
Tests on stationary logger with engine at idle and operating revolutions were recorded using Siglab VNA software and the resultant figures copied and pasted in here under results. Data is not weighted in accordance with the BS 6841 standard. Raw data and analysed results are stored on CD-rom for future reference

C.2. Results

C.2.1 Engine vibration at idle and logger stationary:

The logger was static and the engine revs at idle revolutions. The green curve represents the vibration on the floor below the seat and the blue curve the vibration on top of the seat at the seat buttock interface. The natural resonance of the vehicle is noticeable at 20, 40 and 60Hz. The green curve shows that the vehicle engine at idle has a noticeable resonance frequency at 4Hz. This is the frequency where the human body in the most vulnerable to vibration as it is the first mode frequency of the seated subject. The blue curve shows the reaction of the body to this 4Hz input vibration in that it also peaks at around 4Hz although the body spreads the energy over a wide frequency range using its own internal damping. This happens for all frequencies below 20Hz as the human body experiences more vibration than what the vehicle actually induces upon it.

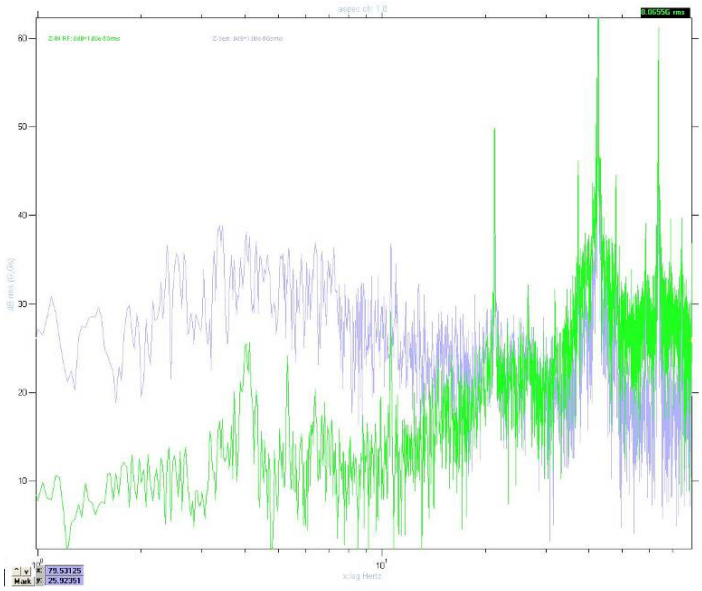

Figure 68 :- Vibration frequency spectrum for logger stationary with engine revs at idle

C.2.2 Engine vibration at operating revs and logger stationary

The logger was static and the engine revs at operating revolutions that would be used for the normal in-field stacking operation. The green curve represents the vibration on the floor below the seat and the blue curve the vibration on top of the seat at the seat buttock interface.

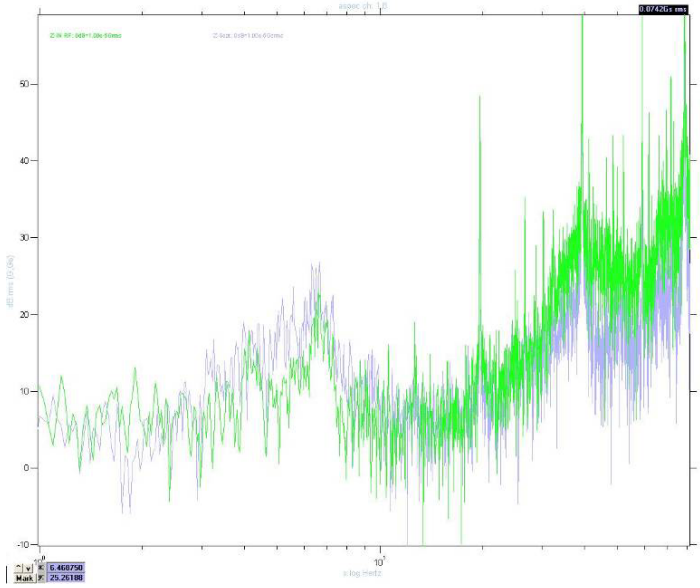

Figure 69 :- Vibration frequency spectrum for logger stationary with engine at operating revs

On the green curve, the 4Hz peak input from the vehicle has actually reduced by about 10 dB, but a new peak at 6.5Hz appeared likely due to the engines operating revs being higher. The human body's reaction to this was possibly to sit more erect in response to the

new stimulus. The vibration levels induced on the human body at 4Hz is less than with idle as would be expected, however still higher than that of the vehicle. The resonances at 20, 40 a 60Hz seem unchanged from the idle case and is likely the first mode of resonance of the vehicle tyre mass spring system.

C.2.3 Vibration during normal in-field log stacking operation

Five cycles of fetching a load of logs and stacking it some 30m away were recorded in every test. Each cycle consisted of one full run and one empty run. Eight tests were recorded representing 40 cycles and after applying the required frequency weighting to the signals in the time domain the results in Table 7 were obtained. The vibration dose value (vdv) measure on the seat was 17.25ms$^{-1.75}$ where the maximum allowed level for a 4 hour work shift is 15ms$^{-1.75}$. Reworking this means that the 15ms$^{-1.75}$ limit is reached within 2hours 17min of each and every 4 hour shift.

Table 7 :- In-field stacking operation results (all data time domain weighted to BS 6841 Wb filter)

Three-wheeled Logger in-field test results

		AVERAGES for all runs						STDeviation for all runs				
Chan	**Axis**	**RMS**	**vdv**	**4hvdv**	**CF**	**evdv**	**EU**	**RMS**	**vdv**	**4hvdv**	**CF**	**evdv**
1	**Zin**	0.847	5.808	15.38	10.55	4.899	106.2	0.10654	0.7945	2.219063	2.344774	0.528946
4	**Zin**	0.873	5.599	14.84	8.728	5.047	98.84	0.06284	0.4223	1.08308	2.178512	0.356188
5	**Zin**	0.896	5.625	14.9	8.693	5.182	101.5	0.05562	0.3962	1.017971	3.457214	0.311389
8	**Zseat**	0.915	6.507	**17.25**	10.39	5.286	97.57	0.10906	0.6713	1.990778	1.957496	0.50892

Maximum Exposure Time **2.286** hours per 4 Hour shift

Looking at the vibration frequency spectrum content one can learn the typical frequencies that cause the above high vibration levels. In Figure 70 the frequency spectrum of the test number 2 is shown. Note the slight differences amongst the three z-in measuring positions. This is contributed mainly to angular movement of the vehicle which does not concern us in this report where we mainly focus on vertical vibration. Important, however is the difference between the z_{seat} and the various z_{floor} axes.

At frequencies lower than 5.25 it is clear that the vibration level on the seat is higher than that below the seat on the floor. At these frequencies it would be better to have the operator sit directly on the floor and not on the seat. At frequencies between 6Hz and 13Hz, the existing seat provides a little attenuation of the vibration input; however between 13Hz and 20Hz, the vibration is higher again on the seat than below. Above 20Hz, the seat provides a little vibration isolation due to the sponge characteristics.

At 2.4Hz the main vibration energy exists due to the vehicle motion and the next peak is at 7Hz. At 2.4Hz the magnitudes of the three z_{floor} .axes are equal which indicates the likeliness of vertical only vibration, probably induced by the front wheels 'suspension'. The peak at 7Hz shows the magnitudes picked up by the front and rear sensors different (although similar left to right) indicating a possible pitch motion caused by the tyre 'suspension' of the rear wheel. The resonance peaks are still present at 20, 40 and 60Hz as with the stationary tests.

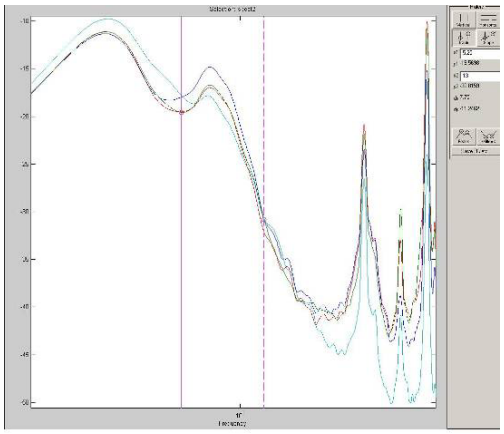

Figure 70 :- Field test 2 Z-axis data frequency spectrum

(blue - $z_{floor\ right\ front}$, red – $z_{floor\ left\ rear}$, green – $z_{floor\ right\ rear}$, cyan - $z_{seat\ centre}$).

C.2.4 Vibration during gravel road run empty

Two tests were recorded with the logger travelling empty over an in-field dirt track. Test #9 is shown in Figure 71 where it is interesting that the z_{seat} (on the seat) vibration level remains higher than the z_{floor} (on the floor) vibration channels up to a frequency of 8Hz. It is likely that due to the 'feet up' sitting posture of the operator that a lot of the vibration is transferred to the upper body through the legs thus inducing more whole body vibration. If compared to the infield stacking operation where the feet pressure alternates from left to right and backwards to forward, this forward driving requires more constant pressure on the pedals to activate forward driving.

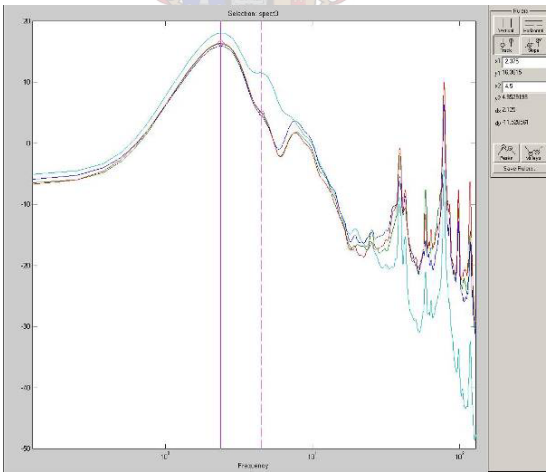

Figure 71 :- Vibration frequency spectrum of dirt track test #9 (empty); channel colours similar to Figure 70.

Note the slight peak at 4.5Hz which is almost non-existent on the z_{floor} curves. This is most likely the natural resonance of the upper body of the operator induced by a possible roll motion of the vehicle. Vibration isolation of the seat only starts upward from 20Hz, similar to that found in Figure 70.
Test #10 frequency spectrum shown in Figure 72 is similar to test #9 above.

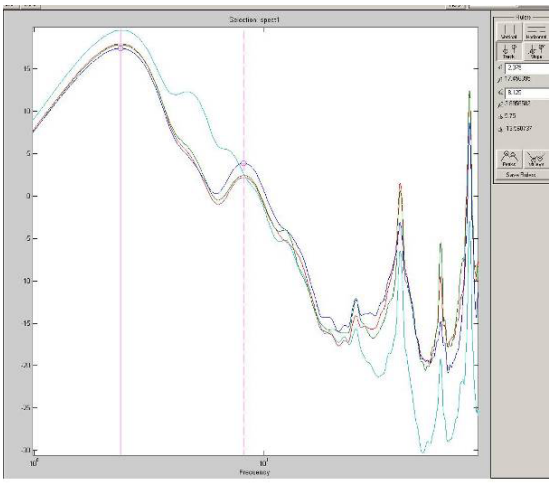

Figure 72 :- Frequency spectrum of test #10 in-field dirt track (empty); channel colours similar to Figure 70.

Note here that the peak at 8.1Hz does not transfer through to the top of the seat as a peak. It is likely a pitch motion triggered by the rear wheel similar to that described earlier and therefore not affecting the vertical vibration.

C.3. Conclusions and Recommendations

The whole body vibration tests on the three-wheeled logger showed that the vibration dose values are exceeded. Only the z-axis vibration was considered in this report, however if the lateral y and fore-aft x axes were added it is likely that the combined multi axis vdv values would even further exceed the recommended vibration dose level.

The frequency content graphs in the results show that during operation the vibration magnitude at frequencies below 5Hz is higher than vibration magnitude above 5Hz. With the logger in stationary, the higher engine rev frequencies dominate the frequency spectrum. As mentioned in the results, there is a resonance of the vehicle at approximately 4Hz during idle. This resonance is at the resonance frequency of the human body and causes excessive vibration of the upper body even at engine idle speed. We would recommend that this resonance of the vehicle body is reduced by damping or anti-resonance techniques.

Suspension of the front wheels relies only on the flexibility of the tyres. This causes major vertical acceleration of the operators body at a peak frequency of 2.4Hz and even after weighting in accordance to BS 6841, the result is still of great concern. More vibration is introduced by the operator's feet into his body, especially when applying constant pressure when driving forward for some distance. This is less when manoeuvring in-field during a stacking operation.

The seat installed in the vehicle requires serious reconsideration. A simple suspension seat or air suspension cushion will reduce the vibration peak at 2.4Hz adequately to conform to the vibration dose limits. The operator is then likely to be able to operate for a full 4 hour shift without the danger of health deterioration.

The data obtained in this study will now also be used to develop an air suspension cushion as part of the human vibration research program at the Engineering Faculty University of Stellenbosch.

Appendix D - Concept design evaluation

Table 8 shows the conceptual design decision matrix with weights, referenced from section 3.3 - Concept design evaluation.

Table 8 :- Concept evaluation decision matrix

CONCEPT DESIGN EVALUATION

	Evaluation Criteria	Weighting	A	B	C	D	E	F	G	H	I	J	K
	Summary Rating:		**-68**	**39**	**234**	**280**	**298**	**386**	**473**	**290**	**226**	**374**	**659**
1	A cushion with three separate pres:	**17**	-1	-1	-1	0	0	1	0	1	1	1	0
2	A mechanical link on will hold the	**7**	-1	-1	0	0	0	1	1	0	0	0	0
3	A simple off the shelf material can	**42**	1	1	1	1	1	1	1	1	1	1	1
4	A single moulding with air chambe	**15**	0	1	1	1	1	1	1	1	1	1	1
5	A tuned pipe exists between each a	**29**	1	1	1	1	1	1	1	-1	-1	-1	1
6	allow maximum vertical travel unc	**19**	1	1	1	1	1	0	1	-1	-1	0	1
7	allow the cushion buttock no more	**24**	-1	0	-1	1	1	1	1	1	1	1	1
8	The membrane used will stretch ur	**13**	-1	-1	-1	-1	-1	-1	-1	-1	-1	0	-1
9	Constant pressure area as the cushi	**32**	-1	-1	-1	1	1	1	1	1	-1	0	1
10	cushion buttock interface to be sha	**5**	-1	-1	1	1	1	1	1	1	1	1	1
11	High linearity	**41**	-1	-1	-1	-1	-1	-1	-1	-1	-1	-1	0
12	Ideally the drums will move with t	**8**	-1	-1	0	0	0	0	1	0	0	0	1
13	Large lateral forces can cause the p	**18**	1	1	1	0	1	1	-1	1	1	1	1
14	Manufacturing simple to keep cost	**39**	1	1	1	0	0	0	1	1	1	1	1
15	Moulding material to be of closed	**31**	0	0	1	1	1	1	0	1	0	1	1
16	No mechanical scissors mechanism	**36**	-1	-1	0	0	0	1	0	1	1	1	1
17	no pinch points (high pressure poir	**6**	1	1	1	1	1	1	1	1	1	1	1
18	one pipe and drum rather than mul	**34**	1	1	1	-1	-1	-1	1	-1	0	0	1
19	One volume which is easily connec	**33**	1	1	1	-1	-1	-1	1	-1	0	0	1
20	Provide support against fore aft bo	**21**	-1	-1	-1	1	1	1	1	1	1	1	1
21	Provide support against fore aft ho	**20**	-1	0	0	1	1	1	1	1	1	1	1
22	Provide support against sideways b	**23**	-1	-1	-1	1	1	1	1	1	1	1	1
23	Provide support against sideways f	**22**	-1	0	0	1	1	1	1	1	1	1	1
24	rubber is used which is a very relia	**43**	1	1	1	1	1	1	1	0	1	1	1
25	seat does not have vertical travel o	**16**	-1	-1	0	0	0	1	1	1	1	1	1
26	Stable as the shaped spring can be	**40**	-1	-1	1	1	1	1	1	1	1	1	1
27	Stable support against body roll	**26**	-1	0	0	1	1	1	1	1	1	1	1
28	support the weight of light to heavy	**35**	1	1	1	1	1	1	1	1	1	1	1
29	The air-cushion will ideally replac	**38**	0	0	0	-1	-1	0	0	1	-1	0	1
30	the body's weight centre axis the sa	**4**	1	1	1	1	1	1	1	1	1	1	1
31	The drums are interlinked with a si	**12**	0	0	0	1	1	1	0	0	0	0	0
32	The drums can be structurally conn	**2**	-1	-1	0	-1	-1	0	0	0	0	0	0
33	The drums can ideally form the ba	**9**	1	1	1	1	1	1	1	0	0	0	0
34	The linearity of the pressure area c	**10**	-1	-1	0	1	1	-1	-1	-1	-1	-1	1
35	The pressure area increase under h	**27**	-1	-1	-1	-1	-1	-1	-1	-1	-1	-1	-1
36	The pressure filler valve is mounte	**1**	1	1	1	1	1	1	1	-1	-1	0	1
37	The rolling membrane air spring ha	**11**	0	0	-1	-1	-1	0	-1	-1	0	-1	-1
38	The sideways force can be prevent	**14**	0	0	0	0	0	0	0	1	0	0	0
39	The spring coefficient of the cushic	**25**	-1	-1	-1	-1	-1	-1	-1	-1	-1	0	-1
40	The stretch of the rubber will not c	**37**	1	1	1	1	1	1	1	1	1	1	1
41	The three pressure chambers will h	**30**	-1	-1	0	-1	-1	-1	0	0	0	0	0
45	Three long drums (cylindrical or re	**3**	0	0	0	0	0	0	0	0	0	0	0
46	Utilize a pipe and drum to increase	**28**	1	1	1	1	1	1	1	-1	-1	-1	1

Concepts:

A	Plastic Ball
B	StablePlasticBall
C	FlatCylinder
D	TwoHorisontalCylinder
E	ThreeFlatCylinders
F	SquareTorus
G	RoundTorus
H	Airbubble
I	OpenFoam
J	CloseFoam
K	TorusInFoam

Appendix E – Simulink model of cushion with solid mass

The Simulink model for the air suspension cushion with solid mass is presented in Figure 73 :- Simulink model of air suspension cushion with and without resonator.

The colour legend used is as follows. Black is the cushion without the pipe and tank. Similar is the green a second cushion without pipe and tank to verify the first. The blue is the pipe and tank connected to the cushion at pressure pC(t). The red represent the random input floor signal and the blue the various measurement points.

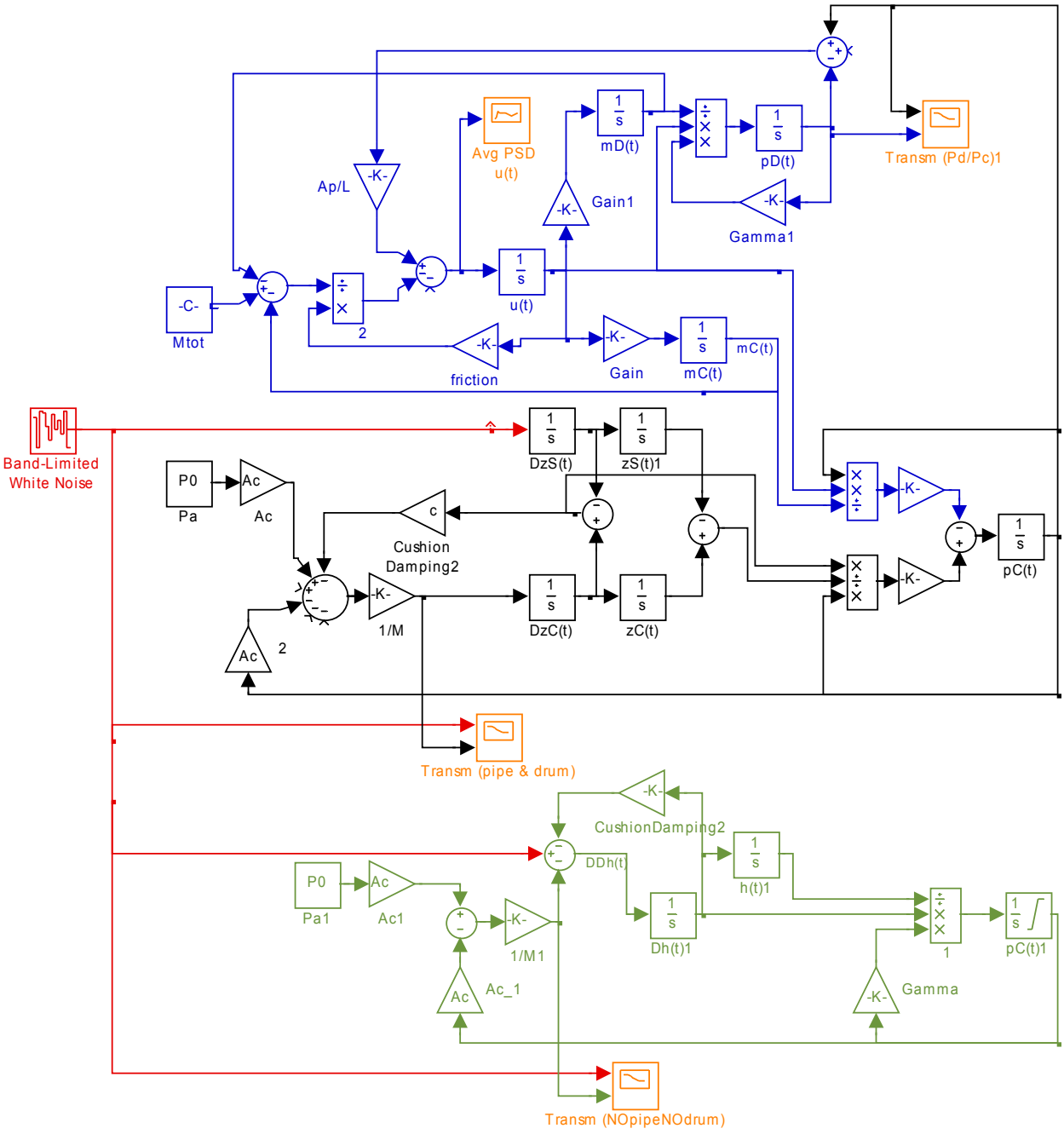

Figure 73 :- Simulink model of air suspension cushion with and without resonator

Appendix F – Simulink model of cushion with human model imposed

The Simulink model has the cushion model as a based with the human superimposed instead of the static mass load. The Figure 74 and Table 9 show the human model diagrammatically with parameters as proposed by Wei & Griffin. Figure 75 details the Simulink model used to determine the transmissibility curve for air suspension cushions with resonators. The part of the model in the blue surround represents the resonator. The part in the red surround represents the human model.

Table 9 :- Parameters used in mechanical human model

parameter	quantity	unit	symbol
Mass	14.62	kg	M0
Mass1	29.25	Kg	M1
Mass2	5.85	Kg	M2
Spring coefficient supporting mass 1	23298	N/m	K1
Spring coefficient supporting mass 2	14728	N/m	K2
Damping coefficient mass 1	364.7	Ns/m	C1
Damping coefficient mass 2	145.9	Ns/m	C2

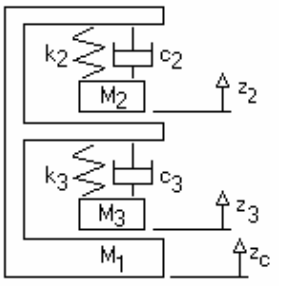

Figure 74 :- Mechanical human model (Wei and Griffin 1998a)

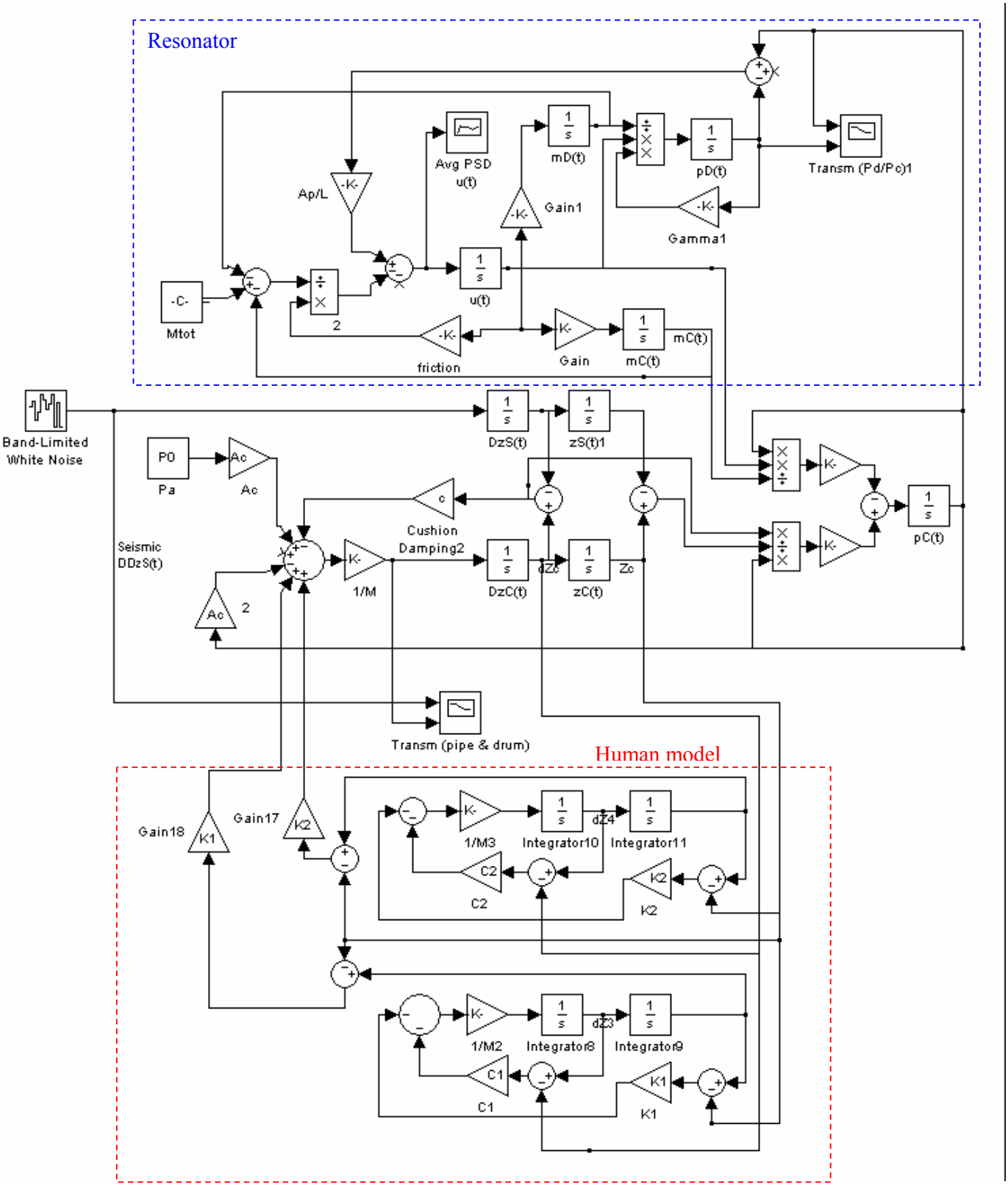

Figure 75 :- Simulink model including the human model